Available online at www.sciencedirect.com

SciVerse ScienceDirect

Procedia Engineering 00 (2012) 000–000

Procedia Engineering

www.elsevier.com/locate/procedia

5th BSME International Conference on Thermal Engineering

Numerical Modelling of Oxy-Fuel Combustion in a Full-Scale Tangentially-Fired Pulverised Coal Boiler

Audai Hussein Al-Abbas[a,b] , Jamal Naser[a,]*, David Dodds[a], and Aaron Blicblau[a]

[a]*Faculty of Engineering & Industrial Sciences, Swinburne University of Technology, Hawthorn 3122, AUSTRALIA*

[b]*Technical College of Al-Musaib , Foundation of Technical Education, Babylon, IRAQ*

Abstract

This paper presents a computational fluid dynamics (CFD) modelling study to investigate Victorian brown coal combustion in a 550 MW utility boiler under the air-fired (standard) and three oxy-fuel-fired cases. The standard case was modelled based on the real operating conditions of Loy Yang A power plant located in the state of Victoria, Australia. A level of confidence of the present CFD model was achieved validating four parameters of the standard combustion case, as well as the previous preliminary CFD studies which were conducted on a lab-scale (100 kW) unit firing lignite and propane under oxy-fuel-fired scenarios. The oxy-fuel combustion cases are known as OF25 (25vol. % O_2 concentration), OF27 (27vol. % O_2 concentration), and OF29 (29vol. % O_2 concentration). The predictions of OF29 combustion case were considerably similar to the standard firing results in terms of gas temperature levels and radiative heat transfer compared with OF25 and OF27 combustion scenarios. This similarity was because of increasing the residence time of pulverised coal (PC) in the combustion zone and O_2 concentration in feed oxidizer gases. Furthermore, a significant increase in the CO_2 concentrations and a noticeable decrease in the nitric oxides (NO_x) formation were noted under all oxy-fuel combustion conditions. This numerical study of oxy-fuel combustion in a full-scale tangentially-fired PC boiler is important prior to its execution in real-life power plants.

Keywords: Oxy-fuel combustion;Victorian brown coal; Combustion chemistry; CO_2 capture; NO_x emission; CFD.

1. Introduction

In general, approximately 85% of electricity production is obtained from solid fuel (coal) in Australia. In the Latrobe valley/Victoria, the Loy Yang power plant has been designed to use brown coal. This source of energy is a major contribution to the greenhouse gases (GHG) emissions. In order to keep a continuous usage of existing power plants and make them environmentally friendly, innovations and research on the brown coal combustion in tangentially-fired furnaces can play an important role to develop this economical energy source. In addition, with increasing concerns from the Kyoto Protocol against the global climate change, developments and research on the brown coal combustion can also make it meet a better sustainable progress for power plants (Chun-Zhu, 2004).

Recently, several advanced combustion technologies have been developed such as Pre-combustion capture, post-combustion capture, and oxy-fuel combustion capture. These technologies are being considered as the most efficient utilization technologies to reduce CO_2, NO_x, and SO_x emissions and fuel consumption (Wall et al., 2009; Kakaras et al., 2007). However, oxy-fuel (O_2/CO_2) combustion technology has been widely considered the most viable technique in the PC power plants. The basic concept of the O_2/CO_2 technology is to use pure oxygen (approximately 95vol.% O_2), produced in air separation units, instead of air (O_2/N_2) in conventional combustion to burn fuel. Due to this high purity of O_2, a very high combustion temperature is achieved in the combustion zone. This elevated temperature can be diluted by recycling part of the flue gas (about 60-80%) to the furnace so as to decrease the radiation heat transfer to the furnace wall. At the end of this process, the partial pressure of carbon dioxide in the flue gas is highly increased; thereby the capturing process of CO_2 will

be easier and economically efficient relative to that in the conventional firing. Nevertheless, NO_x and SO_x are decreased, and a high char burnout is achieved in the exit flue gas (Al-Abbas and Naser, 2012a).

Before switching to apply oxy-fuel combustion technique for conventional full-scale firing boilers, lab-scale furnaces have to be initially examined under a number of oxy-fuel combustion conditions. This strategy is strongly recommended to examine the combustion characteristics and boiler performance. Nevertheless, when the oxy-fuel combustion program was started in the last decade, much research has been carried out in terms of experimental investigations (Andersson, 2007) and numerical studies (Al-Abbas et al., 2011). The most important features of this work focused on the species concentrations, flame temperature levels, char burn-out, NO_x and SO_x formation, and heat transfer. The values of these variables, under oxy-fuel combustion conditions, are connected to the amounts and concentrations of oxygen and carbon dioxide used in the recycled flue gas (RFG). The differences in the thermodynamics properties between the CO_2, in oxy-fuel, and N_2, in the conventional firing atmosphere, can lead to some changes in the combustion characteristics inside the furnace. These amendments should be reduced as much as possible so as to be close to the characteristics of conventional combustion.

From the recent literature, there are a lot of innovations on oxy-fuel combustion technique, which implemented under several operating conditions and combustion environments to reduce the retrofits for the conventional combustion system. However, in the present simulation study, the oxy-fuel combustion approach that conducted experimentally in the Chalmers' lab-scale furnace (Andersson, 2007) has been chosen. This selection was dependent on the preliminary CFD studies (Al-Abbas and Naser, 2012a and b). Whilst the existing (reference) combustion case has been simulated based on the drawings and operation conditions of Loy Yang A power plant that provided by the Energy Technology Innovation Strategy (ETIS) program (Staples and Marshall, 2010). A CFD code, AVL Fire version 2008.2, was used to model and analyze four different combustion environments. Four combustion scenarios were simulated: standard PC combustion, and three oxy-fuel combustion cases, which are known as OF25, OF27, and OF29. User-defined functions (UDFs) required for the PC devolatilization, char burnout, multi-step chemical reactions, mass and heat transfer, carbon in fly-ash, and nitric oxidizes formation/destruction have been written and incorporated into the CFD code. Results, for all combustion cases investigated, are compared. The species concentrations, temperature distributions, gas-phase velocity fields, char burnout, NO_x emissions, and radiative heat transfer obtained for all combustion cases were compared.

2. Model description and methodology

2.1. Geometry and operating conditions of the boiler

The tangentially-fired Victorian (Australian) brown coal 550 MW_e boilers located in the Latrobe Valley mine, was used in this simulation study. The geometric description of the CFD model for the boiler, Loy Yang A, is shown in Figure 1a. The unit produces 430 kg/s of steam flow at 16.8 MPa and 540 ^oC under full load of operating conditions. In Figure 1, the CFD model was extended from the furnace hopper up to the top of the tower. The geometric dimensions of the simulated boiler were 98.84 m, 17.82 m, and 17.82 m for the height, width, and depth, respectively.

The furnace used in this study consists of eight mill-duct systems, two on each side face of the furnace. Only five mills (numbers 1, 2, 5, 6, and 8) are in service and the remaining mills are out of service (numbers 3, 4, and 7). There are three inert burners and three main burners for each mill-duct system. The mill-duct systems are designed for the following purposes: grinding the raw coal into pulverized coal (PC) in the mill, removing the moisture content (62% wt) from the brown coal through the drying shaft, transporting and distributing the PC. The centrifugal separation system is used to deliver pulverized coal from the grinding mill to the inert and main burners of the furnace. This distribution of fuel and gases (fuel-rich mixture) to the main burners is required to maintain combustion stability in the furnace.

Table 1 shows the mass flow rates (kg/s) of air (O_2/N_2) and O_2/CO_2 for the reference (air-fired) and the oxy-fuel combustion scenarios, respectively at each secondary air duct. In the furnace zone, the burners' arrangements on the furnace wall surface were as follows from top to bottom: upper inert burner (UIB), intermediate inert burner (IIB), lower inert burner (LIB), upper main burner (UMB), intermediate main burner (IMB), and lower main burner (LMB). The locations, reference levels (R.L.), of the above-mentioned burners are based on the original ground level of the power plant. The secondary air port ducts were set up above and below each burner in order to improve combustion characteristics. A schematic demonstration of the secondary air ports, in the inert burners, was as follows from top to bottom: upper inert secondary air duct (UISAD), upper intermediate inert secondary air duct (UIISAD), lower intermediate inert secondary air duct (LIISAD), lower inert secondary air duct (LISAD). While in the main burner, the schematic demonstration of the secondary air ports

was shown as follows: upper main secondary air ducts 1 and 2 (UMSAD1& 2), intermediate main secondary air ducts 1 and 2 (IMSAD1& 2), and lower main secondary air ducts1 and 2 (LMSAD1& 2). In order to control the air flow distribution in the central zone of the main burners, a core air duct is installed in the middle of each PC burner, i.e. upper, intermediate, and lower core secondary air ducts (UCSAD, ICSAD, and LCSAD). In representing the convection zone, eight different sources of heat sinks were implemented above the location of hot gas off-takes (HGOTs).

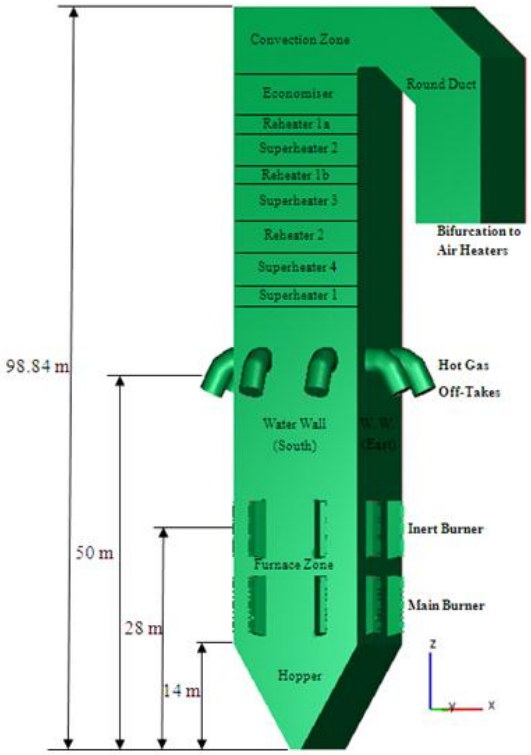

Fig. 1. The geometric description of the CFD model for the boiler, unit 1 at Loy Yang A power station.

Table 1. The mass flow rates (kg/s) of air (O_2/N_2) and O_2/CO_2 for the reference (air-fired) and the oxy-fuel combustion scenarios at each secondary air duct.

Secondary air duct	Distribution ratio (%)	Combustion cases			
		Standard Air-Fired	Oxy-Fuel OF25	Oxy-Fuel OF27	Oxy-Fuel OF29
		Mass flow (kg/s)	Mass flow (kg/s)	Mass flow (kg/s)	Mass flow (kg/s)
Upper inert	5.0%	6.89	5.71	5.3	4.96
Upper intermediate inert	5.0%	6.89	5.71	5.3	4.96
Lower intermediate inert	5.0%	6.89	5.71	5.3	4.96
Lower inert	5.0%	6.89	5.71	5.3	4.96
Upper main	20.0%	27.55	22.87	21.21	19.84
Upper core	6.67%	9.19	7.62	7.07	6.61
Intermediate main	20.0%	27.55	22.87	21.21	19.84
Intermediate core	6.67%	9.19	7.62	7.07	6.61
Lower main	20.0%	27.55	22.87	21.21	19.84
Lower core	6.67%	9.19	7.62	7.07	6.61
Total		137.78	114.35	106.09	99.2

2.2. Numerical description

The geometric model was precisely constructed using the CAD tool, and the dimensions of model geometry were taken from the power plant drawings. The first step of this simulation has been conducted solving of the governing equations of combustion, heat and mass transfer, and turbulent flow under transient mode. The solutions are repeated for all variables in each control volume until the usual convergence limit was achieved with less than 10^{-4}; the CFD code is based on the finite-volume approach. For the convergence criteria, simulations were run up to 48,000 time-steps until the stable quasi steady

state was reached. Then, the numerical results were averaged over the final 8,000 time-steps. After the converged solution was achieved for the two-phase (gases and particles) flow, the second step of the simulation was subsequently implemented for the NO_x formation/destruction models.

The standard SIMPLE algorithm was used solving the combination between the velocity and pressure in Navier-stokes equations. A Lagrangian/Eulerian approach was used for gas-solid two-phase flow. Under the initial simulation set up, the time-step used in this simulation was limited to 0.0005 (s) in order to allow for the temperature profile to stabilize. Once the simulation results become more stable, the time-step is increased up to 0.0025 (s), an appropriate value by the numerical stability. The total number of particles used in this simulation was 50,000 particles, and the share of each in the service mill-duct system was 10,000 particles. In the convection zone of the furnace, heat absorption sources for the water tube wall and the convective tube banks were simulated as heat transfer sink terms (user defined sinks) in the enthalpy equation.

3. Results and discussion

3.1. Temperature distributions

In Figure 2, the distributions of flue gas temperatures are showed along the height of the furnace at the mid cut of X-Z plane for the air-fired, OF25, OF27, and OF29 combustion scenarios. As soon as the reaction processes between PC and oxidizer gases have been started the flame temperature is gradually increased to be at a peak value in the furnace zone as follows: 1591.37 K for air-fired, 1479.0 K for OF25, 1540.3 K for OF27, and 1592.0 K for OF29. It is clearly seen that a reduction in the levels of the gas temperature when the N_2 is replaced by the CO_2 in the secondary air ducts, particularly in the OF25 and OF27cases examined. That obvious decrease in the gas temperature was mainly due to the higher volumetric heat capacity of CO_2 compared to N_2 in the gas mixture. On the other hand, the maximum gas temperatures between air-fired and OF29 combustion cases were approximately identical. That improvement on the gas temperature of the latter oxy-fuel case was because of increasing O_2 concentration in the feed oxidizer gases. However, the inlet flow fields of feed oxidizer gases (O_2/CO_2), in all oxy-fuel cases, were reduced in proportion to the volumetric flow rates by fixed ratios: 83%, 77%, and 72% for OF25, OF27, and OF29, respectively with respect to the conventional firing case.

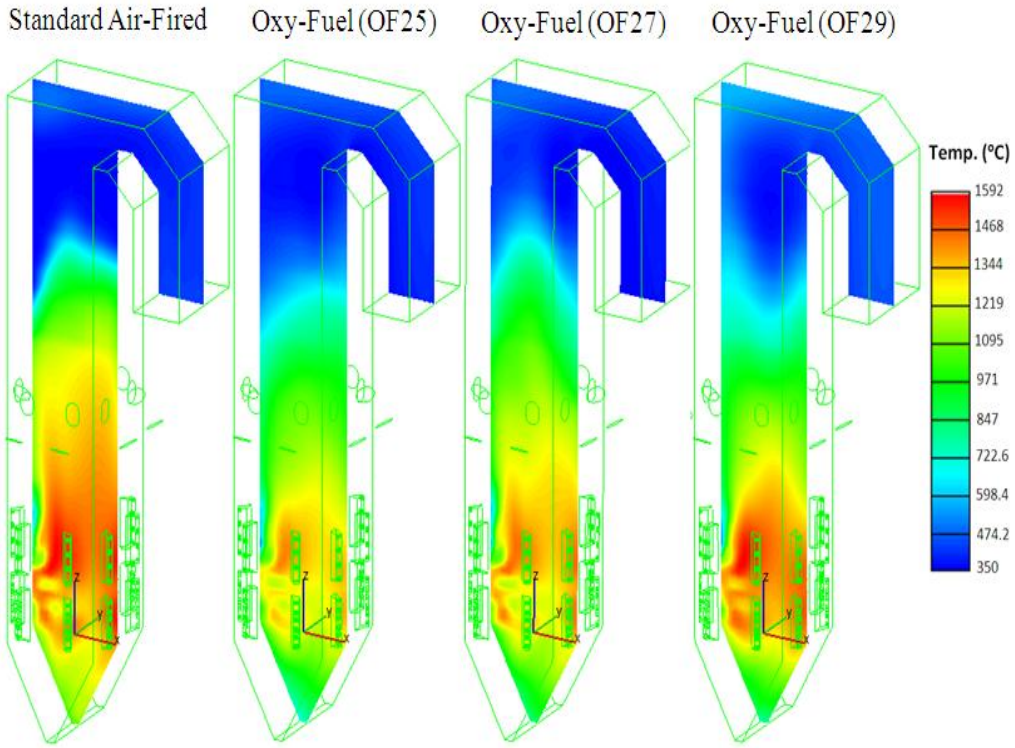

Fig. 2. Distributions of the flue gas temperature (K) along the height of the furnace at the mid cut (X-Z plane) for air-fired, OF25, OF27, and OF29 combustion cases.

Figure 3 presents the average flue gas temperature profiles along the furnace centreline, from bottom of the hopper up to the convective tube banks' location, for all combustion scenarios. As seen in the hopper region (level Z=0 m to level Z=14 m), the gas temperatures are low for all O_2/CO_2 cases compared to that of the conventional firing case. This phenomenon might be due to the availability of oxygen, in this region of the furnace, in the air-fired case. In contrast, no air leakage is considered in all O_2/CO_2 cases, and thus nearly no combustion occurs in the hopper zone. In Fig. 3, two peak gas temperatures exist in the furnace zone. The first peaks appear in the zone close to the main (PC) burners, which considered the fuel-rich mixture region in the furnace. Whilst the second peak values were approximately in the inert burner region, around level Z=28 m. These higher gas temperatures resulted in the reaction between the volatile matters released from the coal and surrounding oxygen, and thus a high amount of heat is generated. After that increase of the gas temperature in the burners region, the value gradually falls due to the heat absorption sinks of the furnace water wall and heat exchanger tubes at the upper zone of the boiler. Also observable in Fig. 3 is that despite similarities in the distributions of gas temperatures, 25% O_2/75% CO_2 mixture case showed low temperature values than other cases, in particular in the furnace zone.

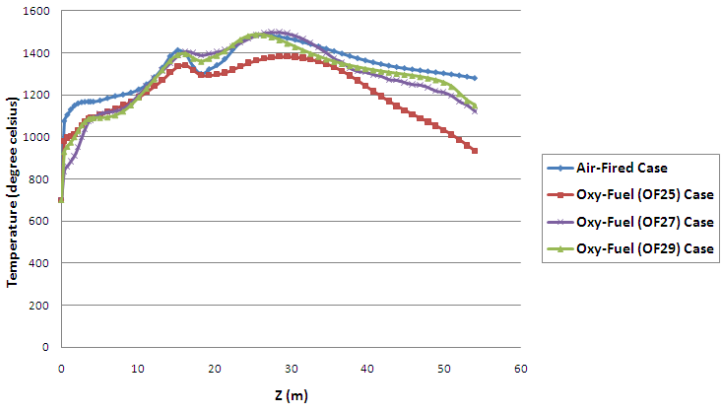

Fig. 3. Profiles of the mean flue gas temperature (K) along the furnace centreline for all combustion scenarios.

3.2. Species concentrations (carbon dioxide)

Figure 4 shows the profiles of carbon dioxide mass fraction (kg/kg) along the furnace centreline (from bottom of the hopper up to the convective tube banks' location) for all cases examined. For all oxy-fuel cases, the values of the CO_2 concentrations were approximately similar along the furnace centreline. In addition, the thermal dissociation mechanism of CO_2 adopted is clearly noticed in the furnace zone (level Z=14 m to level Z=25 m), particularly in the air-fired case. The differences in the CO_2 concentrations between the conventional combustion case and oxy-fuel cases are evident because of adopting the Chalmers' approach in this study. Approximately five times higher CO_2 is achieved for all oxy-fuel combustion scenarios compared to the air-fired case. The concentrations of CO_2 mass fractions at the furnace exit were equal to 18.84, 85.76, 85.01, and 84.18 wt% for the air-fired, OF25, OF27, and OF29, respectively. Due to the higher capability of carbon dioxide to absorb the combustion heat, this elevated CO_2 in the oxy-fuel cases can potentially increase the protection of the furnace wall against the hot flue gases.

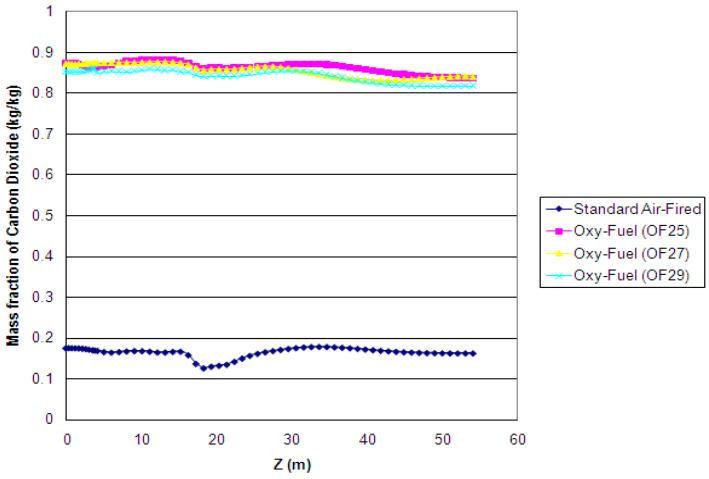

Fig. 4. Profiles of carbon dioxide mass fraction (kg/kg) along the furnace centreline (from bottom of the hopper up to the convective tube banks' location) for all combustion cases examined.

3.3. NO_x emissions

Figure 5 presents the distributions of nitric oxides (NO_x) ppm at the UMB plane and at the UIB plane for all combustion cases. In Fig. 5, there is a significant decrease in NO_x formation in all oxy-fuel combustion scenarios compared to the standard firing case. This reduction can be attributed into two main reasons: firstly due to decrease in the gas temperatures in the combustion zone; secondly due to the suppression of the thermal NO mechanism. It can be seen in Fig. 5 for oxy-fuel combustion cases, the conversion rates of coal-N to NO_x are somewhat increased with oxygen concentrations in the feed oxidizer gases. The concentrations were 375, 180, 240, and 280 ppm, under dry conditions, for the standard (air-fired), OF25, OF27, and OF29 cases, respectively.

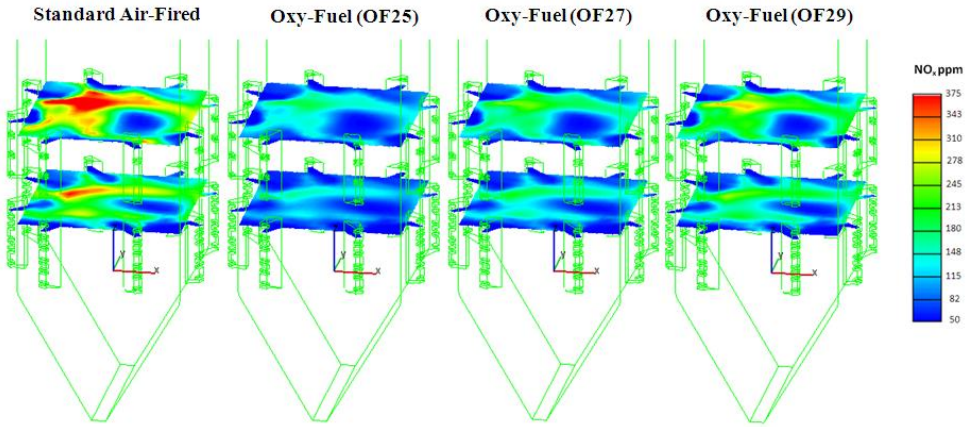

Fig. 5. Distributions of NO_x (ppm) at the UMB plane and at the UIB plane for all cases investigated.

4. Conclusion

In this study, a commercial CFD code, AVL Fire ver.2008.2, has been modified to investigate the Victorian brown coal combustion in a 550 MW tangentially-fired boiler under different combustion media. The obtainable experimental data were used to validate the numerical results under the standard firing condition, a good agreement is achieved. The oxy-fuel combustion approach adopted in a 100 kW facility unit (Chalmers' furnace) was applied to the present large-scale furnace in three oxy-fuel-fired conditions, namely OF25, OF27, and OF29. In the OF25 and OF27 combustion cases, a clear reduction in the gas temperatures was noted compared to the standard firing case. In contrast, OF29 case showed similar gas temperature levels and radiative heat transfer to that of the standard firing case. This is due to augmenting the residence time of coal particles and oxygen concentrations in the gas mixture.

Acknowledgments

This work is carried out with a financial support from the Iraqi Ministry of Higher Education and Scientific Research (www.mohesr.gov.iq) during the scholarship period in Australia.

References

[1] C.-Z. Li, Advances in the Science of Victorian Brown Coal, Elsevier, Oxford, 2004.
[2] E. Kakaras, A. Koumanakos, A. Doukelis, D. Giannakopoulos, I. Vorrias, Oxyfuel boiler design in a lignite-fired power plant, Fuel, 86 (2007) 2144-2150.
[3] T. Wall, Y. Liu, C. Spero, L. Elliott, S. Khare, R. Rathnam, F. Zeenathal, B. Moghtaderi, B. Buhre, C. Sheng, R. Gupta, T. Yamada, K. Makino, J. Yu, An overview on oxyfuel coal combustion--State of the art research and technology development, Chemical Engineering Research and Design, 87 (2009) 1003-1016.
[4] A.H. Al-Abbas, J. Naser, Numerical Study of One Air-Fired and Two Oxy-Fuel Combustion Cases of Propane in a 100 kW Furnace, Energy & Fuels, 26 (2012a) 952-967.
[5] K. Andersson, Characterization of oxy-fuel flames - their composition, temperature and radiation, in, Chalmers University of Technology, Göteborg, 2007.
[6] A.H. Al-Abbas, J. Naser, D. Dodds, CFD modelling of air-fired and oxy-fuel combustion of lignite in a 100 KW furnace, Fuel, 90 (2011) 1778-1795.
[7] A.H. Al-Abbas, J. Naser, Effect of chemical reaction mechanisms and NOx modelling on air-fired and oxy-fuel combustion of lignite in a 100 kW furnace, Energy & Fuels, 26(2012b) 3329-3348.
[8] J.Staples, L. Marshall, Herman Resource Laboratories (HRL) Technology, Mulgrave, Victoria Australia, www.hrl.com.au/, Report No. HLC/2010/105.

Available online at www.sciencedirect.com

SciVerse ScienceDirect

Procedia Engineering 00 (2012) 000–000

Procedia Engineering

www.elsevier.com/locate/procedia

5th BSME International Conference on Thermal Engineering

Influence of Different Alternative Fuels on Particle Emission from a Turbocharged Common-rail Diesel Engine

M. M. Rahman[a], S. Stevanovic[b], R.J. Brown[c], Z. Ristovski*

International Laboratory of Air Quality and Health(ILAQH), Biofuel Engine Research Facilities(BERF)
Queensland University of Technology(QUT), Brisbane, Queensland, Australia-4001

Abstract

Influence of alternative fuels on diesel engine exhaust particle emission was investigated using an ultra-low sulfur diesel fuel as a baseline fuel where two biodiesels (canola & tallow), Fischer–Tropsch and bioethanol were used as alternative fuel. Both the biodiesels coming from canola and tallow feedstocks, as well as F-T were used as 100% to run the engine where up to 40% energy substitution by ethanol was achieved without any sacrifice of engine power output. It was found that up to 30% ethanol substitution reduced both particulate mass (PM) and particle number (PN) emission consistently for all load settings at 2000 rpm, highest 59% reduction in PM and 70% reduction in PN observed at 100% load. As previously suggested the possible mechanism for the observed reduction is the oxidation of particulate matter by OH radicals which are in excess with ethanol fumigation. For 40% ethanol substitution some inconsistency was observed for PM emission at different loads but consistent reduction was found for PN. Condensation of unburned/partially burned hydrocarbons that later condense on existing soot might be responsible for this, as the maximum increase of PM was observed at quarter load where low in cylinder temperature favour to nucleation of unburned hydrocarbons. PM emission was also reduced in case of using 100% FT, and 100% biodiesel and the highest 90% reduction in PM was observed for biodiesel at 100% load with almost no difference between the two biodiesels itself. On the other side a considerable difference was observed between canola and tallow biodiesel in case of PN emission. Canola biodiesel increased PN, due to the presence of the nucleation mode, for almost an order of magnitude for all load and speed settings where no such increase was observed for tallow biodiesel.

Keywords: Alternative fuel; Ethanol fumigation; Biodiesel; Particulate matter; Particle number; Particle size distributions; Diesel engine

Nomenclature

DPM	Diesel particulate matter	B100	100% biodiesel
PM	Particle mass	FT	Fischer–Tropsch(Synthetic diesel)
PN	Particle Number	EXX	% of energy substitution by ethanol fumigation

* Corresponding author. Tel.: +61 7 3138 1129; fax: +61 7 3138 9079.
E-mail address: z.ristovski@qut.edu.au

1. Introduction

Compression Ignition (CI) engine is in the pace of increasing popularity due to its higher thermal efficiency. It powers much of our land and sea transport, provides electrical power, and is used in farming, construction and industrial activities. Despite its significant advantages over Spark Ignition (SI) engines the tail pipe emissions from CI engines, especially particulate matter (PM) and NOx, are still a matter of great concern. Particulate matter emitted by diesel engine affects the Earth's temperature and climate by altering the radiative properties of the atmosphere[1]. All though Particles emitted from diesel engine contribute to the global climate both by direct heating and indirect cooling, the heating effect is dominant. So it is really important for climate change mitigation to reduce the diesel engine particulate matter emissions. Even, short atmospheric lifespan makes black carbon abatement one of the most attractive means to make a significant near-term impact on global warming.

In addition to climate change, chronic exposure of diesel exhaust particles (DEP) may lead to exacerbation of pulmonary diseases such as asthma and bronchitis as well as lung cancer. A few studies[2-4] have also described negative impacts of DEPs on reproductive systems i.e liver functions[3] and brain activity[4]. A recent epidemiological study on underground miners reported an increased risk of lung cancer mortality associated with DPM exposure[5]. By considering the health risk associated with DPM, International Agency for Research on Cancer (IARC), which is part of the World Health Organization (WHO), classified diesel engine exhaust as carcinogenic to humans. This adverse health effect of DPM is related to both the physical properties and chemical composition of particles. Physical properties of DPM that influence respiratory health include particle mass, number and size distribution, surface area and mixing status of particles[2]. As for example deposition of particles in different parts of the lung depends on their size, the smaller the particles the higher the deposition efficiency. Even small particle can penetrate deep into the lung. Furthermore, Smaller the particle, greater the chance of staying longer time in the atmosphere, so smaller particles have a higher probability that they will be inhaled and deposited in the respiratory tract and in the alveolar region. Due to the superiority of particle number over particle mass in determining its health and climate effect, European Union (EU) has already introduced particle number based emission standards for euro-v and euro-vi engines.

Use of after treatment technology is one way of reducing diesel exhaust emissions[6] where alternative fuels can be another potential way[7]. Among different types of alternative fuels biodiesel and synthetic diesel fuel, such as Fischer–Tropsch (F–T), are considered to be the most promising options for CI engines as they can be used in CI engines without engine modification[8]. Ethanol, as an alternative fuel, also has the potential to be used in CI engines[9], but its very low cetane number and poor solubility in diesel, especially at low temperature, is key barrier on its way of implementation. Fumigation of ethanol into the intake manifold of the engine where vaporized ethanol mixes with incoming air can resolve the issue of poor solubility when blending ethanol with diesel. In this study, a six cylinder 6 liter turbocharged heavy duty Cummins diesel engine was used to investigate the effect of afore mentioned alternative fuels on diesel emission with a special emphasis on particle emission.

2. Experimental Methods

PM and NOx emission measurement was performed from the exhaust of a 6 cylinder, turbocharged-after cooled, common rail diesel engine. Specification of the engine has shown in table-1. Engine was soupled to an ECU controlled hydraulic dynamometer for adjusting the engine load and speed. An ultra low sulphur diesel fuel was used as a baseline fuel to run the engine where two biodiesel (canola & tallow), a synthetic diesel F-T (Fischer–Tropsch) and bio ethanol were used as alternative fuel. Both the biodiesels coming from canola and tallow feedstocks, as well as F-T were used as 100% basis to run the engine where up to 40% energy substitution by ethanol was achieved without any sacrifice of engine power output. Energy substitution by ethanol was accomplished by fumigating the ethanol into engine intake air.

Table 1: Engine Specification

Model	Cummins ISBe220 31
Cylinders	6 in-line
Capacity (L)	5.9
Bore × Stroke (mm)	102 × 120
Maximum power (kW/rpm)	162/2500
Maximum torque (Nm/rpm)	820/1500
Compression ratio	17.3
Aspiration	Turbocharged & after cooled
Fuel Injection	Common rail
Emissions certification	Euro III

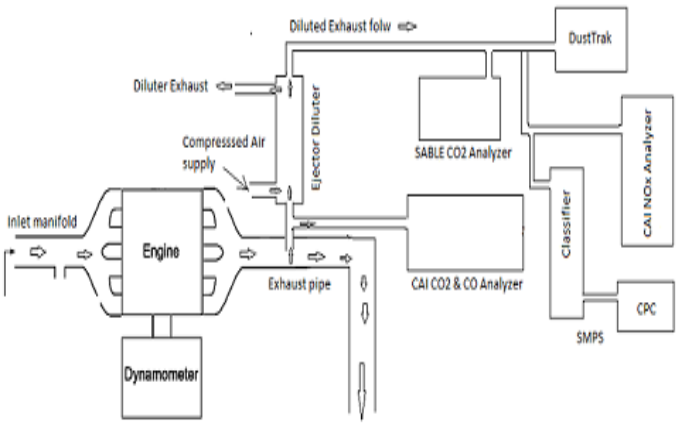

Figure 1: Schematic diagram of experimental set up

Figure-1 displays the experimental setup used to sample exhaust from diesel engine exhaust pipe. An ejector diluter made by Dekati was used to dilute the raw exhaust from the engine exhaust pipe, where raw exhaust is mixed with particle free compressed air. The purpose of the dilution is to bring down the temperature as well as the concentration of gases and PM within the measuring range of the instrument. A HEPA filter was used to provide particle free compressed air for the diluter. Diluted exhaust was then sent to different gaseous and particle measuring instrument for measurement. A CAI 600 series CO_2 analyzer was used to measure the CO_2, and CO concentration directly from the raw exhaust. A second CO_2 meter (SABLE, CA-10) was used to record the CO_2 from the diluted exhaust. Dilution ratio was calculated from two CO_2 measurements by using the following formula.

$$Dilution\ Ratio\,(DR) = \frac{CO_2\ (Raw) - CO_2(Bckground, CAI)}{CO_2\ (Diluted) - CO_2(Bckground, SABLE)}$$

A CAI 600 series CLD NO_x analyzer was used to measure the NO_x and NO_2 from diluted exhaust. $PM_{2.5}$ emissions was measured by a TSI DustTrak(Model 8530). DustTrak readings were converted into a gravimetric measurement by using the tapered element oscillating microbalance to DustTrak correlation for diesel particles published by Jamriska et al[10]. Particle number and size distribution was measured by scanning mobility particle sizer (SMPS) consists of TSI 3080 classifier and TSI 3025 butanol base condensation particle counter (CPC).

3. Results and Discussions

3.1. PM 2.5 emission from different alternative fuels

Figure-2 shows the brake specific PM2.5 emission at engine speed 2000 rpm. For 25% and 100% load, PM reduced consistently with the increase of ethanol percentage and maximum 59% reduction was observed for 30% ethanol substitution at 100% Load. For 40% ethanol substitution PM increased slightly at 100% load which was well below the PM of neat diesel but around 44% increase was observed at 25% load resulted in highest PM emission among all fuels and engine load settings. On the other hand, no such reduction in PM was observed due to ethanol substitution for 50% and & 75% load. The most significant reduction in PM2.5 was achieved when using biodiesel and this trend was consistent regardless of the load and speed settings of the engine. Highest 93% reduction was achieved for 100% canola biodiesel while it was 91% for tallow biodiesel. A considerable reduction in PM is also observed for synthetic diesel which was higher than both of the biodiesels but lower than neat diesel and all ethanol substitutions.

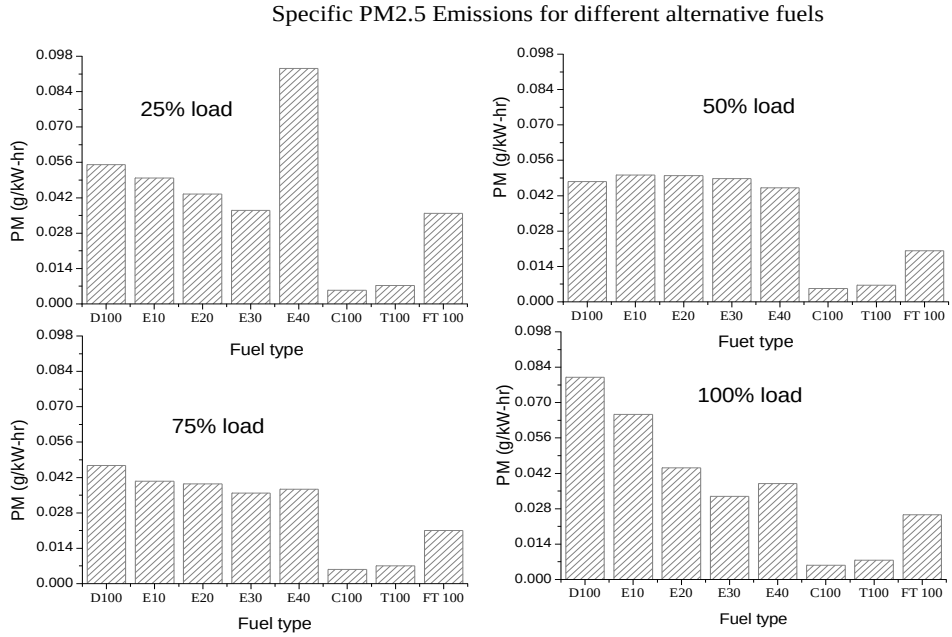

Figure 2: Brake specific PM2.5 emission for different alternative fuels at 2000 rpm engine speed

3.2. Particle number and size distribution form different alternative fuels

The reduction in PM due to alternative fuel is further revealed in particle number and size distribution as shown in figure-3, figure-4(a) and figure-4(b). With the increase of ethanol substitution, brake specific particle number concentration decreased consistently at 25%, 50%, 75% and 100% load, and highest reduction happened for 40% ethanol substitution at 100% load. For 25% load, total particle number concentration at 10% ethanol substitution was higher than neat diesel and 30 nm increase of particle median diameter was found for 40 % ethanol substitution. This increase of particle median diameter indicates why highest PM2.5 emission was observed for 40% ethanol substitution at 25% load. Tallow biodiesel decreased the total particle number concentration with the reduction of 15 nm median diameter. For canola biodiesel, accumulation mode particles reduced but the presence of 20 nm nucleation mode particles are constantly observed during all load and speed settings as shown in figure-4(b) separately. The presence of nucleation mode particle in case of canola biodiesel increased specific particle number emission almost by an order than neat diesel. Particle size distribution for synthetic diesel fuel was found almost similar to that of fossil diesel with slight reduction in total number concentration at 100%, 75% and 50% load, while a small increase in nanoparticle emission was observed at 25% load.

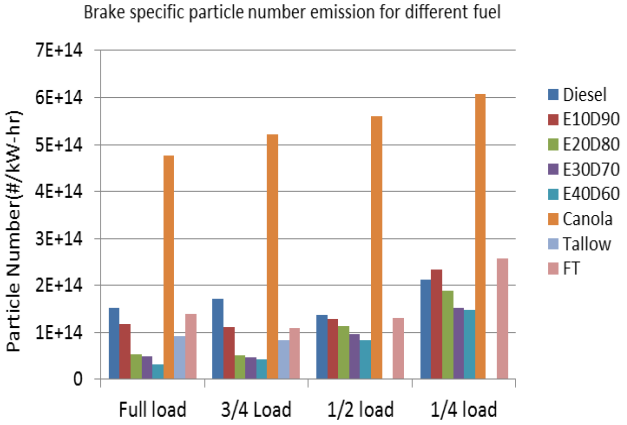

Figure 3: Brake specific particle number emission for different alternative fuels at 2000 rpm engine speed.

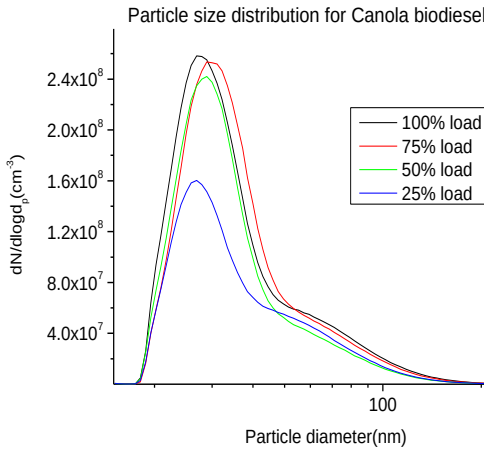

Figure 4(b): Particle size distribution for canola biodiesel

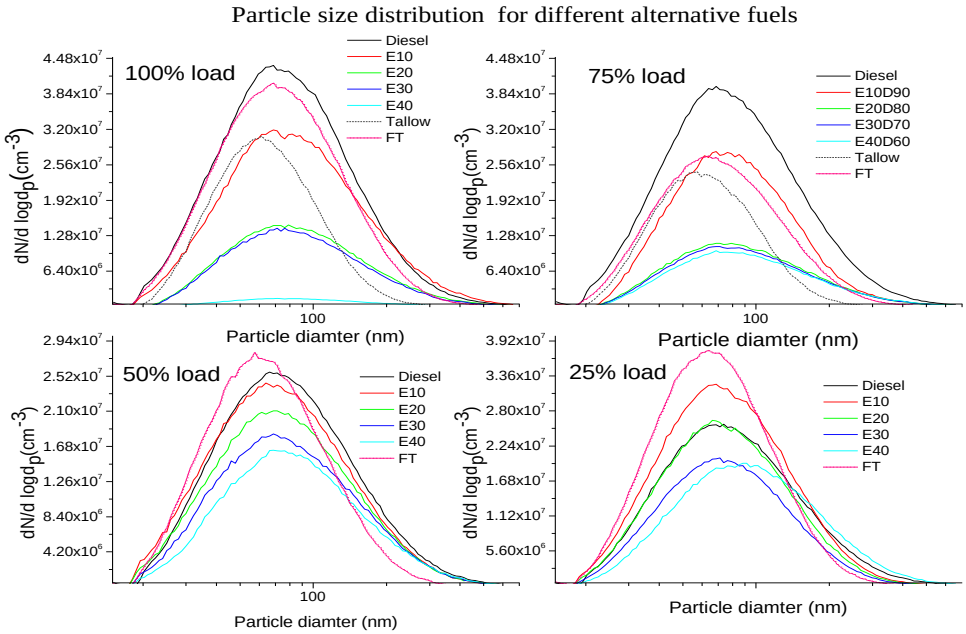

Figure 4(a): Particle size distribution for different alternative fuels at 2000 rpm engine speed

The presence of fuel bound oxygen in the ethanol was the driving force behind the reduction of both PM and PN due to ethanol substitution. As previously suggested[11] the possible mechanism for the observed reduction is the oxidation of particulate matter by OH radicals which are in excess with ethanol fumigation. Higher ratio of hydrogen to carbon, higher volatility and absence of aromatics and sulphur in ethanol also favoured suppression of in cylinder PM formation. For 40% ethanol substitution some inconsistency was observed for PM emission at different loads but consistent reduction was found for PN. Condensation of unburned/partially burned hydrocarbons that later condense on existing soot might be responsible for this, as the maximum increase of PM was observed at quarter load where low in cylinder temperature is favourable to nucleation of unburned hydrocarbons. For biodiesels, the massive reduction of PM is also due to its oxygen content and higher cetane value. Difference in specific PN emission between two biodiesels might be due to its chemical composition. Canola biodiesel composed of 30% more double unsaturated compound than tallow biodiesel which might favour formation of nucleation mode particles. In addition viscosity of and density of canola biodiesel also found higher than tallow biodiesel which may also favour smaller particle emission. For FT, the absence of aromatics and sulphur supposed to be responsible for low PM emission as they act as precursor for PM.

3.3. Effect of different alternative fuels on specific NOx emission

Figure-5 shows the brake specific NOx emission for different alternative fuels at 2000 rpm. For ethanol fumigation, Nox emission decreased from the reference diesel fuel with the increase of energy substitution by ethanol for each engine load. Highest 25% Nox reduction was observed for 40% energy substitution (E40) by ethanol at 100% load where it was 14%, 12% and 9% for E30, E20 and E10 respectively. Same trend was found in NOx reduction at other engine load as well. Low heating value of ethanol which causes low in cylinder temperature is mainly responsible for reduced NOx emission for ethanol fumigation On the other hand brake specific NOx emission increased for both biodiesels and synthetic diesel. Between two biodiesels tallow biodiesel produced less NOx than canola biodiesel. NOx emission increased 25%, 11%, 47% and 32% at 25%, 50%, 75% and 100% load respectively for canola biodiesel while it was 4%, 6%, 5% and 11% for tallow biodiesel at the same engine load. Higher degree of unsaturation of canola biodiesel is found to be responsible for higher NOx emission by canola biodiesel than tallow biodiesel, similar result is also reported by[12] Finally, NOx emission from synthetic diesel was also found higher than neat diesel but lower than biodiesel.

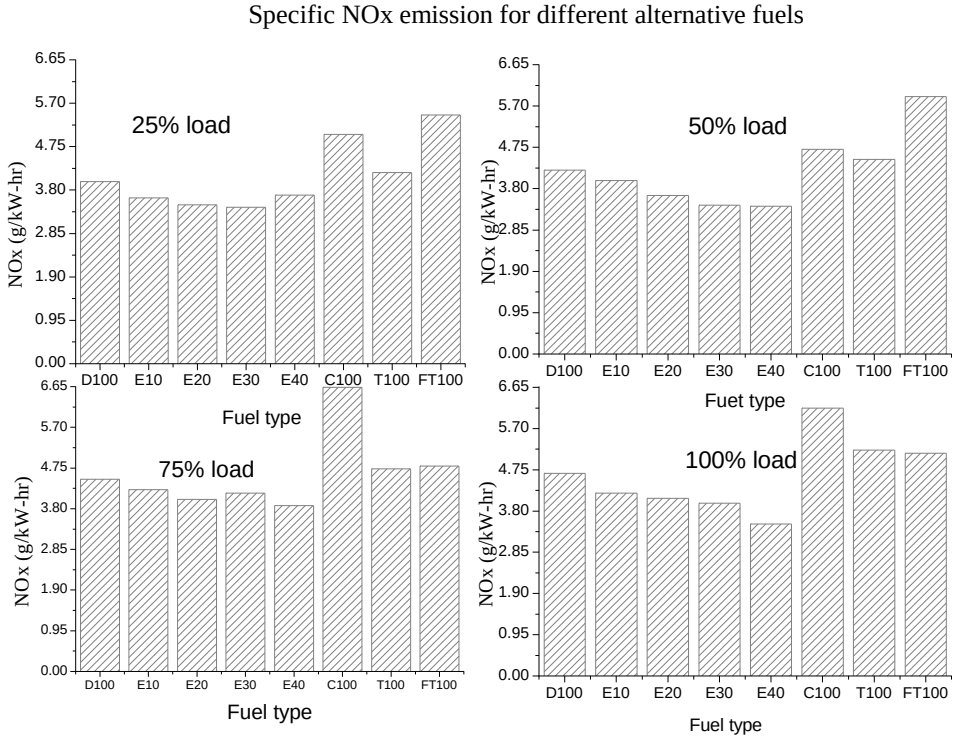

Figure 5: Brake specific NOx emission for different alternative fuels at 2000 rpm engine speed

4. Conclusions

- In general energy substitution by ethanol fumigation reduced both PM and PN emission compared to petroleum diesel and maximum 59% reduction in PM and 70% reduction in PN observed at full load . Up to 30% energy substitution by ethanol reduced PM and PN consistently regardless of the engine operating condition where some inconsistency was observed for 40% ethanol substitution due to nucleation at some engine operating speeds and loads. Ethanol substitution also reduced NOx emission.
- Biodiesel reduced PM most among all used alternative fuels and the highest 93% reduction was observed at full load. But canola biodiesel increased PN almost an order than diesel due to the presence of nucleation mode particles where tallow biodiesel reduced PN significantly with 15 nm reduction in particle median diameter.
- PM emission for FT was found lower than neat diesel and all ethanol fumigation but higher than biodiesel, where no considerable difference was observed for PN.
- Both biodiesel and FT increased specific NOx emission. Between two biodiesels NOx emission from canola was higher than tallow due to the presence of more unsaturated compound in canola biodiesel which may cause prolonged premixed combustion favorable for thermal NOx production.

5. Acknowledgement

Author wishes to thank all the technicians in the Biofuel Engine Research Facilities (BERF) in Queensland University of Technology (QUT) for their valuable contribution during experimental measurement.

6. References

1. Jacobson MZ: **Strong radiative heating due to the mixing state of black carbon in atmospheric aerosols.** *Nature* 2001, **409:**695-697.
2. Ristovski ZD, Miljevic B, Surawski NC, Morawska L, Fong KM, Goh F, Yang IA: **Respiratory health effects of diesel particulate matter.** *Respirology* 2012, **17:**201-212.
3. Folkmann JK, Risom L, Hansen CS, Loft S, Moller P: **Oxidatively damaged DNA and inflammation in the liver of dyslipidemic ApoE-/- mice exposed to diesel exhaust particles.** *Toxicology* 2007, **1:**134-144.
4. Cruts B, van Etten L, Tornqvist H, Blomberg A, Sandstrom T, Mills NL, Borm PJA: **Exposure to diesel exhaust induces changes in EEG in human volunteers.** *Particle and Fibre Toxicology* 2008, **5:**4.
5. Attfield MD, Schleiff PL, Lubin JH, Blair A, Stewart PA, Vermeulen R, Coble JB, Silverman DT: **The diesel exhaust in miners study: A cohort mortality study with emphasis on lung cancer.** *Journal of the National Cancer Institute* 2012, **104:**869-883.
6. Herner JD, Hu SH, Robertson WH, Huai T, Chang MCO, Rieger P, Ayala A: **Effect of Advanced Aftertreatment for PM and NO(x) Reduction on Heavy-Duty Diesel Engine Ultrafine Particle Emissions.** *Environmental science & technology* 2011, **45:**2413-2419.
7. Lapuerta M, Armas O, Hernández JJ, Tsolakis A: **Potential for reducing emissions in a diesel engine by fuelling with conventional biodiesel and Fischer-Tropsch diesel.** *Fuel* 2010, **89:**3106-3113.
8. Xue J, Grift TE, Hansen AC: **Effect of biodiesel on engine performances and emissions.** *Renewable and Sustainable Energy Reviews* 2011, **15:**1098-1116.
9. Surawski NC, Ristovski ZD, Brown RJ, Situ R: **Gaseous and particle emissions from an ethanol fumigated compression ignition engine.** *Energy Conversion and Management* 2012, **54:**145-151.
10. Jamriska M, Morawska L, Thomas S, He C: **Diesel bus emissions measured in a tunnel study.** *Environ Sci Technol* 2004, **38:**6701–6709.
11. Surawski NC, Miljevic B, Roberts BA, Modini RL, Situ R, Brown RJ, Bottle SE, Ristovski ZD: **Particle emissions, volatility, and toxicity from an ethanol fumigated compression ignition engine.** *Environmental Science and Technology* 2010, **44:**229-235.
12. Varatharajan K, Cheralathan M: **Influence of fuel properties and composition on NOx emissions from biodiesel powered diesel engines: A review.** *Renewable and Sustainable Energy Reviews* 2012, **16:**3702-3710.

Available online at www.sciencedirect.com

SciVerse ScienceDirect

Procedia Engineering 00 (2012) 000–000

Procedia Engineering

www.elsevier.com/locate/procedia

5th BSME International Conference on Thermal Engineering

Computational Fluid Dynamic Modelling of a 550 MW Tangentially-Fired Furnace Under Different Operating Conditions

Audai Hussein Al-Abbas[a,b] and Jamal Naser[a,*]

[a]*Faculty of Engineering & Industrial Sciences, Swinburne University of Technology, Hawthorn 3122, AUSTRALIA*

[b]*Technical College of Al-Musaib , Foundation of Technical Education, Babylon, IRAQ*

Abstract

In the present paper, a computational fluid dynamics (CFD) modelling study was performed for the combustion of the brown coal in a large-scale tangentially-fired furnace (550 MW) under different operating conditions. The AVL Fire CFD code has been used to model the furnace. The mathematical models of coal combustion with the appropriate kinetic parameters were written and added to the code as user defined functions. It consists of pulverised coal (PC) devolatilization, char burnout, heat and mass transfer, and nitric oxide formation. The simulation of the PC combustion was carried out using multi-step reaction chemistry schemes. The level of confidence of this numerical model was based on the previous validations of the lignite combustion in a lab-scale furnace, as well as the validation parameters of the present furnace at the standard existing conditions in terms of temperature values and species concentrations. Performance of the boiler under different operating conditions was investigated, from which the effects of air and coal mass flow rates were considered at full load with different operating schemes of coal mills (out-of-service operations). The validated model was used to perform the following investigation parameters: furnace gas temperatures, species concentrations (CO and CO_2), and velocity distributions. This study provides good information to optimize the operations of the utility tangentially-fired boiler with less emissions production.

Keywords: Coal combustion, Victorian brown coal, Emissions, CFD.

1. Introduction

In the state of Victoria in Australia, there is one of the largest basins of brown coal over the world. This vast reserve of brown coal will lead to continuing the low-cost of electricity in the foreseeable future. It is, however, a competitive resource of energy amongst the other sources of fossil fuel and renewable energies. On the other hand, it has a major contribution to the greenhouse gases (GHG) emissions and global warming (Dodds et al., 2011).

In order to design such efficient, clean, and economical brown coal combustion systems, the understanding of the brown coal reactivity and behaviour under different operating conditions is required. Generally, brown coal has a number of advantages such as abundance, low-cost, high reactivity, and low sulphur content. In despite of these benefits, a high moisture content (about 60-70 wt %) is the major disadvantage of brown coal. However, in the existing pulverized brown coal (PC) tangentially-fired boiler, a large amount of the hot exit flue gas, typically 50% of the total flue gas generated, is reused to dry the brown coal within the mill-duct system. During that drying process by the hot gas off-takes (HGOTs), a large amount of water vapour is reproduced as well. In order to avoid any flame stability problems inside the combustion chamber, due to that evaporated steam, a fuel-rich mixture (mainly pulverized coal) is passed through the main burner ducts. Whilst a fuel-lean mixture, including water vapour, inert gases, and remaining of PC, is delivered to the inert burner ducts (upper burners). This distribution of the PC and inert gases into the firing system is favorable, particularly in this type of combustion technology (Ahmed and Naser, 2011).

Computational fluid dynamics (CFD) modelling studies can comprehensively provide a wide range of information for the design of furnace and burner that can reduce the cost of time-consuming experimental investigations. The CFD has the ability to predict well the flame structure, gas temperatures distributions, chemical species concentrations, radiative heat transfer etc., under different combustion conditions. The work programme covered by this paper achieves the development and validation of the computational tool applied to the combustion system which indicates the practical relevance and the long term viability for such a tool.

Currently, few numerical works on full scale boilers have been conducted. Therefore, the objective of this study is to simulate the brown coal combustion in a large-scale tangentially-fired furnace under several operating conditions. A computational fluid dynamics (CFD) code, AVL Fire version 2008.2, was used to model and analyze ten different combustion environments. The investigated combustion cases were dependent on the scenarios of change in the mass flow rates and distribution ratios for the PC and air, as an oxidant. In addition, the operation schemes of turned off (out-of service) burners were also examined under full load operation. The species concentrations (O_2, CO_2, CO, H_2O, and H_2), furnace gas temperature distributions, and velocity fields obtained for all combustion cases were compared.

2. Boiler description and operating conditions

The mesh generation with the geometric description of the CFD model for the boiler, unit 1 at Loy Yang A, is shown in Figure 1a. Under maximum continuous rating (MCR) of operating conditions, the unit produces 430 kg/s of steam flow through the main steam piping at 16.8 MPa and 540 ^{o}C. The computational domain illustrated in Figure 1 was extended from the furnace hopper up to the top of the tower, passing through the transition of round duct to before the bifurcation at the inlet to the air heaters. In this CFD model, the geometric dimensions of the simulated boiler were 98.84 m (height), 17.82 m (width), and 17.82 m (depth).

The tangentially-fired furnace used in this study consists of eight mill-duct systems, two on each side face of the furnace. For each mill-duct system, there are six separate burners, including three inert burners and three main burners, as well as a hot gas off-take (HGOT) that uses to dry the brown coal. The distribution of PC at both the burner mouths was accompanied by the inert flue gas and water vapour from the drying process in the mill. Around 82% of the PC and 34% of the gases is delivered to the main burner (PC burner) and the remaining 18% of pulverized coal and 66% of the gases is transported to the inert burner (vapour burner).

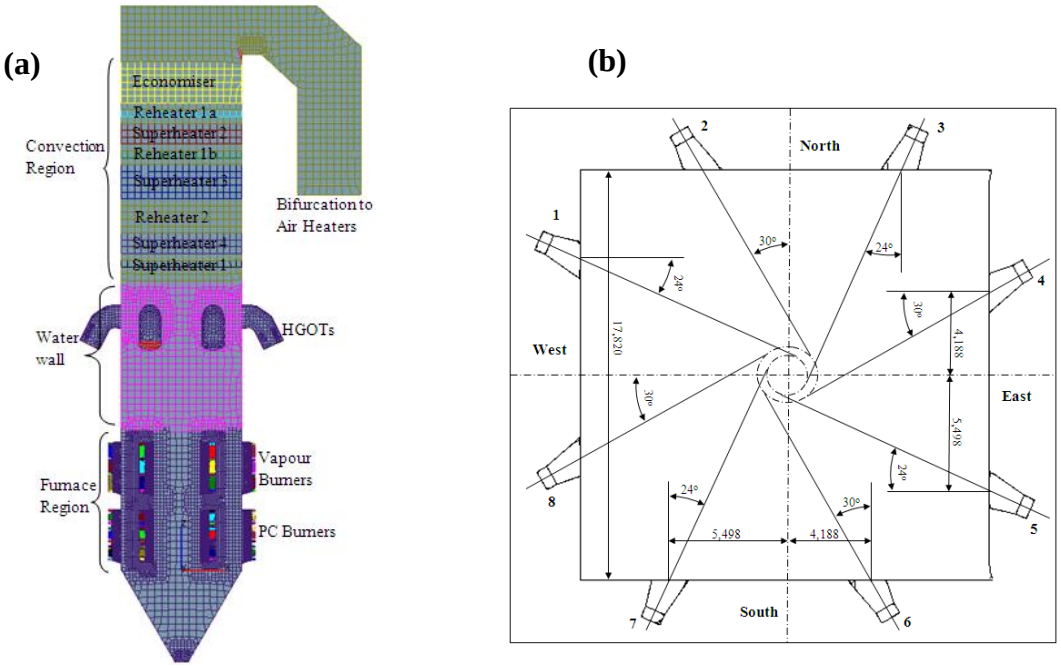

Fig. 1. (a) CFD geometrical model of unit 1 at Loy Yang A power plant; (b) The schematic representation of the burners' configurations.

Regarding the operating conditions, the operating schemes of turned off (out of service) burners under full load operation are summarized in Table 1. Around 81.3 kg/s of PC and 422.8 kg/s of gas mixture are passed through both the inert and

main burners of the furnace at different flow distribution ratios under the standard operating conditions (as specified in cases 1—6).

Table 1: Operation scheme of turned off (out of service) burners under full load operation and 20 % lower and 20 % higher than the standard operating conditions.

Combustion case no.	1	2	3	4	5	6	7	8	9	10
Burners turned off	3, 4, and 7	3,4, and 6	3, 4, and 8	1, 3, and 4	3, 5, and 7	2, 4, and 6	3, 4, and 7	3, 5, and 7	3, 4, and 7	3, 5, and 7
Combustion scenarios	Standard operating conditions						Lower by 20%		Higher by 20%	

Table 2 shows the mass flow rates (kg/s) of air for the standard case and investigated combustion cases at each secondary air duct. The overall number of vapour and PC burners was 48, while 18 of the total burners were practically out of service. Regarding the burner configuration, each burner ports 1, 3, 5, and 7 were inclined by 24^{o} with the perpendicular line to the furnace face, while each the remaining burner ports 2, 4, 6, and 8 were inclined by 30^{o}. This configuration of the burner set up was mostly used in this type of tangentially-fired furnace in order to improve flame stability inside the furnace, as schematically plotted in Figure 1b.

Table 2: The mass flow rates (kg/s) of air for the standard case and investigated combustion scenarios at each secondary air duct.

Secondary air duct	Distribution ratio (%)	Air Standard	20% Lower	20% Higher
		Mass flow (kg/s)	Mass flow (kg/s)	Mass flow (kg/s)
Upper inert	5.0%	6.89	5.51	8.27
Upper intermediate inert	5.0%	6.89	5.51	8.27
Lower intermediate inert	5.0%	6.89	5.51	8.27
Lower inert	5.0%	6.89	5.51	8.27
Upper main	20.0%	27.55	22.04	33.07
Upper core	6.67%	9.19	7.35	11.03
Intermediate main	20.0%	27.55	22.04	33.07
Intermediate core	6.67%	9.19	7.35	11.03
Lower main	20.0%	27.55	22.04	33.07
Lower core	6.67%	9.19	7.35	11.03
Total		137.78	110.21	165.38

3. Mathematical models and numerical description

Numerical simulation of pulverized Victorian brown coal under the air-fired and oxy-fuel combustion conditions were carried out by a computational fluid dynamics (CFD) code. Appropriate subroutines were integrated and incorporated into the CFD code to account for devolatilization and char burnout, convection and radiation heat transfer between particles and gases, and thermal and fuel NO formation/destruction. The mathematical models and results of NO_x formation are not shown in this paper. The devolatilized hydrocarbon fuel is considered as a methane equivalent, as there are no crucial differences between methane and the gaseous product attained from devolatilization of coal utilized. For precise calculations, the multi-step reaction mechanisms are carried out in this simulation study. The main reactions of the coal combustion model can be, however, expressed in three homogeneous and three heterogeneous chemical reactions, as follows: The chemical equations for devolatilized methane burned with oxygen, in a three-step reaction, are given in below:

$$CH_4 + O_2 \longrightarrow CO + H_2 + H_2O + \text{heat} \quad (1)$$

$$CO + H_2O \rightleftharpoons CO_2 + H_2 \quad (2)$$

$O_2 + 2H_2 \rightleftharpoons 2H_2O$ (3)

While the chemical equations for char burned with oxygen, carbon dioxide, and water vapour are written as follows:

$C_{char} + 1/2O_2 \longrightarrow CO + heat$ (4)

$C_{char} + CO_2 \longrightarrow 2CO$ (5)

$C_{char} + H_2O \longrightarrow CO + H_2$ (6)

For the gas phase flow, non-steady state Eulerian partial differential equations (PDEs) were solved for mass, momentum, enthalpy, a number of species mass fractions, and turbulent fields. Turbulence is modelled using the standard k - ε turbulent model, which has been demonstrated a sufficient accuracy in the turbulent flow calculation, particularly in the near-burner region of previous simulation study (Al-Abbas and Naser, 2012). The eddy-breakup (EBU) turbulent combustion model is used to control the mixing rate of species. A number of mathematical models were coupled through the source terms of PDEs for calculating the coal devolatilization and char combustion models, turbulence, coal particle temperatures and trajectories, and the heat transfer models.

The coal combustion has been modelled, in this study, by using two main complex reaction processes. Firstly, the first order reaction model of Badzioch and Hawksley, 1970 is applied to calculate the rate of production of the volatile released. The pre-exponential factor and activation factor of the Arrhenius form are $0.2 * 10^5$ s^{-1} and 5941 $J.kmol^{-1}.K^{-1}$, respectively, taking from the work of Anthony et al., 1975. Secondly; the char oxidation rate is modelled by a global diffusion control power-law, which was proposed by Field et al., 1967. In this heterogeneous reaction, the oxidation rate of the char is governed by the diffusion of bulk oxygen partial pressure to the particle's external surface. The pre-exponential factor and activation factor of this model are equal to 497 ($kg . m^{-2}. s^{-1}. (N.m^{-2})^{-1}$) and 8540 ($J\ kmol^{-1}.K^{-1}$), respectively. Regarding the heat transfer models, the discrete transfer radiation method (DTRM) has been used because of its ability for a better prediction in participating media, especially in furnaces.

4. Results and discussion

4.1 Temperature distribution

Figure 2 presents the effects of different operating conditions on the flame shape in the combustion zone at the 1650K iso-surfaces for all combustion cases examined. The effects of different turned off burners operations under full load are presented in panels (a)-(f), while in panels (g)-(j) the effects of mass flow rates and distribution ratios for the brown coal particles and mill gases are investigated. That was done by using the validated CFD model (Al-Abbas et al., 2012) under two different combustion scenarios: 20 % lower (cases 7 and 8) and 20 % higher (cases 9 and 10) than the standard combustion case, as shown in Tables 1 and 2. This iso-surface temperature can clearly show the flame distributions in the furnace and determines as a result the boiler performance at different combustion conditions. The operation scheme of the combustion cases used in this study was basically dependent on the inclined angles of each burner ports, as schematically plotted in Fig. 1b. However, this strategy of testing is used to improve the turbulent mixing of PC with the feed oxidizer gases in the tangentially-fired furnace which essentially dependents on the location of the central vortex in this type of furnaces. This improvement on the combustion conditions can bring several benefits to the combustion characteristics and reduces the fouling and slagging problems on the surfaces of the heat exchanges. Regarding the cases investigated under full load operation, it can be seen that the flame temperature distributions of cases 2 and 5 showed a clear tendency toward the out-of-service burners. This feature might be caused due to the movement of the central vortex toward the turned off burners. A good distribution of the flame was achieved in cases 3 and 6 because of turning off the opposite burners. In panels (g) and (h), the flames are concentrated in the near-burner region due to the reduction in the mass flow rates of combustibles. Whereas the combustion flames are uniformly distributed in the burner and water wall regions for both cases 9 and 10 due to the higher aerodynamic effect of the PC and air adopted in these two cases.

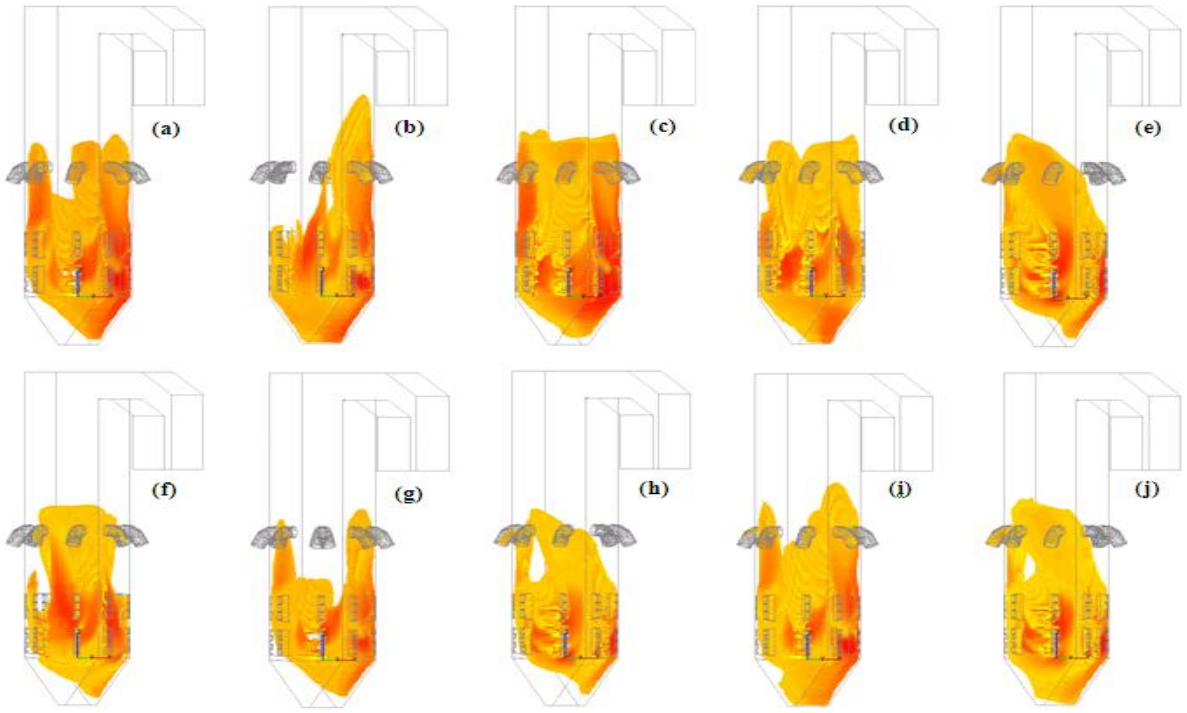

Fig. 2. Iso-surfaces of the combustion flames at 1650K: (a) case 1, (b) case 2, (c) case 3, (d) case 4, (e) case 5, (f) case 6, (g) case 7, (h) case 8, ((i) case 9, (j) case 10.

4.2 Velocity distribution

Figure 3 presents the cross-section cuts of the gas velocity vector on the upper intermediate inert of the secondary air duct for the combustion cases (cases 1-6 as specified in Table 1) that work under full load operation. Connecting to Fig. 2, cases 3 and 6 showed a good flow field distribution in the furnace. In these two cases, the tangential distributions of the gas velocity vectors (central vortexes) were approximately close to the central zone of the furnace compared to the other combustion cases. As a result, this good tangential circulation of the gases led to improve the flame distribution, as seen in Fig. 2. In contrast, the central vortexes in cases 2 and 5 were away from the central position of the furnace and skew toward the furnace wall.

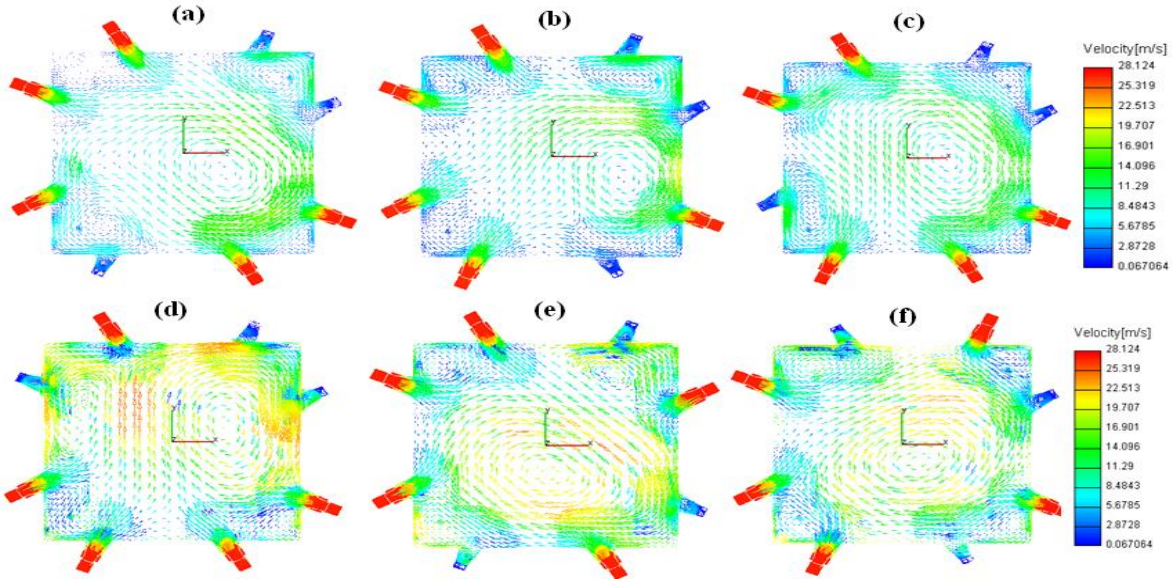

Fig. 3. Gas velocity vector on the upper intermediate inert of the secondary air duct for six combustion cases: (a) case 1, (b) case 2, (c) case 3, (d) case 4, (e) case 5, (f) case 6.

4.3 Species concentrations

Figure 4 a and b presents the distributions of mass fraction of CO_2 and CO respectively along the central line (X and Y = 0.0) of the furnace in the region of combustion zone (burner region) for different combustion cases: 2, 3, 5, 6, 9, and 10. Both figures show that there are two peak values for all combustion cases examined. The maximum values were firstly close to the main burners (PC burners), while the second max. values were in the inert burner region. These two values were resulted due to the availability of the high O_2 concentrations in these regions. In the case 6, the concentrations of CO_2 and CO were lower than those of the other combustion cases. As mentioned earlier, this improvement might be caused due to the good mixing condition adopted in this case.

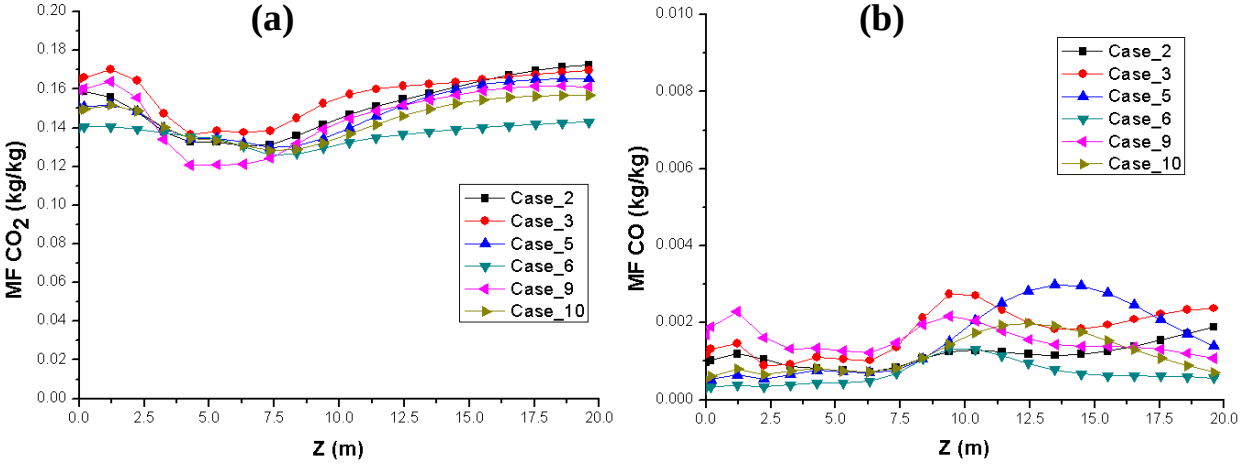

Fig. 4. (a) Mass fraction (MF) of carbon dioxide for combustion cases (2, 3, 5, 6, 9, and 10) along the central line of the furnace in the burner regions; (b) Mass fraction of carbon monoxide for combustion cases (2, 3, 5, 6, 9, and 10) along the central line of the furnace in the burner regions.

5. Conclusion

A CFD model of a 550 MW tangentially-fired furnace at Loy Yang A power plant has been developed. The validated model was used to investigate the combustion characteristics and boiler performance under different firing conditions. The combustion scenarios of this work were based on the effect of the mass flow rates and distribution ratios for the PC and air in the combustion zone. Ten different combustion cases were investigated. The first six combustion cases were based on the change of the out-of-service burners under full load operation, while the rest cases were carried out at 20 % lower and 20 % higher than the standard operating conditions, as specified in Table 1. Temperature distributions, velocity distributions, and species concentrations are compared for all cases examined. The numerical results showed that both the cases 3 and 6 provide good flow field distributions and resulted in an improvement in the flame distribution in the furnace and water wall regions. A slight reduction in the CO_2 and CO concentrations was observed in the case 6 compared to the other combustion cases. This work may lead to optimize the operating conditions of the commercial tangentially-fired furnaces.

Acknowledgments

The financial support provided by the Iraqi Ministry of Higher Education and Scientific Research is gratefully appreciated during the scholarship period (2009-2012) in Australia.

References

[1] D. Dodds, J. Naser, J. Staples, C. Black, L. Marshall, V. Nightingale, Experimental and numerical study of the pulverised-fuel distribution in the mill-duct system of the Loy Yang B lignite fuelled power station, Powder Technology, 207 (2011) 257-269.

[2] S. Ahmed, J. Naser, Numerical investigation to assess the possibility of utilizing a new type of mechanically thermally dewatered (MTE) coal in existing tangentially-fired furnaces, Heat and Mass Transfer/Waerme- und Stoffuebertragung, 47 (2011) 457-469.

[3] A.H. Al-Abbas, J. Naser, Effect of chemical reaction mechanisms and NOx modelling on air-fired and oxy-fuel combustion of lignite in a 100 kW furnace, Energy & Fuels, (2012), DOI: 10.1021/ef300403a

[4] S. Badzioch, P.G.W. Hawksley, Kinetics of thermal decomposition of pulverized coal particles, Industrial and Engineering Chemistry: Process Design and Development, 9 (1970) 521-530.

[5] D.B. Anthony, J.B. Howard, H.C. Hottel, H.P. Meissner, Rapid devolatilization of pulverized coal, Symposium (International) on Combustion, 15 (1975) 1303-1317.

[6] D.W.G. M.A. Field, B.B. Morgan and P.G.W. Hawksley, Combustion of pulverized coal. Leatherhead: The British coal utilization research association, (1967) 186–210.

[7] A.H. Al-Abbas, J. Naser, D. Dodds, CFD modelling of air-fired and oxy-fuel combustion in a large-scale furnace at Loy Yang A brown coal power station, Fuel, (2012), DOI: 10.1016/j.fuel.2012.06.028.

Available online at www.sciencedirect.com

SciVerse ScienceDirect

Procedia Engineering 00 (2012) 000–000

Procedia Engineering

www.elsevier.com/locate/procedia

5th BSME International Conference on Thermal Engineering

Impact of Alternative Fuels on the Cement Manufacturing Plant Performance: An overview

Azad Rahman[a,*], M.G. Rasul[a], M.M.K. Khan[a], S. Sharma[a]

[a]*Central Queensland University*
School of Engineering and Built Environment
Rockhampton, Queensland 4702, Australia

Abstract

Cement manufacturing is a high energy consuming and heavy polluting process. To reduce the energy and environmental costs cement producers are currently using a blend of alternative fuels with conventional fossil fuels. Alkaline environment, high temperature and long processing time allow cement kiln to burn a wide range of alternative fuels including waste and hazardous materials. This paper summarizes and reviews literatures on the usage of different types of alternative fuel and their impacts on the plant performance. The past research suggests that the maximum benefit can be derived by using an appropriate blend of different types of alternative fuels together with fossil fuels. However, the studies on quantification of appropriate mixing ratio of different alternative fuels to increase the plant performance are scant. Further study is required to determine the correct blending ratios. This literature review is focused on the relationship between performance and blending of different alternative fuels used by leading cement manufacturing groups.

Keywords: Cement; Alternative fuel; Plant performance; Energy efficiency

1. Introduction

The production of cement consumes large quantities of raw materials and energy (thermal and electricity). This process requires approximately 3.2 to 6.3 GJ of energy and 1.7 tons of raw materials (mainly limestone) per ton of clinker produced [1, 2]. Being an energy intensive industry, thermal energy used in cement industry accounts for about 20–25% of the production cost [3]. The typical electrical energy consumption of a modern cement plant is about 110–120kWh per ton of cement. In the manufacturing process thermal energy is used mainly during the burning process, while maximum share of electrical energy is used for cement grinding [3].

Generally fossil fuels such as coal, petroleum coke (petcoke) and natural gas provide the thermal energy required for cement industry. Usage of alternative fuel (AF) becomes more popular to the cement manufacturer due to increasing fossil fuel prices, limited fossil fuel resources and environmental concerns. AF cover all non-fossil fuels and waste from other industries including tire-derived fuels, biomass residues, sewage sludge and different commercial wastes [4].

The rotary kiln used in cement manufacturing is able to burn a wide range of materials due to the long exposure time at high temperatures, intrinsic ability of clinker to absorb and lock contaminants into the clinker and the alkalinity of the kiln environment. Materials like waste oils, plastics, waste tires and sewage sludge are often proposed as alternative fuels for the

* Corresponding author. Tel.: +61 422 438 437;
E-mail address: a.rahman2@cqu.edu.au

cement industry. Meat and bone meal are also considered now as alternative fuel [5]. Biomass waste and spent pot linings produced in aluminum smelters [6] are recently identified as potential alternative fuels for cement industry.

Alternative fuels utilization in cement industry reduces the production cost and achieves higher thermal energy efficiency thus increase plant performance. The objective of this study is to review the available literature on the performance of cement manufacturing plants using different blends of alternative fuels. There are several key performance indicators to measure the performance of cement manufacturing plant and most of them are related to the thermal efficiency of the plant. This article summarizes the current practices of using alternative fuels in cement industry and attempts to draw a relationship between the usage percentage of AFs and the plant performance. A variety of research journals, conference proceedings, books, industrial sustainability reports and reliable websites are included in this review. A brief discussion has been appended to understand the correlation between the blended AFs and plant performance which might be useful for cement producers and the researchers.

2. Cement manufacturing process

The main process routes for the manufacturing of cement vary with respect to equipment design, method of operation and fuel consumption [7]. Cement manufacturing process basically includes quarry, raw meal preparation, preheating of raw meal, kiln, clinker cooling, grinding, storage and dispatch. Figure 1 shows a basic process flow of cement manufacturing. The basic chemistry of the cement manufacturing process begins with the decomposition of calcium carbonate ($CaCO_3$) at about 900°C to leave calcium oxide (CaO, lime) and liberate CO_2; this process is known as calcination. This is followed by the clinkering process in which the calcium oxide reacts at high temperature (typically 1,400°–1,500° C) with silica, alumina and ferrous oxide to form the silicates, aluminates and ferrites respectively which forms the clinker. This clinker is then ground together with gypsum and other additives to produce cement. Fuels are required to generate thermal energy during the process of calcination in preheater tower and during the clinkerization process in Kiln.

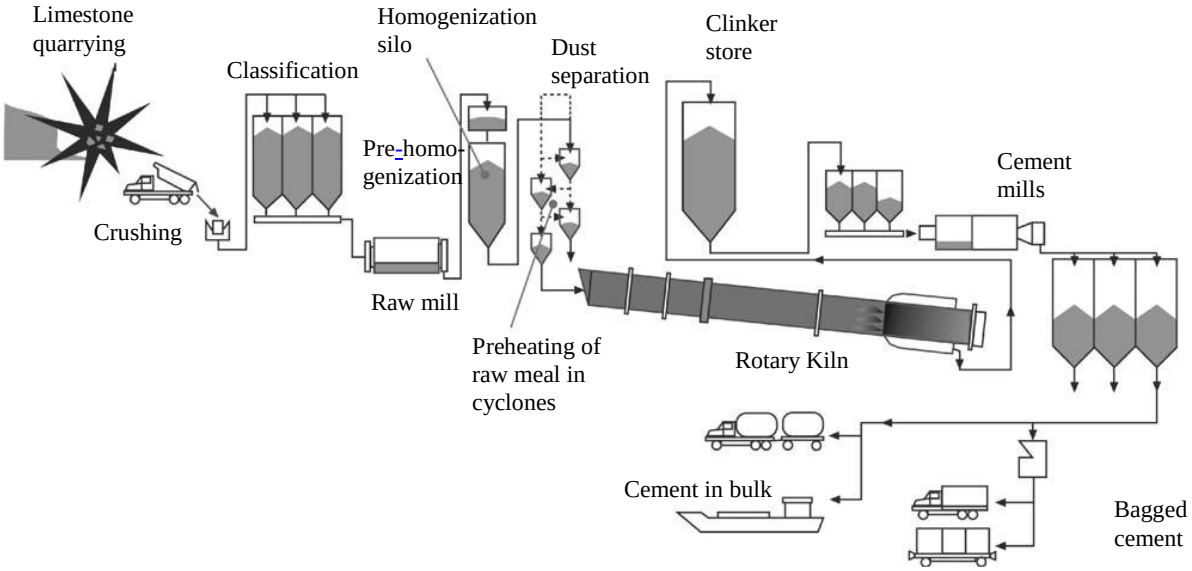

Fig. 1: Cement manufacturing process (Kaantee et al., 2004)

3. Alternative fuels

Most natural and artificial materials contain some energy which can be utilized by the cement industries to meet the requirement of the thermal energy. The use of AF for cement clinker production is of high importance for the cement manufacturers as well as for the environment. Alternative fuel utilization at commercial level in cement industry is as old as about 30 years now. In calciner lines, close to 100% alternative fuel firing at the precalciner was achieved at very early stage [8]. Use of AFs in rotary kilns is still in progress. Reports show that in some kilns up to 100% substitution rates have been achieved [9], while others are facing some limitations regarding environmental, social and product quality issues. In

any case, AF utilization requires adaptation by the cement industry. Modern multi-channel burners and thermograph systems are in use these days which help in controlling the AF feed rate and the flame shape to optimize the burning behavior of the fuels [8].

Generally the cement producers choose the AFs on the basis of price and their availability but these criteria of selecting AFs are not adequate. Composition of the fuel including the energy content, moisture and volatile contents are very important criteria to select an AF. It is also important to consider all forms of AFs such as: liquid, solid, semi-solid, powdered or in the form of big lumps. Different types of AFs require a flexible fuel feeding system, through which AF could be fed either directly into the burning zone at kiln or in the pre-heating system [5].

3.1 Criteria of alternative fuel

There are no set criteria for selecting AFs today. The specific criteria that a material must meet in order to be considered as a fuel is typically set by the individual cement producer according to their own needs. AFs are generally a mixture of various wastes and therefore consistency in their composition cannot be guaranteed. There is a need for ensuring the chemical contents of the AF that meets regulatory requirements for environmental protection. The following properties are expected to be considered as alternative fuels [3, 10]:

- Physical state of the fuel (solid, liquid, gaseous),
- Content of circulating elements (Na, K, Cl, S),
- Toxicity (organic compounds, heavy metals),
- Composition and content of ash and content of volatiles,
- Calorific value — over 14.0 MJ/kg,
- Chlorine content — less than 0.2% and Sulfur content — less than 2.5%,
- PCB content—less than 50 ppm, heavy-metals content — less than 2500ppm [out of which: mercury (Hg) less than 10 ppm, and total cadmium (Cd), thallium (Tl) and mercury (Hg) less than 100 ppm].
- Physical properties (scrap size, density, homogeneity),
- Grinding properties,
- Moisture content,
- Proportioning technology,
- The emissions released,
- The cement quality and its compatibility with the environment must not decrease,
- Alternative fuels must be economically viable.
- Availability

3.2 Advantages and disadvantages

Alternative fuels are generally cheaper than the fossil fuels because most of the AFs are generated from wastes which only require some processing cost. A mixture of fossil fuels and AF in optimal proportion is used to produce the thermal energy required in cement industry. The significant advantage of alternative fuel substitution is the preservation of non-renewable energy sources [11] and the reduction of waste disposal sites. Switching to alternatives fuels presents several challenges as they have different characteristics compared to the conventional fuels. Poor heat distribution, unstable precalciner operation, blockages in the preheater cyclones, build-ups in the kiln riser ducts, higher SO_2, NO_X, and CO emissions, and dusty kilns are some of the major challenges which need to be addressed [12]. One potential constraint on the implementation of alternative fuels is the final clinker composition since the combustion by-products are incorporated into clinker [13]. The substitution of AFs inherently requires initial investment costs associated with adjustment or replacement of burner, establishment of alternative fuel delivery systems, new fuel storage facilities, and fuel distribution systems [14].

3.3. Usage of alternative fuel

The cement manufacturing industry is under increasing pressure from the environmental protection agencies to reduce the emissions. The usage of AFs in cement manufacturing not only helps to reduce the emission but also has significant ecological benefits of conserving non-renewable resources [12]. The substitution rate of fossil fuel by AFs varies from country to country. Most of the European countries are way ahead in the usage percentage of AFs than the rest of the world. The substitution rate of different countries is shown in Table 1 [15]. World's leading cement producers are currently using AFs in a large extent and pursuing to increase it even more by 2020. Conventional fossil fuel substitution rate and the

percentage of different AFs usage by different cement production group are available in their sustainable development reports. Table 2 summarizes the percentage of different wastes which are currently being used as AFs in five selected leading cement producer groups [16-21]. Cemex group are currently using industrial and household waste as a major portion of their AFs. Heidelberg, Holcim and Italcementi group are using range of AFs but Lafarge group is utilizing only four types of AFs. It is also found from Table 2 that most common AF is used tires which are utilized by all the selected manufacturing group up to some extent.

Table 1: Usage of AFs in different countries [15]

Country or Region	% Substitution	Country or Region	% Substitution
Netherlands	83	Czech Republic	24
Switzerland	47.8	EU (prior to expansion in 2004)	12
Austria	46	Japan	10
Norway	35	United States	8
France	34.1	Australia	6
Belgium	30	United Kingdom	6
Germany	42	Denmark	4
Sweden	29	Hungary	3
Luxembourg	25	Finland	3

Table 2: Percentage of different type of waste used as AF

Waste type used as Alternative fuel (%)	Holcim Group (2011)	Cemex Group (2011)	Heidelberg Group (2011)	Italcementi Group (2011)	Lafarge Group (2011)
Waste oil	5		3.7	8.5	22.1
Solvent & liquid waste	11		4.7	21.9	
Tires	10	16	11.6	14.9	19.7
Impregnated sawdust	6				
Plastic	9		26.4	4.7	33.1
Industrial & household waste (solid)		65		13.8	
Industrial waste & other fossil based fuel	30				
MBM	2	4	6.1	15.7	
Agricultural Waste	9	10	4.2	11.1	
Wood chip & Other Biomass	15	5	24.5		25.1
Sewage sludge	2		4.2	1.7	
RDF				7.8	
Other alternative fuel			14.6		

4. Plant performance indicator

The cement industry needs to ensure sustainable and environmentally friendly use of natural resources while increasing profit margins. This is the responsibility of the cement producers to develop new strategies that will optimize the performance of the manufacturing process in response to the changing conditions. To measure the performance of the manufacturing process a number of companies utilize some Key Performance Indicators (KPI). Selecting appropriate KPIs at the company level and implementing them in the operational level is also a new challenge faced by the cement industry.

To move towards the sustainable development an important requirement for the cement companies is the performance measurement. Investigation of cement plant's performance requires data from different sources, which need to be collected and evaluated properly. The raw data from the sources are often unavailable due to the confidentiality policy of the plant. Inconsistent data because of the limited accuracy of the instruments are also another problem [22]. Within the cement

industry, many companies are operating environmental indicators as facility level KPIs and some companies have introduced indicators based on energy efficiency and the usage of AFs and raw materials [23]. Base lining and benchmarking are two related approaches for performance measurement. Base lining involves comparing plant performance over time, while benchmarking involves comparing performance relative to an established best practice level of performance [24].

The potential KPIs for cement plant performance can be categorized by energy efficiency, environmental performance, economical benefits, social performance etc. According to the WBCSD report on sustainable cement industry [23], the most important KPIs are;

- Tonnes of cement per mega joule of energy
- Fuel & raw material substitution rates (%)
- Non-product output (kg of waste) per tonne of cement
- Net CO_2 (kg) per tonne of cement
- Incident rate (injury, illness) per 200,000 hours

Apart from the last one on the list all are directly involved with the fuel source hence with the AFs. In this article the impacts of AFs are studied on the basis of available data from different sources. Five selected cement manufacturing group's data has been analyzed to understand the influence of alternative fuel on plant performance.

5. Data & analysis

There is variability in the data due to both differences in company performance and differences in kiln process. To illustrate that, Table 3 represents specific thermal energy consumption of clinker manufacturing with different kiln process [25]. Still several literatures try to figure out the baseline of the performance measurement. Table 4 gives an example of such effort [23].

Table 3: Specific thermal energy consumption in different kiln process [25]

Kiln process	Thermal energy consumption (GJ/tonne clinker)
Wet process with internals	5.86–6.28
Long dry process with internals	4.60
1-stage cyclone pre-heater	4.18
2-stage cyclone pre-heater	3.77
4-stage cyclone pre-heater	3.55
4-stage cyclone pre-heater plus calciner	3.14
5-stage pre-heater plus calciner plus high efficiency cooler	3.01
6-stage pre-heater plus calciner plus high efficiency cooler	<2.93

Table 4: Baseline Performance of the Cement Industry [23]

Indicator	Approximate Value
Tonnes of cement per MJ	Each tonne of cement consumes roughly 3000 MJ of total electrical and thermal energy
Fuel & raw material substitution rates (%)	Fuel ranges from 0 to 25% Raw material from 0 to 10%
Non-product output (waste per ton of cement)	Airborne and waterborne releases are generally known, but definitions of solid waste vary
Net CO_2 (kg) per ton of cement	Each tonne of Cement generates approximately 900 kg of net CO_2 emissions
Incident rate (injury, illness) per 200,000 hours	Ranges from 1 to 5 incidents per 200,000 hours

Three out of the five world's largest cement producers are located in the EU-27: Lafarge (France), Heidelberg Cement (Germany) and Italcementi (Italy), with the other two being Holcim (Switzerland) and Cemex, (Mexico) [26]. As the plant level data is not available in literature the group level data [16-21] for the aforementioned cement manufacturing companies

have been considered for the current study. Table 5 summarized the percentage of AFs in fuel mix and the average thermal energy efficiency of the manufacturing group. The annual sale of cement is also included to indicate the annual production of the groups. Apart from Heidelberg group all have increased the percentage of AFs in their fuel mix. Thermal energy efficiency was achieved with the increment of AF usage with an exception for Cemex group.

Table 5: Thermal efficiency of cement manufacturing group

Company	Sales of cement (million tons)		% of thermal energy from alternative fuel		Thermal energy efficiency (MJ/ton clinker)	
Year	2009	2011	2009	2011	2009	2011
Holcim Group	131.9	144.3	12.0	12.2	3606	3510
Cemex Group	72	75	16.4	24.7	3693	3757
Heidelberg Group	79.3	87.8	22.7	21.2	3793	3797
Italcementi Group	55.7	51.1	5.4	5.8	3970	3805
Lafarge Group	149.4	160	10.9	13	3670	3657

Most important KPI for cement manufacturing plant from the environmental point of view is the gross and specific CO_2 emission. This and other KPIs for the cement manufacturing group are assembled in Table 6. In the table air emission data includes the amount of NO_X, SO_2, dust and other heavy metal and organic components. Clinker cement ratio is also included in the table as it is also considered as an important KPI [23] and directly involved with the thermal energy consumption and CO_2 emission rate. Lafarge group manage to improve their clinker cement ratio and in the course they manage to reduce net CO_2 emission which occurs during the calcinations process of clinker production.

Table 6: KPIs of cement manufacturing groups

Company	Gross CO_2 emission (Million tons)		Net CO_2 (Kg) per ton of cement		Air emission (kg of waste) per ton of cement		Clinker cement ratio	
Year	2009	2011	2009	2011	2009	2011	2009	2011
Holcim Group	92.6	102.0	613	608	1.43	1.34	70.7	70.9
Cemex Group	41.7	43.3	658	660	1.58	1.53	75.1	75.1
Heidelberg Group	41.8	47.4	649.3	650.5	2.15	2.40	76.4	75.5
Italcementi Group	35.03	34.43	717	708	2.14	2.12	81.6	81.3
Lafarge Group	93	98	628	611	2.57	2.21	75	73

6. Discussion

The usage of AFs in cement industry increases day by day to meet the objectives of sustainable development, however it should not impose an adverse effect on the plant performance. Five selected cement manufacturing groups' data has been presented in this paper to understand the link between the usage percentage of AF and the plant performance. Four major KPIs have been scrutinized from the available data. Percentage of different wastes which are currently used in cement industry as AF has also been analyzed to understand the correlation between them and the plant performance.

Among the selected groups, Cemex Group was found to be the highest fossil fuel substitution rate achiever. Industrial and household solid wastes constitute the major part of AFs used by Cemex group. Generally Industrial and household solid wastes contains more moisture than coal and hence the thermal energy requirement per ton of clinker production is higher for Cemex group. The positive side was the reduction of waste per ton of cement production (reduces about 3% in two years).

Holcim group secured second place by the sale margin in year 2009 and 2011. The percentage of AFs usage remains almost same during those two years along with the ratio of different waste materials. The thermal energy efficiency for the Holcim group drop from 3606 MJ/t to 3510 MJ/t. Specific air emission of Holcim group reduced slightly while gross CO_2 emission increased due to the increase of cement production.

Lafarge group posted highest sale of cement both in year 2009 and 2011. They also increased the fossil fuel substitution rate by AFs from 10.9 to 13 in two years. Their AFs include solvent & liquid waste, tires, industrial & household waste and biomass almost in equal proportion. Thermal energy consumption for Lafarge group was reduced from 3670MJ/t to 3657MJ/t. The most commendable achievement of Lafarge group is the net CO_2 emission per ton of cement which dropped from 628 kg to 611kg in two years.

Percentage of thermal energy from AFs in Heidelberg group reduced to 21.2 in 2011 from 22.7 in 2009. Thermal energy consumption increased slightly from 3793MJ/t to 3797MJ/t. Air emission per ton of cement was also increased during that period by 10%. Similar increment was found in the figure of gross and net CO_2 emission.

Italcementi group was way behind in using AFs in cement manufacturing compared to other cement manufacturing groups. It also reflected on their thermal energy consumption and air emission data. Italcementi group also had some trouble regarding the clinker cement ratio compared to other manufacturing groups. It is pertinent to mention here that the net CO2 emission for all the groups are way below the base line as mentioned in Table 4. Still cement manufacturer try hard to reduce it even more along with the reduction of other emissions (NO_X, SO_2 and dust).

From the above study it is clear that usage percentage of alternative fuel can influence the plant performance in terms of their thermal efficiency. Still the magnitudes of its influence need to be determined quantitatively through extensive study with specific plant data. The percentages of waste that are currently being used as alternative fuel by the cement producer groups are available in literature. However, it is difficult to establish a relationship between the percentage of waste and plant performance on the basis of available data.

Currently, authors are undertaking a project to investigate the feasibility of using different wastes as alternative fuel for cement industry and to optimize their usage. Process engineering software ASPEN PLUS is being used to model the heating system of a full-scale cement plant, using different alternative fuels on the basis of combustion mechanism. This software is focused on clinker chemistry, thermodynamics in the rotary kiln and also the effect of alternative fuels on material flow, emissions and product quality. Through simulation the usage of wastes will be maximized along with controlling the above factors. ASPEN PLUS could also be used to calculate the heat balance of the entire process using established thermodynamics principles of material and energy conservation. In the process of optimizing the usage of alternative fuel, the plant performance will be determined through most suitable KPIs.

7. Concluding remarks

In this study, group level data of the leading cement manufacturer have been analyzed and discussed to draw a relationship between the usage of AFs and plant performance. The analysis reveals that CO_2 emission and other air emissions such as NO_X, SO_2 and dust can be reduced by increasing the usage of AFs. Thermal energy consumption of the plant can also be reduced by using certain wastes as AFs. Extensive study is required to find out the degree of the impact on the plant performance by the usage of AFs. A research group at Central Queensland University is studying different alternative fuels based on their intrinsic properties available from the local cement plant/s to improve the performance of the manufacturing process.

References

[1] Van Oss, H.G., Padovani, A.C., 2002, Cement Manufacture and The Environment, Part I: Chemistry & Technology, Journal of Industrial Ecology 6 (1), p. 89.

[2] Van Oss, H.G., Padovani, A.C., 2003, Cement Manufacture and The Environment, Part II: Environmental Challenges and Opportunities, Journal of Industrial Ecology 7 (1), p. 93.

[3] Madlool, N.A., Saidur, R., Hossain, M.S., Rahim, N.A., 2011, A Critical Review on Energy Use and Savings in the Cement Industries, Renewable and Sustainable Energy Reviews 15 (4), p. 2042.

[4] Nielsen, A.R., Aniol, R.W., Larsen, M.B., Glarborg, P., Dam-Johansen, K., 2011, Mixing Large and Small Particles in a Pilot Scale Rotary Kiln, Powder Technology 210 (3), p.273.

[5] Kaantee, U., Zevenhoven, R., Backman, R., Hupa, M., 2004, Cement Manufacturing Using Alternative Fuels and the Advantages of Process Modelling, Fuel Processing Technology 85 (4), p. 293.

[6] Lechtenberg, D., 2009, Spent Cell Linings from the Aluminium Smelting Process as an Alternative Fuel and Raw Material for Cement Production, Global Cement Magazine, January, p. 36-37.

[7] European Commission, Reference Document on the Best Available Techniques in the Cement and Lime Manufacturing Industries. BAT Reference Document (BREF), European IPPC Bureau, Seville, Spain, 2011.

[8] Schneider, M., Romer, M., Tschudin, M., Bolio, H., 2011, Sustainable Cement Production—Present and Future, Cement and Concrete Research 41(7) p. 642.

[9] Cemex News, 2011, UK Cement Plant Set 100% AF record, Global Cement Magazine, April, p. 57.

[10] Mokrzycki, E., Uliasz-Bochenczyk, A., 2003, Alternative fuels for the cement industry, Applied Energy 74, p. 95.

[11] Willitsch, D.F., Sturm, G., Wurst, F., Prey, T., Alternative Fuels in the Cement-Industry, Report of PMT-Zyklontechnik GmbH, Krems, Austria, 2002.

[12] Trezza, M.A., Scian, A.N., 2000, Burning Wastes as an Industrial Resource: Their Effect on Portland Cement Clinker. Cement and Concrete Research, 2000; Vol. 30, No. 1: 137-144.
[13] Chinyama, MPM., 2011, Alternative Fuels in Cement Manufacturing, in "*Alternative fuel*" M. Manzanera, Editor. InTech, Rijeka, Croatia.
[14] Akkapeddi, S., 2008, Alternative Solid Fuels for the Production of Portland Cement, MSc. Thesis, Auburn University, Alabama, December.
[15] WBCSD Report, "Guidelines for the Selection and Use of Fuels and Raw Materials in the Cement Manufacturing Process, Fuels and Raw Materials" December 2005. www.wbcsdcement.org/pdf/tf2_guidelines.pdf, viewed on 12th October 2011.
[16] Heidelberg Cement Group, Sustainability KPI 2011, http://www.heidelbergcement.com/NR/rdonlyres/912D789C-C7B4-43CC-ABA7-6C0FF837A6A5/0/IndicatorsSustainability_2011.pdf, viewed on 28th July 2012.
[17] Holcim Ltd. 2011, Corporate Sustainable Development Report 2011, http://www.holcim.com/fileadmin/templates/CORP/doc/SD12/holcim_csd_2011_WEB.pdf, viewed on 28th July 2012
[18] Italcementi Group, Sustainability Disclosure 2011, http://www.italcementigroup.com/NR/rdonlyres/1734D444-F2DE-41FA-9914-8A943E385975/0/ITC_Sostenibilita_2011UK.pdf, viewed on 6th June 2012.
[19] Italcementi Group. Sustainability Report 2010, http://www.italcementigroup.com/NR/rdonlyres/613C7701-5A4A-4FCD-BEDD-2400E49C98A5/0/sdReport2010.pdf, viewed on 19th March 2012.
[20] Lafarge Group, Sustainability Report 2011, http://www.lafarge.com/05182012-publication_sustainable_development-Sustainable_report_2011-uk.pdf, viewed on 6th June 2012.
[21] Cemex Group, Sustainable Development Report, 2011, http://www.cemex.com/InvestorCenter/files/2011/CX_SDR2011.pdf, viewed on 6th June 2012.
[22] Gallestey, E., Castagnoli, D., Colbert, C., New Levels of Performance for the Cement Industry. http://www02.abb.com/global/gad/gad02077.nsf/lupLongContent/D23B7F13F1201AE7C1256EA7003BF848, viewed on 10th May 2012.
[23] Fiksel, J., 2002. Substudy 5: Key Performance Indicators. WBCSD. http://dev.wbcsdcement.imsplc.com/pdf/battelle/final_report5.pdf, viewed on 10th May 2012.
[24] Boyd, G. and. Zhang, G., Measuring Improvement In Energy Efficiency of the US Cement Industry with the ENERGY STAR Energy Performance Indicator, Energy Efficiency, DOI 10.1007/s12053-012-9160-z, published online 25 May 2012.
[25] GERIAP, Company Toolkit for Energy Efficiency, Industry Sectors – Cement, 2005. http://www.energyefficiencyasia.org/docs/IndustrySectorsCement_draftMay05.pdf, viewed on 10th May 2012.
[26] European Commission Report, Energy Efficiency and CO_2 Reduction in the Cement Industry, 2010. http://setis.ec.europa.eu/newsroom-items-folder/cement-energy-efficiency/at_download/Document, viewed on 24th April 2012

Available online at www.sciencedirect.com

SciVerse ScienceDirect

Procedia Engineering 00 (2012) 000–000

Procedia Engineering

www.elsevier.com/locate/procedia

5th BSME International Conference on Thermal Engineering

Investigation of the Effects of Diesel Injection Rate Shapes on Combustion and Pollutant Formation of a Dual Fuel (Diesel/Natural Gas) Engine with Multi-Dimensional CFD Model

*Bahram Jafari[a], Seyyed Mostafa Mirsalim[b], Davood Domiri Ganji[a]

[a]*Nooshirvani University of technology, Babol, 47148-71167, Iran*
[b]*Polytechnic University of technology, Tehran, 15875-4413, Iran*

Abstract

The utilization of natural gas engines for power generation and other stationary applications has grown dramatically in the last two decades. This is due largely to the favourable emissions characteristics and more recently, favourable power density and thermal efficiency. Conventional compression ignition engines can easily be converted to a dual fuel (Diesel/Natural gas) mode of operation in order to use natural gas as a main fuel and diesel as pilot injection to initiate combustion. The objective of this study is to simulate combustion process, pollutant formation and flow field in the combustion chamber of D87 dual fuel engine. A three dimensional CFD model for flow field, spray, spray-wall interactions, combustion and emissions formation processes have been used to carry out the computations. This work is presented to study the effect of different diesel pilot injection rate shapes in constant amount of diesel pilot fuel and piston bowl shape. Results show that the improvement of air-fuel mixture formation and combustion process at optimized injection rate shape. The results of model in addition to approving the corresponding data in the literature are also compared with the experimental data and shown good agreement.

Keywords: Dual fuel engine, Combustion, emission, pilot injection rate shape

Nomenclature

k	*Turbulence kinetic energy [m2/s2]*
C	*Constant coefficient*
S	*Stoichiometry coefficient*
Greek symbols	
ε	Dissipation rate [m2/s2]
ρ	Density [kg/m3]
Subscripts	
fu	*Fuel*
ox	*Oxidizer*
pr	*Product*

* Corresponding author. Tel.: +98-911-127-6472; fax: +98-121-220-3252.
E-mail address: Bahramjafari@gmail.com

R	*Reaction*
Abbreviations	
ATDC	*After top dead center*
BTDC	*Before top dead center*
IVC	*Intake valve close*
EVO	*Exhaust valve open*
SOI	*Start of injection*
CA	*Crank angle*
DOI	*Duration of injection*
IMEP	*Indicated mean effective pressure*

1. Introduction

Direct-injection diesel engines have proved to be an efficient option in heavy-duty applications like transportation or power generation. However, due to the natural conditions of high pressure and temperature in the combustion process, diesel engines emit considerable amounts of pollutants, especially nitrogen oxides (NOx) and soot. International regulations ratified in recent years have imposed more stringent limits on pollutant emissions in internal combustion engines. To comply with these regulations with the common rail injection system which is widely used in recently developed engines, several new fuel injection strategies on conventional diesel combustion have been investigated in direct injection diesel engines.

An experimental study was carried out to visualize the spray and combustion inside an AVL single-cylinder research diesel engine converted for optical access by Tsung-Cheng Wang et al. The results showed that optically accessible engines provide very useful information for studying the diesel combustion conditions, which also provided a very critical test for diesel combustion models. The high IMEP conditions were successfully achieved in the optical engine experiments, which show sensitivity to injection pressure, charge condition, and combustion chamber geometry [1].

Rolf Egnell had a simple approach to studying the relation between fuel rate heat release rate and NO formation in diesel engines. The calculations showed that by increasing the length of the injection period and maintaining a smooth and even fuel rate, the NO formation could be reduced with very limited reduction of the indicated thermal efficiency [2].

Pressure modulated injection and its effect on combustion and emissions of a heavy duty diesel engine had been investigated by H. Erlach et.al. The results with separated pilot injection were found to be sensitive to pilot timing, pilot injection pressure and fuelling during pilot injection. The pilot injection should be timed as closely to the main injection as possible in order to avoid excessive NOx formation during the combustion of the pilot fuel. The pressure during the pilot injection should be high enough to ensure sufficient mixing to restrict soot formation. The amount of pilot fuel should be a compromise between providing enough combustion products to lower the flame temperature during the main combustion and avoiding excessive soot formation [3].

In order to comply the regulations, better emission performance and fuel economy, natural gas fuelled engines are being developed. Natural gas is usually used in spark ignited engines because of its relatively high octane number. As a matter of fact, it is very probably to occur knock in this type of engine and then the compression ratio of this type of engines can't be made as high as diesel. As a result, the thermal efficiency of spark ignited natural gas engines is inferior to that of conventional diesel engines. To overcome this shortcoming, a combustion system using natural gas as a dual-fuel in diesel engines has been proposed in recent years.

The diesel/natural gas (dual fuel) engine has been developed as one of the alternatives to the conventional diesel engine in order to utilize natural gas, a plentiful alternative fuel. It is very important to improve thermal efficiency and to reduce exhaust emissions.

It also showed that by Pierpont and et.al [4] at high load engine operating conditions raising the injection pressure effectively reduces particulate emissions. As to how to optimize combustion chamber to cope with high-pressure injection, in-depth understanding of the cross influence between the injection and the configuration of combustion chamber is inevitable. Since evaporative and non-evaporative diesel spray behave quite differently in terms of spray penetration and dispersion.

There have been several fundamental studies on dual fuel engines in recent years. Hountalas and Papagiannakis[5] simulated the combustion process for natural gas engines with a pilot diesel fuel injection and the ignition source has been modelled by using a two-zone combustion model. A semi-empirical spray model was used for diesel combustion simulation. Hountalas and Papageogakis [6] studied natural gas injection, mixing, and spark ignition parameters using the KIVA-3 Code. A one step global reaction mechanism was used to simulate the combustion chemistry. There are also some studies on dual fuel engine misfire and knock. Karim [7] studied light load misfire and high load knock. Uyehara [8] discussed how to control dual fuel engine emissions by studying the combustion of both the diesel and dual fuel engines.

Pilot injection rate shape is one of the best ways to restrict direct injection dual fuel engines emission. According to that, many shapes for injection rate are provided based on its fuel spray ignition. This prevents the engine from knocking and allows a high compression ratio comparable to that of conventional diesel engines. The effect of injection rate shaping has been investigated by Youtong Zhang et al. [9]. The injection rate shapes were varied to investigate their effects on dual fuel combustion. These profiles were included a rising, falling, and top-hat (constant) rate.

However, there are a few studies about the effect of the pilot injection rate shape on the performance of a dual fuel engine. In this work, three dimensional CFD code FIRE has been used to study the effect of injection rates on combustion process in the dual fuel engine.

2. Model description

The commercial computational fluid dynamics (CFD) code FIRE was used to perform the numerical simulation of combustion and emission formation in D87 dual fuel engine. The engine specification and operating condition that is used in this work are shown on Table 1.

This engine is a DI engine in diesel mode. But in the dual fuel mode, natural gas is injected in intake port and a mixture of air and fuel imports into the cylinder. Air-fuel mixture is compressed during the comparison stroke. But, the mixture needs a pilot as an ignition source. Near to TDC, pilot diesel fuel is injected into the cylinder and combustion is started. The ratio of diesel to natural gas in D87 dual fuel engine is 20% to 80%, respectively.

Table1. Engine Specifications

Engine type	Diesel engine	Dual Fuel engine
Engine speed	1500 rpm	1500 rpm
Bore × stroke	150×180 mm	150×180 mm
Power	1000 kW	800 kW
Compression ratio	15:1	11.5:1
Injector type	Common-rail	Common-rail
Number of nozzle holes	8	8

Figure 1 shows the 45° sector computational mesh of combustion chamber in three dimensional at TDC. Since an 8-hole nozzle is used, only a 45° sector has been modeled. This takes advantage of the symmetry of the chamber geometric setup, which significantly reduces computational runtime. Number of cells in the mesh is 19385 cells at TDC. This fine mesh size will be able to provide good spatial resolution for the distribution of most variables within the combustion chamber. Calculations are carried out on the closed system from IVC at -150°CA ATDC to EVO at 120°CA ATDC.

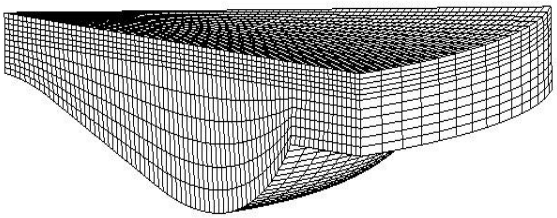

Fig.1. Computational mesh at TDC

At the applied code, the compressible, turbulent and three dimensional transient conservation equations are solved for reacting multi-component gas mixtures with the flow dynamics of an evaporating liquid spray by Amsden et al. [10]. The turbulent flows within the combustion chamber are simulated using the RNG k-ε turbulence model which is presented by Han and Reitz [11], modified for variable-density engine flows.

2.1. Spray, combustion and emissions models

The spray module is based on a statistical method that refers to as discrete droplet method (DDM). This method operates by solving ordinary differential equations for the trajectory, momentum, heat and mass transfer of single droplets, each being a member of a group of identical non-interacting droplets termed a parcel. Thus one member of the group represents the behavior of the complete parcel.

The Kelvin-Helmholtz Rayleigh-Taylor (KH-RT) model is selected to represent spray breakup [12]. In this model Kelvin-Helmholtz (KH) surface waves and Rayleigh-Taylor (RT) disturbances should be in continuous competition of breaking up the droplets.

The Dukowicz model [13] was applied for treating the heat-up and evaporation of the droplets. This model assumes a uniform droplet temperature. In addition, the rate of droplet temperature change is determined by the heat balance, which states that the heat convection from the gas to the droplet either heats up the droplet or supplies heat for vaporization.

The Shell auto-ignition model was used for auto-ignition modeling. In this generic mechanism, 6 generic species for hydrocarbon fuel, oxidizer, total radical pool, branching agent, intermediate species and products were involved. In addition the important stages of auto-ignition such as initiation, propagation, branching and termination were presented by generalized reactions, described in [14].

Combustion process is modeled by Eddy Breakup model [15]. In the eddy break-up model, the rate of consumption of fuel is specified as a function of local flow properties. The mixing-controlled rate of reaction is expressed in terms of the turbulence time scale k-ε, where k is the turbulent kinetic energy and ε is the rate of dissipation of k. With s as the stoichiometry coefficient, CR and C′R are model constants, a transport equation for the mass fraction of fuel is solved, where the:

$$S_{fu} = -\rho \frac{\varepsilon}{k} \min\left[C_R m_{fu}, C_R \frac{m_{ox}}{s}, C'_R \frac{m_{pr}}{1+s} \right] \tag{1}$$

The two first terms of the minimum value of operator determine whether fuel or oxygen is present in limiting quantity, and the third term is a reaction probability which ensures that the flame is not spread in the absence of hot products.

NOx formation model is derived by systematic reduction of multi-step chemistry, which is based on the partial equilibrium assumption of the considered elementary reactions using the extended Zeldovich mechanism [16] describing the thermal nitrous oxide formation.

The overall soot formation rate is modeled as the difference between soot formation and soot oxidation. Soot formation is based on Hiroyasu model and the soot oxidation rate is adopted from Nagle and Strickland-Constable [17].

All above equations are taken into account simultaneously to predict spray distribution and combustion progress in the turbulent flow field, wall impingement and diesel combustion rate using two stage pressure correction algorithms.

2.3. Numerical Model

The numerical method used in this study is a segregated solution algorithm with a finite volume-based technique. The segregated solution is chosen due to the advantage over the alternative method of strong coupling between the velocities and pressure. This can help to avoid convergence problems and oscillations in pressure and velocity fields. This technique consists of an integration of the governing equations of mass, momentum, species, energy and turbulence on the individual cells within the computational domain to construct algebraic equations for each unknown dependent variable. The pressure and velocity are coupled using the SIMPLE (semi-implicit method for pressure linked equations) algorithm which uses a guess-and-correct procedure for the calculation of pressure on the staggered grid arrangement. It is more economical and stable compared to the other algorithms. The upwind scheme is employed for the discretization of the model equations as it is always bounded and provides stability for the pressure correction equation.

3. Results and discussion

3.1. Model validity

Before using the three dimensional CFD model to examine the effect of different injection rate shapes on combustion process, it is necessary to validate its predictive ability. For this reason, it has been used the experimental data for both of diesel and dual fuel D87 engine. Parameter tuned is: in-cylinder pressure. Figures 2 and figure 3 indicate the comparison of

simulated and experimental in-cylinder pressures against the crank angle for the D87 diesel and dual fuel engine in full load condition, respectively.

The good agreement of predicted in-cylinder pressure with the experimental data can be observed. It is due to time step and computational grid independency of obtained results. It means that, if the number of mesh be fewer than it, it causes fault and maybe diverge and if be more than it, the computational time will be increased.

Maximum difference in in-cylinder pressure is acceptability in numerically solution. The accuracy of calculated in-cylinder pressure illustrates the ability of this model in prediction of mixture formation and combustion process. Therefore, the CFD and combustion simulation model performed in this study are able to represent the real combustion process inside diesel and dual fuel engine and have the capability to be implemented for further calculation.

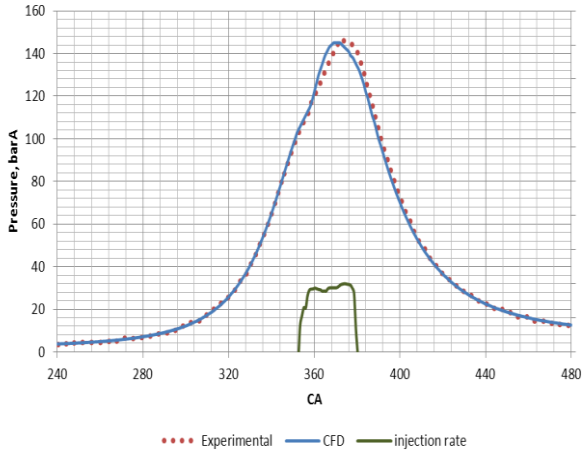

Fig.2. Comparison of calculated and measured in-cylinder pressure with SOI at -9.4 ºCA ATDC in diesel engine

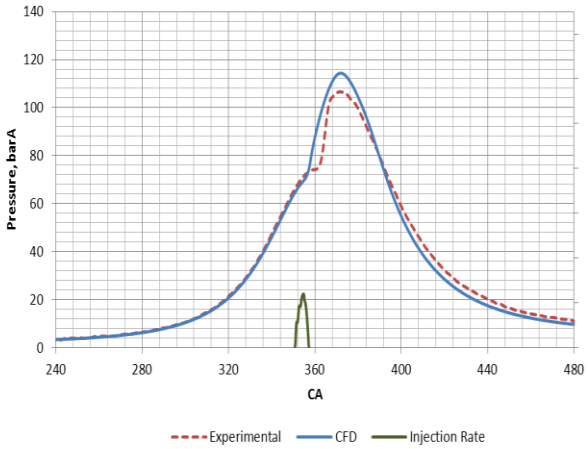

Fig.3. Comparison of calculated and measured in-cylinder pressure with SOI at -9.4 ºCA ATDC in dual fuel engine (20% diesel+80% natural gas)

As can be seen from figure 2 and figure 3, in the dual fuel engine, mean cylinder pressure has been decreased in compared to diesel fuel engine. In-cylinder pressure represents engine performance. Therefore, engine performance was decreased in dual fuel engine.

As mentioned about the diesel engine, improvement of air and pilot diesel fuel mixture formation in ignition delay is a possible way to increase of combustion efficiency and engine performance. The quality of mixture formation varies with the injection parameters such as injection rate shape. Hence, the influence of different diesel injection rate shapes on combustion and emissions has been investigated in this work in a dual fuel engine.

3.2. Effect of injection rate shape

In order to investigate the effect of different injection rate shapes, a fixed amount of natural gas and diesel fuel has been considered. The predicted results are presented in this section for five injection rate shapes. Figure 4 shows the applied injection shape curves.

With two common rails, one for low pressure fuel and the other for high pressure fuel, the injection rate shape control by controlling the fuel injector supply pressure, from the two rails. Case1, case2 and case3 are controlled by a next-generation common rail system (NCRS) [19]. Case3 and Case4 are produced via a conventional common rail system (CRS).

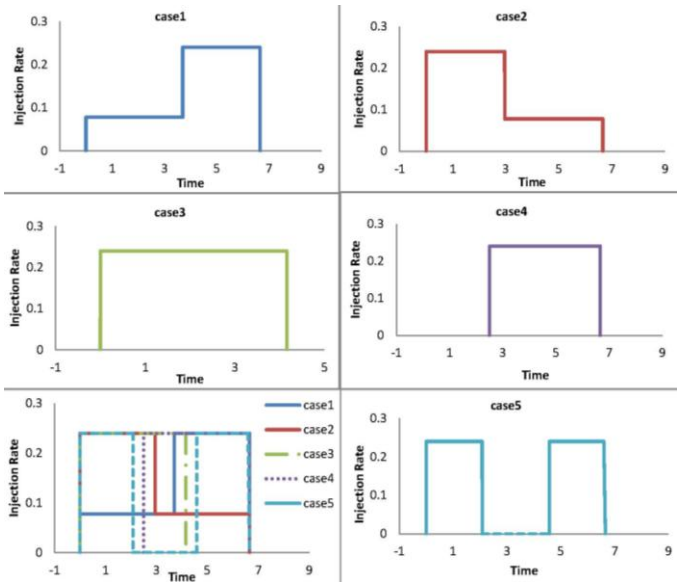

Fig.4. Different injection rate shapes

Duration of injection (DOI) for different cases can be determined according to Table 2. These injection rates are dimensionless and Fire code uses them as a normalized profile.

Table2. DOI of different injection rate shapes

Rate Shape	DOI (CAD)
Case1	6.66
Case2	6.66
Case3	4.16
Case4	4.16
Case5	6.66

In order to equalize the area under the curve for all cases, these values are modified. By using of these curves, the CFD code divides all mass in the whole identified course to ensure that all mass inject to the combustion chamber.

Figures 5 to 9 show the predicted mean in-cylinder pressure, heat release rate, mean in-cylinder temperature, NOx and soot emission for five injection shape cases. It can be seen that case3 has the highest peak pressure and temperature.

When injection velocity is increased at the first of injection in case2 and case3, droplets penetrate slightly further into the combustion chamber because of high momentum liquid droplets and higher injection velocity. This leads to the increase of air entrainment into the fuel spray because of the longer spray path before impinging piston bowl. Also, higher injection velocity at the first of injection results in smaller diesel fuel droplet at ignition delay. This is due to the aerodynamic forces induced by the relative velocity between liquid fuel ligaments or bigger droplets and the surrounding gas intensify break-up of the droplet. Therefore, distributions of droplets are reduced at ignition delay and improvement of mixture formation. Injection velocity in case4 is equal to case3. But, start of injection in case4 has been retarded in compared to case3.

Therefore, the peak pressure was decreased in case4. Also, case1 with the longest DOI has retarded the combustion (Figure 1) thus decreasing the mean in-cylinder pressure and temperature as well as the NOx mass fraction. It is generally believed that NOx is formed in local high temperature regions present in the cylinder during premixed combustion. With these conditions present, and because the fuel-air charge is not homogeneous, the excess oxygen and nitrogen combine at high rates to form NOx. Also, NOx formation rapidly slows down during the later portion of the combustion process, and most of the NOx which has formed 'freezes' as it mixes with cooler cylinder gases and as the bulk cylinder temperature drops during the expansion stroke.

It is shown that split injection in case5 is effective at reducing soot emission. The quantity of soot particles in the emissions is determined by the balance between the rate of formation and subsequent oxidation. During the second phase of combustion, the 'diffusion burn', particulates are formed. Air mixing with the outer edges of the fuel jet sustains the diffusion burn. Fuel in the interior of the spray jet is subjected to high temperatures and pressures but it is starved for oxygen, leading to soot production. Injection pause causes the second pulse of injected fuel enters into a high-temperature region which is left over from the combustion of the first pulse of injection. Soot formation is therefore significantly reduced owing to the injected fuel is rapidly consumed by combustion before a rich soot producing region can accumulate. Also, injection pause promotes the oxygen availability for soot oxidation.

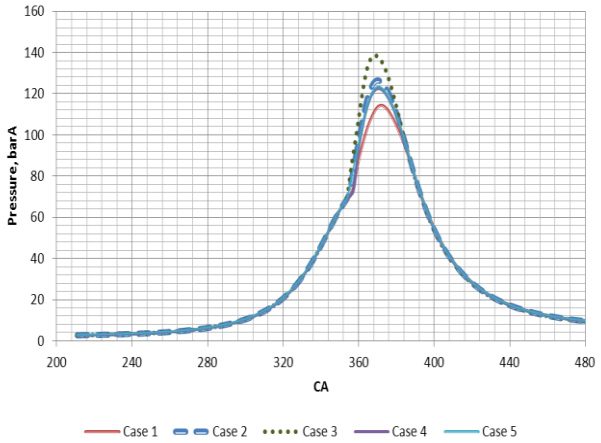

Fig.5. Mean in-cylinder pressure comparing between different injection rate shapes

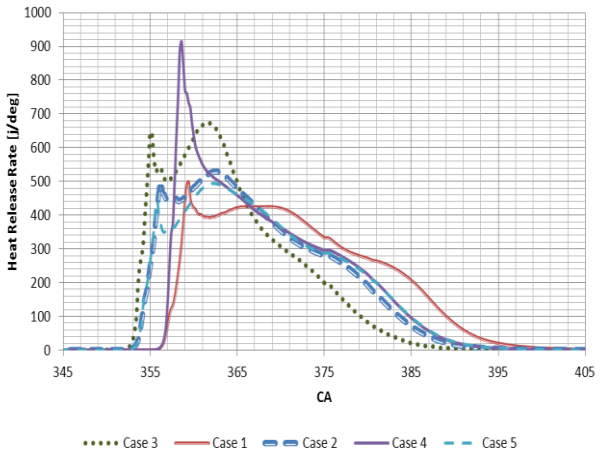

Fig.6. Heat release rate comparing between different injection rate shapes

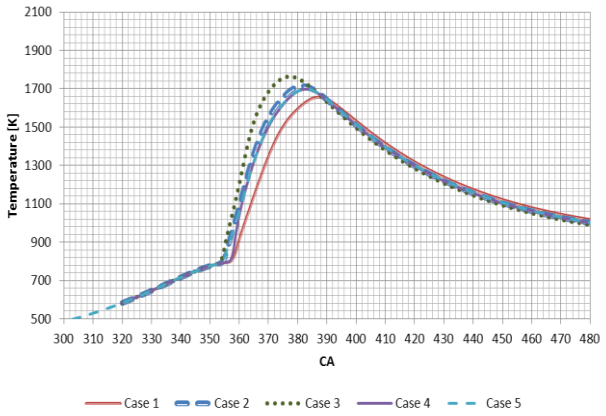

Fig.7. Mean in-cylinder temperature comparing between different injection rate shapes

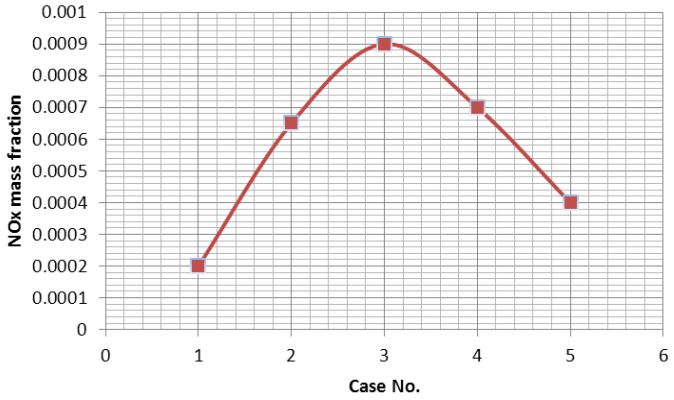

Fig.8. Effect of different injection rate shapes on NOx emission production

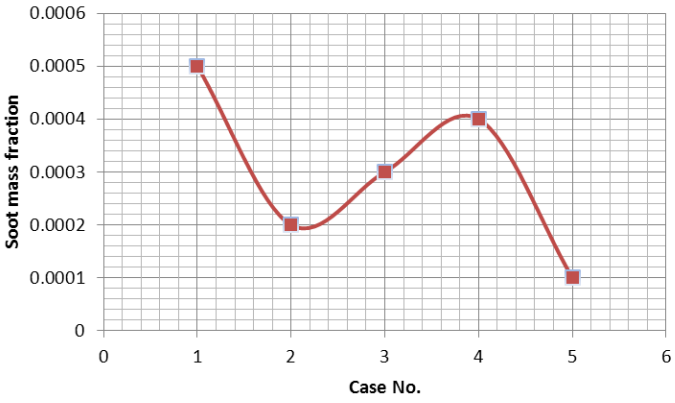

Fig.9. Effect of different injection rate shapes on soot emission production

The gross indicated mean effective pressure that is the integral of the cylinder pressure with respect to the change in cylinder volume over the compression and expansion strokes only is calculated by using equation below [18]:

$$IMEP = \Delta\theta / V_s . \sum_{i=n_1}^{n_2} p(i).dV(i) / d\theta \qquad (2)$$

P (i) = cylinder pressure at crank angle position i
V (i) = cylinder pressure at crank angle position i
V_s = cylinder swept volume
n_1= BDC induction integer crank angle position
n_2 = BDC exhaust integer crank angle position

IMEP as a performance result doesn't have much difference between cases and as shown in table2 there is no obvious dispute in the output power despite of differencing in peak pressure.

Table.2. Indicated mean effective pressure

Case number	IMEP
Case 1	19.436
Case 2	19.775
Case 3	19.888
Case 4	19.662
Case 5	19.662

Figure 10 shows the contour plots of spray distribution and mixture formation when combustion process has been started in a cross-section taken diagonally across the bowl and split ting it in half at 360 °CA and 370 °CA, respectively. As can be seen in figure 10, air-fuel mixture flows towards both the piston bowl and squish regions in case2. Therefore, enough time for mixing is available at ignition delay which leads to higher peak value of premixed combustion and combustion temperature.

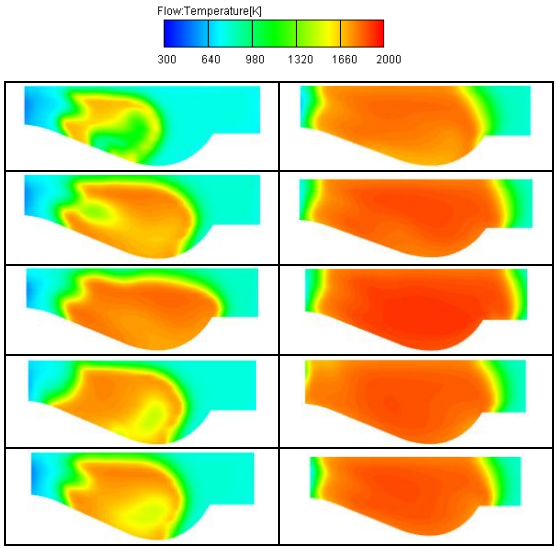

Fig.10. 2D Contours of temperature, up to down in square, case 1 to 5 for 360 ºCA (first column) 370 ºCA (second column) respectively

1. CONCLUSIONS

In this work, the effect of different injection rate shapes on combustion process and emission formation have been investigated as well as engine performance by using multi-dimensional CFD code in a Dual fuel engine operating in high engine load condition and the following results are obtained.

As shown in case 1, combustion process has been retarded and NOx has been reduced because in-cylinder temperature is decreased. Case3 has the highest peak temperature as well as more NOx mass fractions compared to other cases. Case5 mode exhibits average results among the five types.

The use of different injection rate shapes affects the combustion related properties and can be used as an alternative way to control combustion in the dual fuel engines. Due to Case5 is a combination of Case1 and 2, then its soot and NOx is lower than others. As matter of fact it can be the best Case.

References

1. Tsung-Cheng Wang, Joong-Sub Han, Xingbin Xie, Ming-Chia Lai, Naeim A. HeneinErnest Schwarz and Walter Bryzik, 1999. Direct visualization of high pressure diesel spray and engine combustion. SAE1999-01-3496.
2. Rolf Egnell, 1999. A Simple Approach to Studying the Relation between Fuel Rate Heat Release Rate and NO Formation in Diesel Engines. SAE 1999-01-3548.
3. Erlach. H., Chmela. F., Cartellieri .W. and Herzog. P., 1995. Pressure Modulated Injection and Its Effect on Combustion and Emissions of a HD Diesel Engine. SAE 952059.
4. Pierpont. D.A. and Reitz. R.D., 1995. Effects of Injection Pressure and Nozzle Geometry on D.I. Diesel Emissionsand Performance, SAE Paper 950604,1995.
5. Hountalas, D.T. and Papagiannakis, R. G., 2001. A Simulation Model for the Combustion process of Natural Gas Engines with Pilot Diesel Fuel as an Ignition Source. SAE 2001-01-1245.
6. Hountalas, D. T. and Papagiannakis, R. G., 2001. Development of a Simulation Model for Direct Injection, Dual fuel, Diesel- Natural Gas Engines. SAE 2001-01-0286.
7. Karim, G.A., 2000. Combustion in Gas Fuelled Compression-Ignition Engines. ASME ICE-Vol. 35-1.
8. Uyehara, O. A., 1995. Prechamber for Lean Burn for Low NOx. SAE 950612.
9. Youtong Z., Song-Charng K. and Rolf D. R., 2003. Modelling and Simulation of a Dual Fuel (Diesel/ Natural Gas) Engine with Multidimensional CFD. SAE 010755.
10 Amsden, A. A., O'Rourke, P.J. and Butler, T.D., 1989, KIVA ll. a computer program for chemically reactive flows with sprays. Los Alamos National Laboratory, NO. LA-11560-MS.
11. Han, Z., Reitz, R.D., 1995. Turbulence modelling of internal combustion engine using RNG k-ε models, Combustion Science Technology, 106.267-295.
12. Beale, J.C., Reitz, R.D., 1999. Modeling Spray Atomization with the Kelvin-Helmholtz/Rayleigh-Taylor Hybrid Model. Atomization and Sprays, 9.623-650.
13. Dukowicz, J.K., 1979. Quasi-Steady Droplet Phase Change In the Presence of Convection. Informal Report Los Alamos Scientific Laboratory, LA7997-MS.
14. Halstead, M., Kirsch, L., Quinn, C., 1977. The Auto Ignition of Hydrocarbon Fueled at High Temperatures and Pressures-Fitting of a Mathematical Model. Combustion Flame, 30. 45-60.
15. Magnussen, B.F., Hjertager, B.H., 1976. On Mathematcal Modeling of Turbulent Combustion with Special Emphasis on Soot Formation and Combustion. In the Proceedings of the 16th Symp on Combustion, pp. 719-729.
16. Zeldovich, Y. B., Sadovnikov, P. Y., Frank, D. A., Kamenetskii, 1974. Oxidation of Nitrogen in Combustion, Translation by M. Shelef. Academy of Sciences of USSR, Institute of Chemical Physics, Moscow-Leningrad.
17. Kong, S. C., Sun, Y. and Reitz, R. D., 2007. Modeling Diesel Spray Flame Lift-Off, Sooting Tendency and NOx Emissions Using Detailed Chemistry with Phenomenological Soot Model. ASME J. Eng. Gas Turbines Power.
18. Hrjit,s.rai., Michael, f.j., Colin, P.Loader., 1999. Quantification and reduction of IMEP errors resulting from pressure transducer thermal shock in an S.I Engine. SAE 1999-01-1329
19. Susumu Kohketsu., Keiki Tanabe., Koji Mori., 2000. Flexibly Controlled Injection Rate Shape with Next Generation Common Rail System for Heavy Duty DI Diesel Engines. SAE 2000-01-0705

Available online at www.sciencedirect.com

SciVerse ScienceDirect

Procedia Engineering 00 (2012) 000–000

Procedia Engineering

www.elsevier.com/locate/procedia

5th BSME International Conference on Thermal Engineering

Waste transformer oil as an alternative fuel for diesel engine

Md Nurun Nabi*, Md Shamim Akhter, Md Atiqur Rahman

Department of Mechanical Engineering, Rajshahi University of Engineering and Technology, Rajshahi-6204, Bangladesh.

Abstract

The current study investigates the suitability for using waste transformer oil (WTO) as an alternative fuel for compression ignition (CI) engine. For this purpose different properties of the WTO were determined. The different properties include density, kinematic viscosity, cetane number, calorific value, flash and fire points, fourier transform infra-red (FTIR). The investigation includes two parts. In the first part of the investigation, different properties and engine performance were conducted. In the latter part of the investigation WTO was refined by well know transesterification process and again different fuel properties and engine performance were conducted. In the text, the refined waste transformer oil is designated as RWTO. All fuel properties with WTO and RWTO were compared with those of conventional diesel fuel (DF). All properties were close to those of DF. FTIR results revealed that the WTO is a diesel like hydrocarbon. The engine performance with WTO and RWTO was much better than that of DF. Based on the findings, WTO and RWTO are suggested to be alternative fuels for CI engine.

Keywords: Waste transformer oil, fuel properties, *CI engine, alternative fuel.*

1. Introduction

The engine and fuel researchers are devoted to explore alternative fuels as the present world largely depends on petroleum fuel for generating power, vehicle movement and agriculture sectors. Price hike, limited reserve of petroleum oils and stringent emission regulation also forced researchers to find alternative fuels. In Bangladesh, there is limited petroleum reserve to meet the demand of the petroleum product and for this reason it is necessary to spend a lot of foreign currency for importing fuel every year. Recent price hike of petroleum oil incurs lots of money. Bangladesh imports most of the petroleum oils from Middle East. In this point of view, waste transformer oil (WTO) can be an alternative source for petroleum oils. WTO has significant physiochemical properties. WTO can meet a portion of our demand without any hesitation. There is a huge unused amount of transformer oil in Bangladesh which is rejected every year. This oil is not used for any other purpose**.** So, WTO is an important source for meeting the demand of diesel in Bangladesh. Bangladesh imports approximately 2.4 million ton diesel each year [1]. It is well known that the transformer oil is used mainly in the electrical transformer for insulation purpose. Moreover, cooling is another purpose of using transformer oil in the electrical transformer while the transformer is running. Among various properties, one of the main properties of transformer oil is to sustain high temperature during operation. When an electrical transformer is in operation, the transformer oil is subject to mechanical and electrical resistance. For a certain period of time, it is recommended to check the electrical and chemical properties of the transformer oil. By using WTO, Bangladesh can reduce importing a huge amount of petroleum products from foreign countries**.** Our attention goes to the WTO. WTO results from the power generation and transmission station. At present 100 per cent transformer oil is not used in place of diesel fuel (DF) to run the engine rather blends of WTO and DF

* Corresponding author. Tel.: +8801748037304; fax: +880721750832.
E-mail address: nahin1234@hotmail.com

are used to run the engine. Transformer oils are an important class of insulating oils. They act a heat transfer medium in the transformer. Transformer oil have negligible amount of contamination which have adverse effect on the electrical properties [2]. In general, transformer oil is produced from wax-free naphthenic oils. After certain period of time of operation in the transformer, the oil is thrown out in the form of waste. But after testing the transformer oil blends (transformer oil and diesel fuel) it has been seen that the property of transformer oil is comparable to that of diesel [3]. Based on the earlier findings, the current study investigated the possibility of using WTO as a diesel substitute.

2. EXPERIMENTAL SETUP AND PROCEDURE OF EXPERIMENTATION

2.1 Materials and methods

The engine used in this experiment was a single cylinder, water-cooled, NA, 4-stroke, DI diesel engine. The specifications of the engine are shown in Table 1. The experiments were conducted with conventional DF and different blends of WTO. The engine speed was measured directly from the tachometer attached with the dynamometer. The outlet temperatures of cooling water and exhaust gas were measured directly from the thermocouples (Ni-Cr) attached to the corresponding passages. The dynamic fuel injection timing was set at 24º BTDC (before top dead centre). The engine speed was kept fixed at 800 rpm. An inclined water tube manometer, connected to the air box (drum) was used to measure the air pressure. Fuel consumption was measured by a burette attached to the engine. A stopwatch was used to measure fuel consumption time for every 10 cm^3 fuel. To investigate the suitability of WTO as DF three different blends were prepared. All percentages of different blends were volumetric percentages. The blends are WTO10 (WTO 10% and DF 90%), WTO15 (WTO 15% and DF 85%), and WTO20 (WTO 20% and DF 80%). Similar blends (RWTO10, RWTO15, and RWTO20) were prepared with RWTO. The RWTO was prepared by well-known transesterification process. In this process, methanol was used as alcohol and NaOH was used as catalyst. The brake power (BP), input power, BSFC and brake thermal efficiency were calculated by equations 1, 2, 3 and 4 respectively.

$$BP = W \times N \times 0.45 \times 0.746/5000 \quad \text{(kW)} \quad \text{----(1)}$$

Where, W is load in lb and N is engine speed in rpm.

$$\text{Input power} = \dot{m}_f \times CV/3600 \quad \text{(kW)} \quad \text{----(2)}$$

Where, $\dot{m}_f$ is the mass flow rate of fuel in kg/hr and CV is the calorific value of fuel in kJ/kg.

$$BSFC = \dot{m}_f / BP \quad \text{(kg/kWh)} \quad \text{----(3)}$$

$$\text{Brake thermal efficiency} = 100/((\dot{m}_f/BP)(CV/3600)) \quad (\%) \quad \text{----(4)}$$

Table 1Engine specifications

Engine type	**4-stroke CI engine**
Number of cylinders	One
Bore x Stroke	80 x 110 mm
Cooling	water cooling
Compression ratio	16.5
Rated power	4.476Kw@1800 rpm
Injection pressure	14 MPa (low speed, 900 -1099 rpm)
	20 MPa (high speed, 1100-2000 rpm)
Injection timing	24°BTDC

Table 2 Fuel properties of WTO, RWTO and DF

Properties	**WTO**	**RWTO**	**DF**
Density[kg/m^3]	895	874	860
Kinematic viscosity[cSt]	10.1	6.2	3.08
Flash point [°C]	140	125	90
Fire point [°C]	145	132	95
Gross calorific value[kJ/kg]	41775	43813	44500
Cetane number	42	50	48

2.2 Fuel characterization

In this section the different fuel properties include density, kinematic viscosity, cetane number, calorific value, flash and fire points, elemental analysis (CHONS), FTIR are discussed. The density was measured according to the ASTM D1298 method, kinematic viscosity was determined as per ASTM D445 method, cetane number was ascribed as per ASTM D613 method, gross calorific value was determined as per D5865 method, flash and fire points were determined according to

ASTM D93. Viscosity is one of the important properties for DF as it affects fuel atomization. Cetane number indicates the ignition quality of a DF. Some selected properties of WTO and neat DF are shown in Table 2.

2.2.1 Fourier transform infrared (FTIR) spectra for neat DF and neat WTO

The target of the current investigation is to explore the alternative fuel for CI engine. To fulfil the target WTO is selected as a possible source for alternative fuel. However, before making any final conclusion it is necessary to examine WTO's suitability as CI engine's fuel. Considering the above fact, FTIR analysis of WTO was performed as FTIR gives an idea about the suitability of WTO as DF. FTIR gives the idea of the WTO to identify the basic compositional groups. The FTIR instrument produces the IR-spectra of the WTO. It provides the absorption spectrum in percentage incident intensity, along the wave numbers 4000 to 500 cm. The standard IR-spectra of hydrocarbons were used to identify the functional group of the components of the WTO. The IR-spectra of WTO was compared with that of DF.

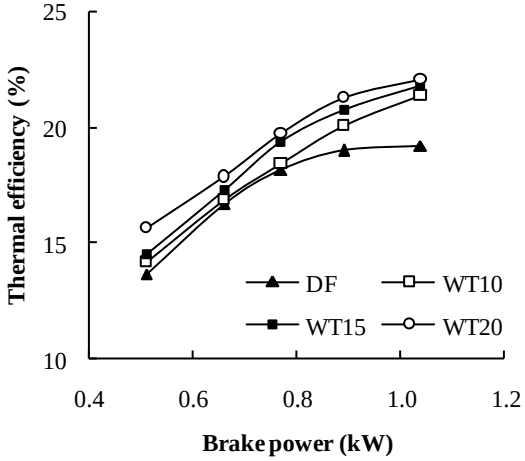

Figure 1 Effect of WTO on brake thermal efficiency

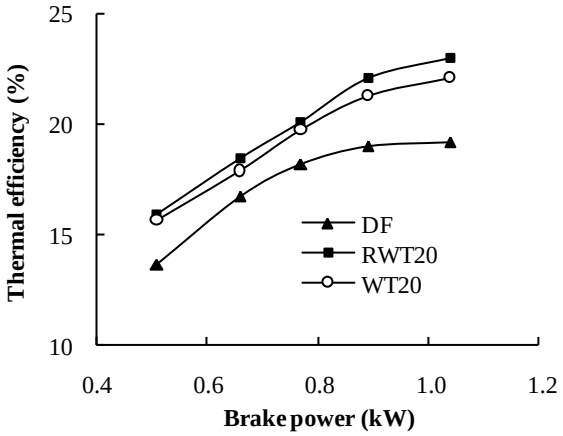

Figure 2 Effect of RWTO on brake thermal efficiency

3. RESULTS AND DISCUSSION

3.1 Effect of WTO and RWTO on brake thermal efficiency

The variation of brake thermal efficiency with engine load using all types of fuels/blends is shown in Figures1and 2. The brake thermal efficiency was calculated by the ratio of brake power to input power shown in Equation 4. From this Figure it is observed that the brake thermal efficiency increases with the increase in engine load (brake power) for all fuels/blends. It is interesting to note that compared to DF, all WTO blends show higher brake thermal efficiency. The maximum value of brake thermal efficiencies with WTO10, WTO15, WTO20 blends and DF were found to be 21.37%, 21.8%, 22.1% and 19.2% respectively. The higher thermal efficiencies with WTO blends were attributed to the fact of lower BSFC with the different blends of WTO compared to DF. Equations 3 and 4 indicate that brake thermal efficiency is reciprocal of BSFC. As the BSFC is lower with WTO blends, brake thermal efficiencies increase.

Figure 2 shows a comparison of thermal efficiencies with the blends of WTO20 and RWTO20. The thermal efficiencies with the WTO20 and RWTO20 were compared those of DF. Compared to DF, WTO20 blend show higher thermal efficiencies as described in Figure 1. WTO was refined by the transesterification process. Viscosity is one of the important fuel properties that affect fuel atomization. Higher viscosity leads to poor atomization results in poor combustion and engine emissions. One of the important targets of using transesterification process is to reduce fuel viscosity. Table 2 reveals lower viscosity with RWTO compared to WTO. It is clearly visible that the thermal efficiencies with WTO20 and RWTO20 blends are higher than those of DF. It is interesting to note that compared to WTO20, RWTO20 shows higher thermal efficiency. The higher thermal efficiency with RWTO20 may be attributed to the fact of lower viscosity with RWTO20 blend. The other blends of RWTO20 show similar trends (results not shown). Pullagura et al. [3] conducted experiments with 100% used transformer oil (WTO) and a blend of 40% WTO and diesel fuel in a single cylinder, 4-stroke, air cooled direct injection diesel engine. Authors also inducted hydrogen in the intake manifold. Authors compared the experimental

results with UTO40 and UTO100 with those of diesel fuel. They reported higher thermal efficiencies with both blends compared to diesel fuel. The current investigation is a good agreement with that of Pullagura et al.

4.2 Effect of WTO and RWTO on BSFC

Figures 3 and 4 show BSFC with different fuels/blends. It can be seen from the Figures that the BSFC decreases with the increase in engine load. It is interesting to note that the BSFC is lower with all WTO blends relative to DF. Pullagura et al. [3] lower brake specific energy consumption (BSEC) with WTO blends compared to DF. Though the BSEC is not shown in the current investigation but it can be calculated by simply multiplying the BSFC with the calorific value of the fuel. Thus, as the BSFC is lower with the WTO blends the BSEC will also be lower with all WTO blends.

Figure 4 compares the BSFC among WTO20, RWTO20 and DF. It is obvious that the BSFC for the WTO20 and RWTO20 blends are lower than that of DF. BSFC is better with RWTO20 blend compared to the WTO20 blend. It was observed that the fuel consumption of all types of fuels tested decrease with an increase in brake power.

4.3 Variation of exhaust gas temperature with DF, WTO and RWTO

The variation of exhaust gas temperature with brake power is shown below. The exhaust gas temperature of WTO10,WTO15, WTO20are 100°C, 100°C, 101°C respectively whereas diesel is 98°C. The reason is may be due to high auto ignition temperature for increase in exhaust gas temperature [4]. Due to this fact, the heat that is generated due to the compression stroke gets shifted its direction toward the exhaust side and increases the exhaust gas temperature.

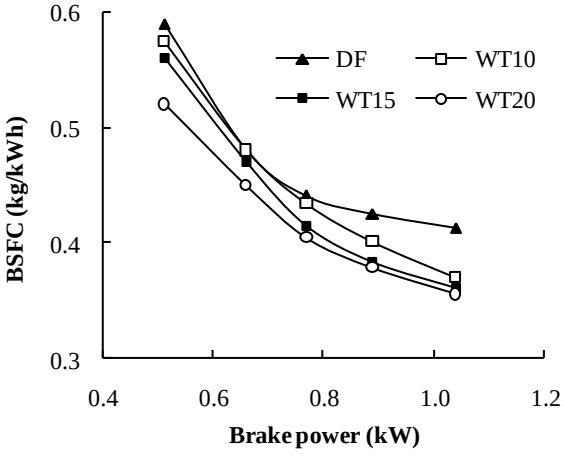

Figure 3 Effect of WTO on BSFC

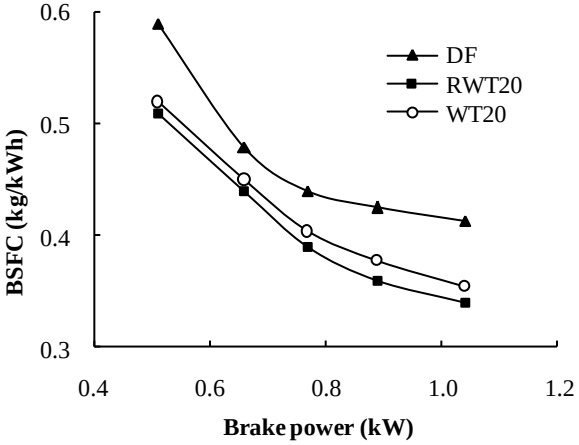

Figure 4 Effect of RWTO on BSFC

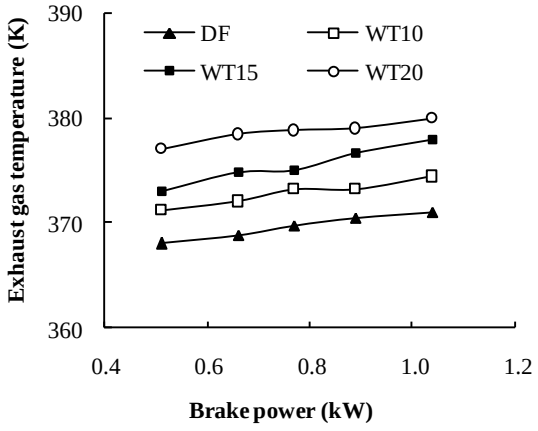

Figure 5 Effect of WTO on exhaust gas temperature

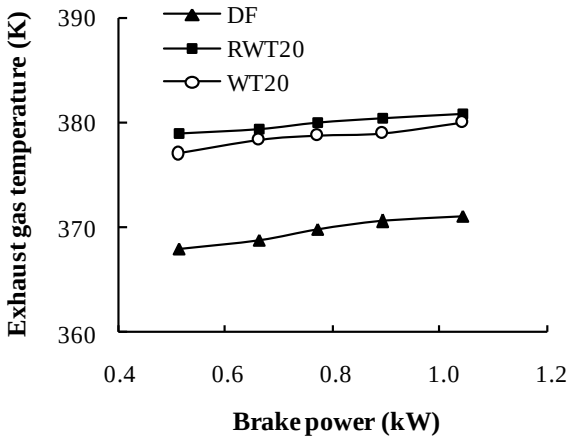

Figure 6 Effect of RWTO on exhaust gas temperature

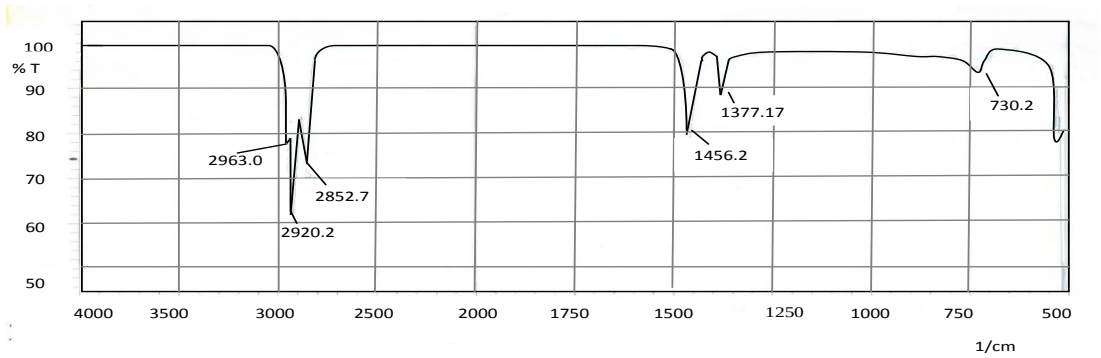

Figure 7 FTIR of neat WTO

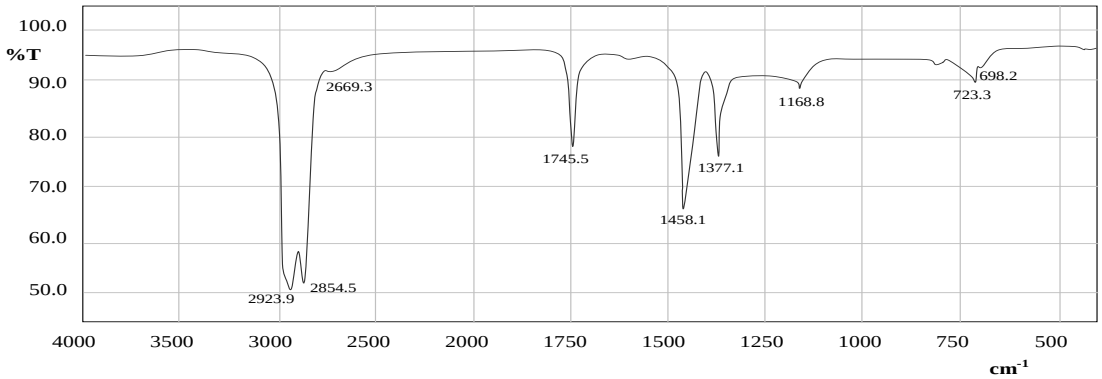

Figure 7 FTIR of neat diesel fuel

Table 3

Neat DF			Neat WTO		
Frequency range (cm^{-1})	**Bond types**	**Family**	**Frequency range (cm^{-1})**	**Bond types**	**Family**
2923.9-2854.5	C-H stretching	Alkanes	2963-2852.7	C-H stretching	Alkanes
1458.3	C-H bending	Alkanes	1456.2	C-H bending	Alkanes
1377.1	C-X	Fluoride	1377.17	C-X	Fluoride
723.3	=C-H bend	Alkanes	730.2	C-H out of plane bend	Alkanes

The FTIR spectrums of diesel and transformer oil were recorded after scanning on FTIR is shown in fig. The table represents the functional group, compositional analysis for the DF and WTO. For DF, the strong absorbance frequencies 2923.9 and 2854.5 cm^{-1} represent C-H stretching. The absorbance peaks 1458.1 cm^{-1} represented the C-H bending which indicates the presence of alkanes. For WTO100 strong absorbance peaks 2963$cm^{-1}$and 2852.7 cm^{-1}represented the C-H stretching. The absorbance peaks 1456.2 cm^{-1} and 730 cm^{-1} represented the C-H bending and C-H out of plane bend respectively indicating the presence of alkanes. From the FTIR graph it is seen that major transmittance spectrums peaks both of the fuels are alkanes. Based on the above discussion it is clear that both of the oil is saturated hydrocarbon. The presence of hydrocarbon groups C-H indicates that the liquid has a potential to be used as fuels.

5. Conclusions

The objective of this experiment was to use transformer oil as an alternative fuel. The pure diesel was used as base fuel for comparing the properties and performance parameters. The performance test was conducted on a diesel engine at a constant speed of 800. The results of the current investigation may be summarized as follows:

1. The viscosity of transformer oil 10.1 cSt which is 69% higher than viscosity of diesel (3.08 cSt) at 33°C and calorific value of diesel was higher than transformer oil by 6%. The flash and fire points of transformer oil were

140°C and 145°C respectively while for diesel, flash and fire points were 90°C and 95°C respectively. This shows transformer oil is safer for storage. The cetane number was 42.

2. The brake thermal efficiency for each blend was found to be high because of proper combustion. The brake thermal efficiency for UTO10, UTO15, UTO20 were found to be 21.37%, 21.8%, 22.1% respectively where baseline diesel was 19.2% for the same power output.

3. The fuel consumption for UTO10 for UTO 15 for UTO 20 was higher as compared to DF due to the lower heating value.

4. The exhaust gas temperature of UTO10, UTO15, UTO20were 100°C, 100°C, 101°C respectively which were higher than baseline diesel (98°C) due to the more residence time and higher viscosity.

6. ACKNOWLEDGEMENTS

Authors wish to acknowledge their sincere appreciations to higher education quality enhancement project (HEQEP, CP-521) of university grant commission (UGC), Bangladesh for partially financing the current investigation.

7. REFERENCES

[1] Rahman MA (student ID 032038) Samsuddoza SM. (student ID 032047), 2008. Biodiesel production from soybean oil and emission and performance comparison of biodiesel and biodiesel-diesel blends in di diesel engine, Undergraduate thesis, ME department, Rajshahi University of Engineering and Technology (RUET), Bangladesh.

[2] Goedde GL, Yerges AP. Dielectric fluid for use in power distribution equipment. US Patent 1998; 5,766, 517.

[3] Pullagura G, Kumar KR, Verma PC, Jaiswal A, Prakash R, Murugan S., 2012. Experimental investigation of hydrogen enrichment on performance and emission behavior of CI engine. International Journal of Engineering Science and Technology 4(3), pp. 1223-1232.

[4] Senthil Kumar M, Ramesh A, Nagalingam B., 2001. Complete vegetable oil fuelled dual fuel compression ignition engine. SAE Technical Paper Series 2001-28-0067.

[5] Sivaprakasam S., 2007. Optimization of the transesterification process for bio diesel production and use of biodiesel in a compression ignition engine. Energy & fuel 21, pp. 2998-3003.

Available online at www.sciencedirect.com

SciVerse ScienceDirect

Procedia Engineering 00 (2012) 000–000

Procedia Engineering

www.elsevier.com/locate/procedia

5th BSME International Conference on Thermal Engineering

Effect of oxygen carriers on performance of power plants with chemical looping combustion

Bilal Hassan[a], Tariq Shamim[a]*

[a]*Mechanical Engineering Program, Masdar Institute of Science and Technology, P.O. Box 54224, Abu Dhabi, UAE*

Abstract

The paper pursues process based analyses on power plants employing multi-stage chemical looping combustion (CLC) technology for carbon capture using different oxygen carrying materials and fuels. The aim is to determine any specific process based advantages offered by different oxygen carriers. CLC is an innovative combustion concept, which offers a potentially attractive option to capture CO_2 with a significantly lower energy penalty than other existing carbon-capture technologies. In the CLC process, the combustion of fuel is split into two separate reactions carried out in two separate reactors: an oxidation reaction and a reduction reaction, by introducing a suitable metal oxide as an oxygen-carrier that circulates between the two reactors. This study investigates the viability of nickel, copper and iron as oxygen carriers using them with natural and synthesis gas fuels. It was conducted by developing an Aspen Plus based model, which employed the conservative principles of mass and energy. Equilibrium based reactor models with no oxygen-carrier (OC) deactivation were assumed. The choice of oxygen carrier and its effect on key operating parameters such as air, fuel and oxygen carrier mass flow rates, operating pressure, and the waste heat recovery were investigated for each fuel. For all OCs, the maximum temperatures were observed at stoichiometric OC mass flow rates for the given fuel supply. The peak reduction reactor temperatures were obtained with copper OC, which may require inerts or other temperature reduction strategies to avoid thermal deterioration. Maximum thermal efficiencies were observed for iron and nickel OCs. However, iron requires considerably larger OC mass flow rates compared to nickel and copper.

Keywords: Greenhouse gas; CO_2 capture; Aspen; chemical looping combustion; oxygen carrier.

1. Introduction

The gradual shift towards a warmer global climate has been indisputably accepted at various international environmental forums. CO_2 has the biggest contribution towards global warming because of the highest emission rate amongst other greenhouse gases and very long residence time within the atmosphere [1]. To reduce the CO_2 concentration within the environment, various carbon capture and sequestration (CCS) strategies have been developed. Chemical looping combustion (CLC) is considered as one of the promising schemes for making carbon capture more energy efficient [2]. CLC is also preferred on the basis of having lower environmental impact in comparison to other carbon capture technologies.

Initially presented as a novel idea for enhancing combustion efficiency by [3], the current interest in CLC is mainly due to its inherent ability to capture CO_2. The main idea of CLC, as shown in Fig. 1, is to split the combustion of the fuel into two separate reactions carried out in two separate reactors: an oxidation reaction and a reduction reaction, by introducing a suitable metal oxide as an oxygen-carrier (OC) that circulates between the two reactors. In this approach, the fuel and solid

* Corresponding author. Tel.: +971-2-810-9158; fax: +971-2-810-9333.
E-mail address: tshamim@masdar.ac.ae

metal oxide enter the reduction reactor, where the metal oxide releases oxygen under the fuel-rich reducing environment. The released oxygen reacts with the fuel, which is oxidized to CO_2 and H_2O. After extracting work, CO_2 can easily be separated from H_2O in a condenser. The reduced metal oxide exits the reduction reactor and is transported to the oxidation reactor, where it is re-oxidized in the presence of air. The oxygen-depleted air and the oxidized metal oxide are separated at the exit of the oxidation reactor. The work is extracted from the separated gas stream whereas the oxidized metal oxide is circulated back to the reduction reactor.

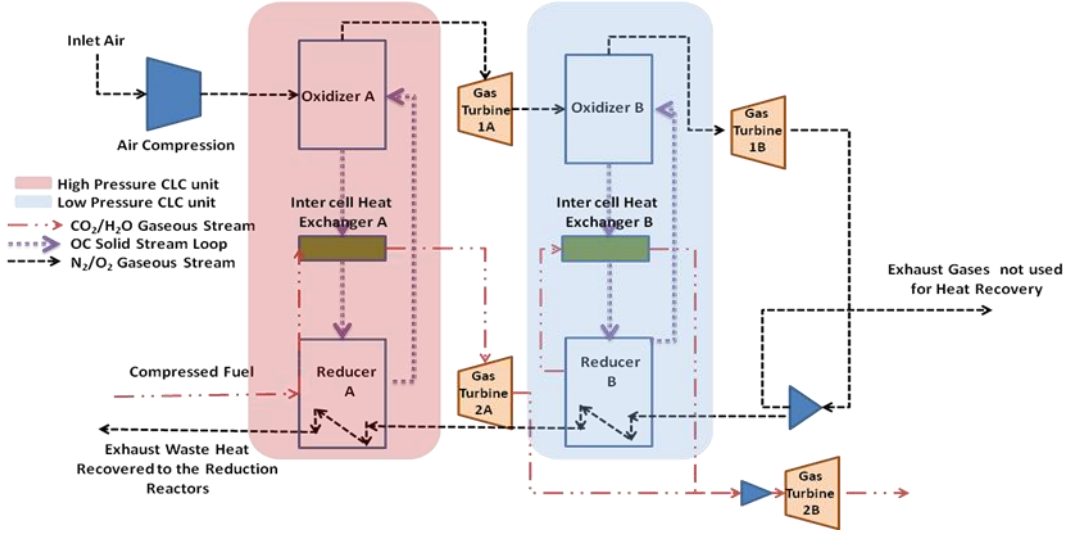

Fig. 1. Schematic representation of the natural gas fueled CLC power plant used in current study

The solid OC particles, which are responsible for repeated exchanges of lattice oxygen between the reduction and oxidation reactors, are an important component of an effective CLC unit. For efficient operation, the OC particles should: have strong affinity to completely react with incoming gaseous fuel; be stable at high temperatures; be fluidizable; resist agglomeration; defy frictional wear; have low production cost; and have minimal environmental impact [4-5]. Besides high fuel conversion and high melting points, other parameters such as density, active surface area, pore volume, particle size and crushing strength are also important parameters for selecting an OC, as described in [6,7].

The integration of CLC technology with power generation systems has been investigated in several studies [e.g., 8]. The prime target of such studies has been enhancement of overall plant thermal efficiencies and possible comparison with similar plants without CLC [9]. Most of these studies are based on specific combinations of power plant arrangements, fuels and OCs. In our previous work [9-10], we conducted parametric analyses to investigate the possible impact of key operating variables on overall plant thermal and exergetic efficiencies. Our work was focused on a natural gas based power plant with nickel as the OC. However, since the possible operating conditions are closely dependent on the reactivity of OC [6-7], it is essential to extend the parametric analysis by including the effects of different OCs and fuels. The present study is motivated by recognizing this gap in literature. It employs a system level model of a CLC based power plant and investigates the effect of different OCs (nickel, copper and iron) and fuels (natural gas and synthesis gas) on the relationship between the plant's key input and output parameters.

2. Methodology

To see the effect of the different OCs on plant performance, a parametric analysis has been performed on a multi-stage, CLC power plant (Fig. 1) using each OC on the Aspen Plus simulation engine. The exhaust heat from the oxidation reactors is recovered to the reduction reactors as shown in the plant schematic. The high temperature solid, OC streams discharged from the oxidation reactors are used to heat the gaseous streams released from the reduction reactors in the inter cell heat exchangers A and B. The reactors were modeled on equilibrium or minimization of Gibbs free energy principle with no OC deterioration. The reaction kinetics and fluid dispersion velocities were not considered. Complete separation of solid and gaseous product streams ejecting from the reactors is assumed.

The Aspen simulation results are used to calculate stream exergies and plant exergetic efficiencies using the definitions described in [10]. The thermo-mechanical and chemical exergies were considered in the current analysis. The model was validated by comparing the results with the work of Anheden and Svedberg [8] and excellent agreements were found between the results of the two models (within 1%) as reported elsewhere [9-10].

3. Results and discussions

3.1. Base Case Scenarios

Base case scenarios have been used in the current case study to reduce the number of simulations. In the parametric analysis, all conditions are fixed to base case values except the varied parameter. Separate base case scenarios have been defined for the case of natural gas and synthesis gas fueled CLC plants as shown in Table 1. The OC feed rates in all base case scenarios are equal to the stoichiometric amounts of OC required for the fuel supply. Other parameters such as exhaust heat recovery, air supply and operating pressure are constant in the base case scenario for a given fuel type. Hence, any significant deviations in the efficiency, temperature and emission profiles shall be primarily due to the particular OC used. The synthesis gas fueled plant is operated on a lower pressure as compared to the natural gas fueled plant in accordance with optimized parameters used by [8].

Synthesis gas has lower heat capacity in comparison to natural gas and thereby, requires lower air mass flows to attain effective CLC operating temperatures. With low air flow rates, there is limited availability of high temperature working fluid for power generation. Hence, synthesis gas fueled plants exhibited thermal efficiencies within the range of 39-41% in comparison to natural gas fueled plants which had peak efficiencies approaching 50%. The operating temperatures for the synthesis gas fueled power plants have been lower in comparison to corresponding natural gas based power plants. This results in lower NO_x and CO emissions which are strongly dependent on oxidation and reduction reactor temperatures respectively. For natural gas operated power plant, iron and nickel OCs attained similar peak thermal efficiencies in comparison to copper which attained a lower peak efficiency of 44%. This is attributed to significantly lower oxidation reaction enthalpy for copper resulting in lower gas turbine inlet temperatures and corresponding lower work outputs. Although copper has a high reduction reactor operating temperature but since the mass flow rate of the CO_2 rich stream is much lower, the effect of the high reduction reactor temperatures on the cumulative plant work output is not substantial.

3.2. Effect of Air Flow Rate on different OC's and Fuels

The air supply primarily affects the oxidation reactor temperature. However, these effects are resonated throughout the CLC cell due to the cyclic operation. The general trends in the temperature profiles shown in Fig. 2 are similar for either fuel. Primarily, maximum temperatures are attained at stoichiometric supply of air for the available supply of OC (base case scenario). With further increase in air mass flow, the exothermic oxidation reactions are unable to sustain the high temperature resulting in a gradual decline. Nickel, copper and iron based OCs have similar oxidation reactor temperature profiles. For both cases of synthesis gas and natural gas, the highest temperature in the oxidation reactor is for nickel. This is attributed to nickel's highly exothermic oxidation reaction enthalpy.

Copper dominates other OCs with significantly higher reduction reactor temperature profiles for both synthesis gas and natural gas. This is primarily attributed to its very exothermic reduction reaction. However, copper as OC is disadvantaged for having a low melting temperature within the range of 1220-1320 K. Although nickel and iron OCs have similar reduction reaction enthalpies but substantial differences are evident between their reduction reactor temperature profiles. This is attributed to considerably higher OC mass flow rates for iron based OC (stoichiometric mass flow for a given

Table 1. Parameter values and the results for base case conditions

BASE CASE SCENARIOS	Base Case Plant Configuration Parameter Values									Base Case Results							
	Fuel	OC	Feed Mass Flows		Stoichiometric OC mass flow rate as per fuel mass flow		Heat Recovery	CLC Loop Pressures		Efficiencies		Temperatures		Emissions			
	Fuel Type	Bulk OC Employed	Total Fuel Supply	Total Air Supply	High Pressure Loop	Low Pressure Loop	Fraction of Exhuast Heat Recovered	High Pressure (HP)Loop	Low Pressure (LP)Loop	Plant Thermal Efficiency	Plant Exergetic Efficiency	HP Oxidation Reactor	LP Reduction Reactor	CO	NOx	CH4	SOx
	Units		kg/hr	kg/hr	kg/hr	kg/hr	%	bars	bars	%	%	K	K	PPM	PPM	PPM	PPM
	Natural Gas	NiO/Ni	3600	180000	42192	10548	21.5	30	15	49.5	66.5	1504	1034	193	1265	0	0
		CuO/Cu	3600	180000	45746	11436	21.5	30	15	44	67	1333	2134	6500	508	0	0
		Fe_2O_3/Fe_3O_4	3600	180000	333408	83352	21.5	30	15	49.7	66.1	1464	1623	295	1200	0	0
	Syn Gas	NiO/Ni	3600	30000	6200	1700	21.5	18	9	40	69.2	1424	1537	403	714	0	210
		CuO/Cu	3600	30000	6720	1740	21.5	18	9	39.7	68.8	1259	2210	2700	260	0	240
		Fe_2O_3/Fe_3O_4	3600	30000	51538	12650	21.5	18	9	40.6	69	1463	1484	355	900	0	200

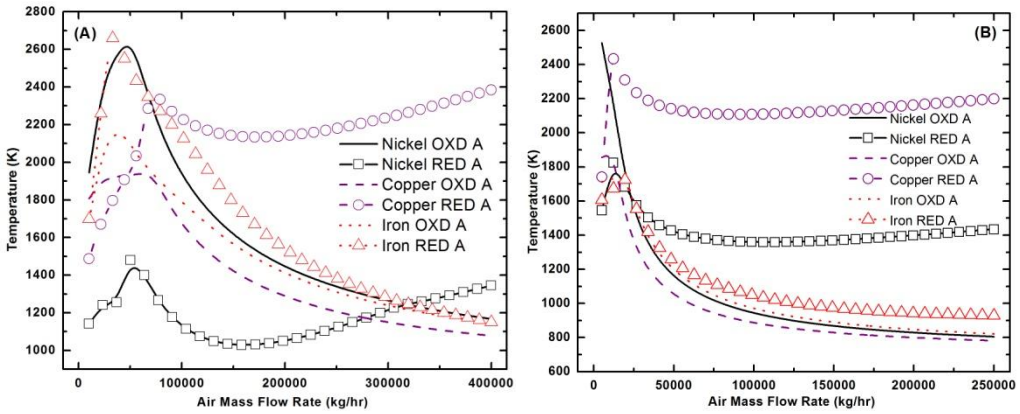

Figure 2 Effect of air mass flow rate on reactor temperature profiles with different OCs using fuels: (A) natural gas; and (B) synthesis gas.

amount of fuel), which results in effective thermal energy exchange between the two reactors located within the loop. This results in high temperatures within both reactors and consequently high plant thermal and exergetic efficiencies.

Maximum thermal efficiencies were attained at roughly three times the stoichiometric air flow rate due to availability of more working fluid as shown in Fig. 3. A decreasing trend in exergetic efficiency is seen for both fuels (Fig. 3). With increasing air mass flows, the plant temperatures fall resulting in lower cumulative work outputs and higher irreversibilities resulting in lower exergetic and thermal efficiencies. Initially, with insufficient air supply incomplete combustion of incoming fuel occurs resulting in substantial quantities of combustible species emitted within the exhaust. This results in high output chemical exergies and correspondingly high overall exergetic efficiencies.

3.3. Effect of Fuel Flow Rate on different OC's and Fuels

The fuel feed rate is to be tailored in accordance with the air and OC mass flow rates to achieve effective CLC plant performance. The effects of fuel flow rates on the reactor temperatures and thermal and exergetic efficiencies are shown in Figs. 4 and 5. Maximum reactor temperatures were attained for fuel feed rates slightly higher than stoichiometric amounts required for the circulating OC within the CLC cell. Peak thermal efficiencies were attained at stoichiometric proportions of fuel and OC for all three OCs used in the current study.

The oxidation and reduction reactor temperature profiles for the natural gas and synthesis gas scenarios are generally similar. However, with nickel OC, the reduction temperature profiles for different fuel supplies are markedly different. Nickel has an endothermic reaction with natural gas and an exothermic reaction with synthesis gas (combination of CO and H_2). Hence, with natural gas, the reduction reactor temperature decreases sharply to as low as 600 K. In contrast, with synthesis gas, the reduction reactor temperatures rise steadily till they exceed stoichiometric proportions and begin declining with excess fuel. Iron has similar reaction enthalpies as nickel but the reduction and oxidation reactor temperatures are roughly similar due to the much higher OC mass flows and thermal exchange between the two reactors. The oxidation reactor temperature profiles for all three OCs remained stable in fuel rich conditions, although reduction reactor

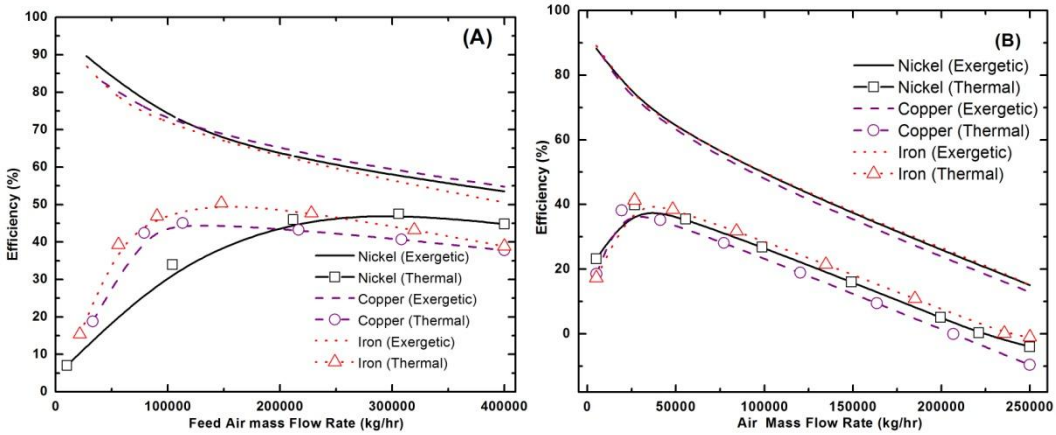

Figure 3 Effect of air mass flow rate on plant thermal and exergetic efficiencies with different OCs using fuels: (A) natural gas; and (B) synthesis gas.

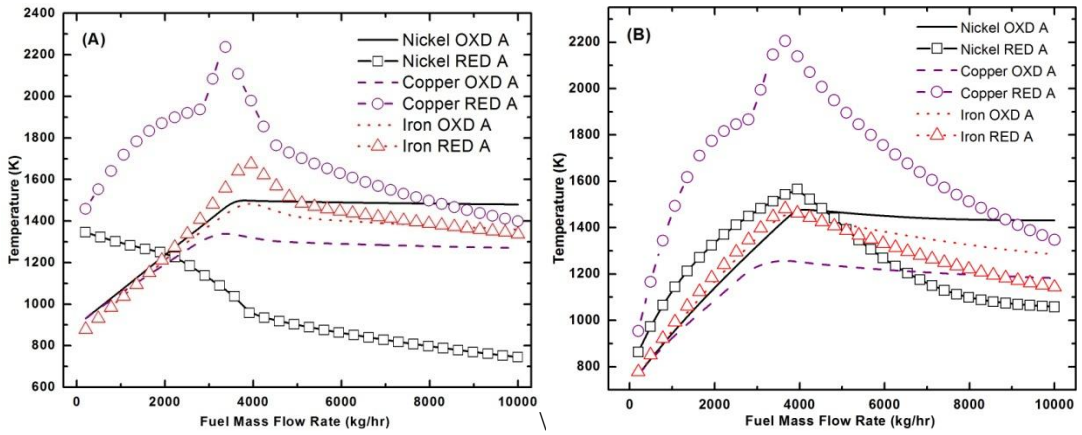

Figure 4 Effect of fuel mass flow rate on reactor temperature profiles with different OCs using fuels: (A) natural gas; and (B) synthesis gas.

temperatures declined in this zone. This is primarily attributed to exothermic oxidation reductions which are shifted forward by low temperature feeds incoming from the reduction reactors.

The exergetic and thermal efficiency profiles for the different OCs and fuel types are very similar. The thermal efficiency profiles decline for fuel rich and OC rich mixtures due to lower operating temperatures and corresponding lower cumulative work output. CLC plants operated on iron OC presented maximum thermal efficiency of 50% at stoichiometric fuel supply rates. This is attributed to considerably higher OC mass flow rates (in case of iron) which allow effective thermal exchange between reduction and oxidation reactors resulting in high operating temperatures for both reactors. The exergetic efficiency profiles with varying fuel mass flow rates are similar for all OCs and fuels. At stoichiometric conditions, the exergetic efficiencies are within the range of 60-70%.

3.4. Effect of OC Flow Rate on different OC's and Fuels

The mass of OC circulating within the CLC loop affects the overall cell performance. The optimal OC mass flow rate shall depend on the particular combination of OC and fuel used. Depending on the oxygen transfer capability, different OCs shall require different OC mass flow rates for a given amount of fuel. The equilibrium based methane conversion efficiency for NiO/Ni (0.98 at 1000°C), Fe_2O_3/Fe_3O_4 (1 at 1000°C) and CuO/Cu (1 at 1000°C) are high. Hence, plants modeled on equilibrium basis should present similar results. The exergetic and thermal efficiency profiles are similar for all three OCs in both synthesis gas and natural gas fueled power plants as shown in Fig 6. This similarity in profiles is attributed to high equilibrium based fuel conversion for all three OCs. As OC mass flow rates increase beyond stoichiometric proportions, the efficiencies remain steady at peak value depicting minimal decrease. The averaged exergetic efficiency of synthesis gas fueled power plant was slightly higher in comparison to corresponding natural gas fueled power plant. However, the exergetic efficiencies for both power plants remained within the range of 60 to 75%. Initially, with insufficient OC available for complete combustion of incoming fuel, substantial levels of combustible species are emitted within the exhaust resulting

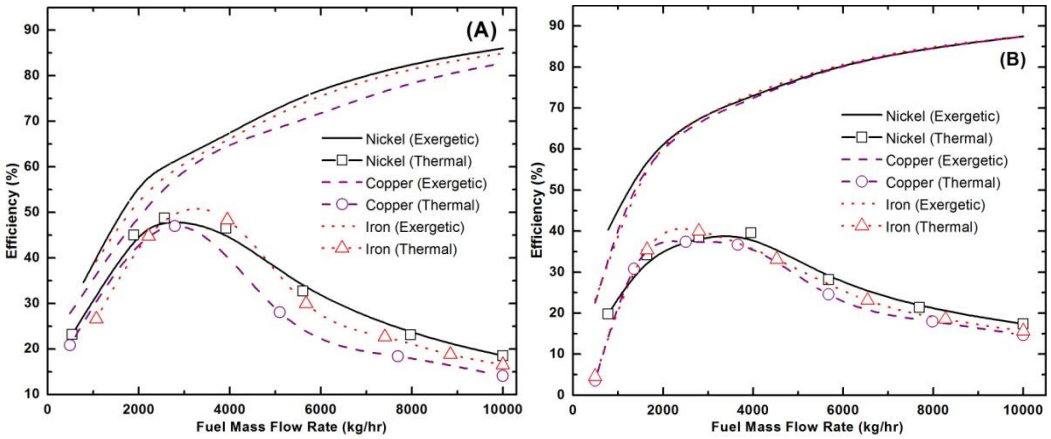

Figure 5 Effect of fuel mass flow rate on plant thermal and exergetic efficiencies with different OCs using fuels: (A) natural gas; and (B) synthesis gas.

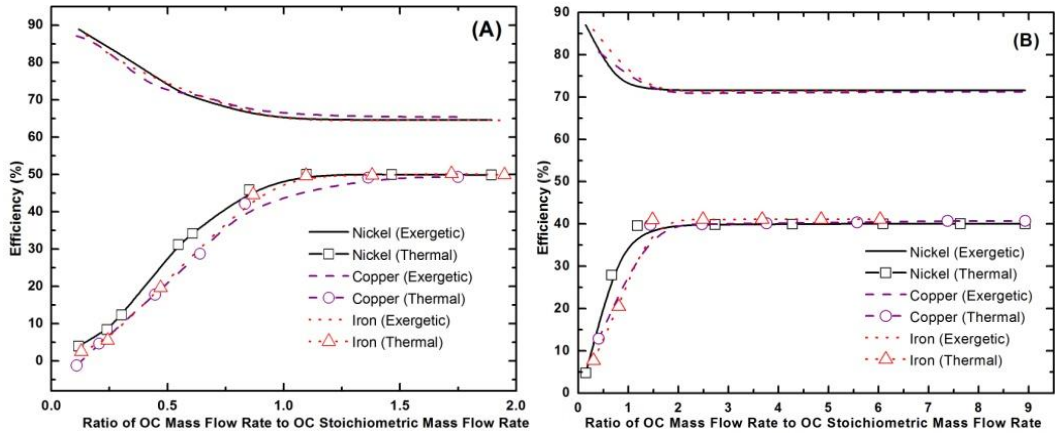

Figure 6 Effect of OC mass flow rate on plant thermal and exergetic efficiencies with different OCs using fuels: (A) natural gas; and (B) synthesis gas.

in high output chemical exergies and overall exergetic efficiencies. The temperature profiles for synthesis gas are found to be similar to corresponding profiles for natural gas (results are not shown here). Maximum temperature are attained at stoichiometric proportions of OC for the given fuel supply.

4. Conclusions

A comparative process based parametric analysis was performed to analyze the effect of the usage of three different OCs and two different fuels on the performance of a multi-stage CLC power plant. The plant temperatures and efficiency profiles were observed and possible variations between them due to a specific combination of fuel and OC employed were investigated further. Natural gas fueled power plant resulted in higher thermal efficiencies (50%) then corresponding synthesis gas operated power plant (44%) due to higher fuel heat capacities and higher air feed rates. High conversion trends were observed for all three OCs. With iron OC operated CLC plants, the thermal efficiencies were maximum due to high oxidation and reduction reactor temperatures. However, iron requires considerably larger amounts of OC for transferring the same amount of oxygen in comparison to nickel and copper OC. This would require larger power plant capacity and increased capital costs. The stoichiometric proportions of fuel and OC result in maximum thermal efficiencies for all combinations of OC and fuels.

Acknowledgements

The work is financially supported by the MIT/Masdar Institute Collaborative Research funds (Grant # 10MAMA1).

References

[1] Archer, D., 2005. Fate of Fossil Fuel CO2 in Geological Time. Geophys Res 110, p. C09S05.
[2] Kerr, H., 2005. Capture and Separation Technology Gaps and Priority Research Needs, in "*Carbon Dioxide Capture for Storage in Deep Geologic Formations – Results From the CO_2 Capture Project*," D. C. Thomas, S. M. Benson, Editors. Oxford, UK.
[3] Richter, H. J., Knoche, K. F., 1983. "Reversibility of combustion processes," ACS Symposium, pp. 71-85.
[4] Mattisson, T., Lyngfelt, A., Cho, P., 2001. The Use of Iron Oxide as an Oxygen Carrier in Chemical-Looping Combustion of Methane with Inherent Separation of CO_2. Fuel 80, pp. 1953-1962.
[5] Jerndal, E., Mattisson T., Lyngfelt, A., 2006. Thermal Analysis of Chemical-Looping Combustion. Chemical Engineering Research & Design 84, pp. 795-806.
[6] Adanez, J., de Diego, L., Garcia-Labiano, F., Gayan, P., Abad, A., 2004. Selection of Oxygen Carriers for Chemical Looping Combustion. Energy and Fuels 18, pp. 371-377.
[7] Cho, P., Mattisson, T., Lyngfelt, A., 2004. Comparison of Iron, Nickel, Copper and Manganese based Oxygen Carriers for Chemical Looping Combustion. Fuel 83, pp. 1225-1245.
[8] Anheden, M., Svedberg, G., 1998. Energy Analysis of Chemical Looping Combustion Systems. Energy Conversion & Management 39, pp. 1967–1980.
[9] Hassan, B., Shamim, T., 2012. "Parametric and exergetic analysis of a power plant with CO_2 capture using chemical looping combustion," International Proceedings of Chemical, Biological and Environmental Engineering, vol. 27, pp. 57-61.
[10] Hassan, B., Shamim, T., Ghoniem, A. F., 2012. "A parametric study of multi-stage chemical looping combustion for CO_2 capture power plant," Proceedings of the ASME 2012 Summer Heat Transfer Conference, Puerto Rico, Paper# ASME2012-58597.

Available online at www.sciencedirect.com

SciVerse ScienceDirect

Procedia Engineering 00 (2012) 000–000

Procedia Engineering

www.elsevier.com/locate/procedia

5th BSME International Conference on Thermal Engineering

Alternative Fuels for Use in Cement Kilns: Process Impact Modelling

K.T. Kaddatz[a], M.G. Rasul[a], Azad Rahman[a,*]

[a]*Central Queensland University*
School of Engineering and Built Environment
Rockhampton, Queensland 4702, Australia

Abstract

The manufacture of Portland cement is an energy intensive process. It produces significant pollution and uses large amounts on non-renewable resources. With increasing pressures to reduce greenhouse gas emissions due to cement manufacture, research and development of fuel alternatives and their effect on the manufacturing process has become an industry focus. The inherent properties of sintering cement in a rotary kiln allows for a large number of fuels to be burnt which are normally prohibited for use as fuel in other processes. To examine the suitability of a fuel, process modeling and simulation can be undertaken to predict the final impact of that fuel on kiln performance and greenhouse gas emission. With an accurate model and sufficient data, it is possible to conduct simulations for a wider range of alternative fuels. This paper discusses and summarizes the simulation results of three alternative fuels, namely spent carbon lining, used industrial lubricants and used tires, for identifying the most effective fuel source among these three. Among the selected fuels used, industrial lubricant is found to be the best option regarding the CO_2 emission, while the spent carbon lining is the worst one. In contrast, feed material requirements can be reduced by up to approximately 15% by using spent carbon lining. Further research is recommended to justify the findings.

Keywords: Cement; Kiln; Alternative fuels; Process modelling; Energy efficiency.

1. Introduction

Portland cement is one of the most commonly used construction materials in the world. The manufacture of Portland cement is energy intensive, requiring temperatures between 1450°C and 1500°C [1]. The manufacture of Portland cement accounts for approximately 5% of the annual carbon dioxide output. Half of these emissions originate from the burning of fuel and half from the calcination reactions [2]. Due to increasing pressures to implement sustainable and environmentally friendly manufacturing techniques, there has been increased exploration of alternative fuels to power the cement kiln. Testing of possible alternative fuels has been limited by the economic risks associated with real world experimentation with alternative fuels.

Modern Portland cement manufacturing technique was invented in 1824 [3] and, since the move to rotary kilns, very little has changed. As this process has been used for a long period of time, the chemical processes are well understood. The difficulty in modeling the process comes from the number of variables and reactions which take place. Attempting to model every possible reaction is well beyond the scope of this study and would require more specific process data than is available. For the purposes of this study, only a limited range of possible reactions have been considered. The reactions selected for

* Corresponding author. Tel.: +61 422 438 437;
E-mail address: a.rahman2@cqu.edu.au

consideration were those responsible for producing the four most prevalent products Alite, Belite, Calcium Aluminate and Ferrite.

The main process routes for the manufacturing of cement vary with respect to equipment design, method of operation and fuel consumption [4]. The cement manufacturing process basically includes quarry, raw material preparation, preheating of raw material, kiln, clinker cooling, grinding, storage and dispatch. A schematic diagram of the cement manufacturing process is shown in figure 1 [5]. The process begins with decomposition of calcium carbonate ($CaCO_3$) at about 900°C to leave calcium oxide (CaO, lime) and liberate CO_2; this process is known as calcination. Then the clinkering process takes place in the kiln in which the calcium oxide reacts at high temperature (typically 1400°–1500°C) with silica, alumina and ferrous oxide to form the silicates, aluminates and ferrites respectively which make up the clinker. This clinker is cooled and then ground together with gypsum and other additives to produce cement.

To generate the required thermal energy, fuels are burnt in the kiln as well as in the preheater tower. The rotary kiln used in cement manufacturing is able to burn a wide range of materials due to the long residence time at high temperatures, the intrinsic ability for clinker to absorb and lock contaminants into the clinker and the alkalinity of the kiln environment. Materials like waste lubricants, plastics, used tires and sewage sludge are often proposed as alternative fuels for the cement industry. Meat and bone meal is also considered now as an alternative fuel [6]. Several agricultural biomass and industrial wastes are newly identified as potential alternative fuels for the cement industry. Spent carbon lining, an industrial waste of aluminium smelters, is one of the prospective alternative fuel candidates [7].

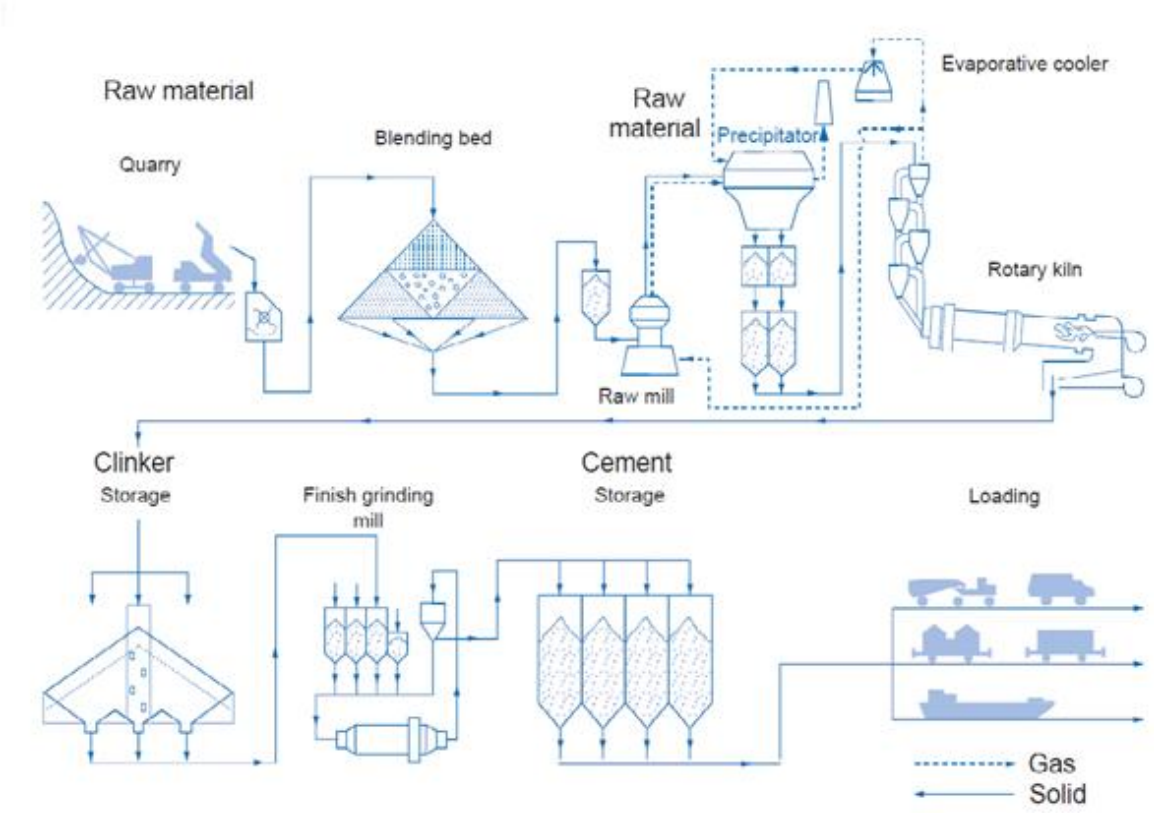

Fig. 1: Schematic presentation of the cement manufacturing process from quarry to dispatch [5]

In order to reduce the risks of trialing a new alternative fuel, this study used a computer process model to predict the effects of selected alternative fuels on kiln performance and CO_2 emissions. These preliminary predictions will allow a larger range of fuels to be tested with minimal cost. Various commercial software packages are available to model and simulate the physical and chemical changes in industrial production. Thermodynamic models are extensively used in chemical and process engineering, materials technology as well as in energy and environmental technology. Most of the studies on modeling cement manufacturing found in the literature are based on computational fluid dynamics (CFD) [8-13]. Kaantee et al. [6] and Zhang et al. [14] used Aspen Plus, a commercial software package, to simulate the cement clinker production focusing on clinker chemistry and thermodynamics in the rotary kiln.

The scope of the study was defined to meet the requirements of testing and implementing selected alternative fuels. Aspen Plus software was initially selected to model the cement manufacturing process of a regional cement plant from which required data was collected. Due to some difficulties in acquiring and using this software package and the lack of technical support, the use of the Aspen Plus model for this study was discontinued. Instead, a Microsoft Excel model is used to investigate suitable waste processing techniques to satisfy the storage, handling and feed requirements. Optimum blending ratios of alternative fuels with the fossil fuel are also studied by using the model. Among the selected alternative fuels, a comparative discussion is appended on the basis of the simulation results.

2. Alternative Fuels

Fossil fuels are most commonly used in the cement industry due to their availability and price. In recent years, due to increasing prices and concerns over climate change, industry has been looking at alternative fuel sources which may be able to partially or totally replace fossil fuels. In the past couple of decades there has been a large amount of research on alternative fuels and their impact on plant performance. The cement plant has the additional advantages of high temperatures and long residence times within the kiln, and fuels normally considered dangerous to burn can be used in these circumstances. Almost all wastes have some calorific value which could be harnessed. However, in order to be economically viable they must meet a number of criteria, the most important of which are listed below [15]:

- Availability.
- Physical state of the fuel (solid, liquid, gaseous).
- Content of circulating elements (Na, K, Cl, S).
- Toxicity (organic compounds, heavy metals).
- Composition and content of ash.
- Content of volatiles.
- Calorific value (typically over 8 MJ/kg is required).
- Physical properties (scrap size, density, homogeneity).
- Grinding properties.
- Humidity content.

In order to create the model, the full chemical breakdowns of each of the fuels are required; this information was gathered from previous studies [6-7]. The current study allows the demonstration of the application of computer modelling to fuel analysis. Three potential alternative fuels, namely spent carbon linings, used industrial lubricants and used tyres have been selected for the current study because of their availability. Though the chemical breakdown of these selected fuels are available in the literature, to ensure the most realistic result, actual plant data have been collected from a regional cement plant. All three alternative fuels have been used or are currently being used by that cement plant. Chemical composition of the alternative fuels, feed material and the coal were collected from the referenced cement plant. Energy and feed material requirement of the process is determined on the basis of the collected data by using a computer model.

End-of-life tyres are a waste product from the automobile industry and became very popular to the cement manufacturers as an alternative fuel to cope with the increasing fuel costs during the mid 80's. High carbon content, high heating value and low moisture content make discarded tyres one of the most used alternative fuels in the cement industry all over the world. Reinforcing wires of tyres can be consumed as a replacement for other raw material containing iron [16] when the whole tyre is used as alternative fuel.

Spent carbon lining (SCL) is a solid waste produced during the manufacture of aluminium metal in electrolytic cells. The carbon portion of the lining serves as the cathode for the electrolysis process. Up to 79% of U.S.-generated SCL was recycled in cement kilns in 2010 [17]. In 2009, 7449 tonnes of SCL were recycled in Australia, mostly in the cement industry as an alternative fuel [18]. Used industrial lubricants generally have high calorific value, and those can be used in cement kilns as alternative fuel with minimal processing cost [19]. The energy content of used lubricants varies due to the different ratios of various chemicals in it, although in most cases the calorific value of used lubricants is higher than coal.

3. Modeling and Simulation

A range of simulation packages are available in order to model the complex chemical processes within modern cement manufacturing plants. Amongst them, ASPEN PLUS, ASPEN HYSYS and ANSYS FLUENT are widely used to model the manufacturing process and to predict the performance characteristics of the plant. ASPEN PLUS and ASPEN HYSYS use a flow sheet simulator to graphically represent each stage of the process allowing for, at a glance, interpretation of the stages of the process. ASPEN PLUS and ASPEN HYSYS enable quick and easy alterations to a process, allowing users to quickly trial a number of different system configurations without requiring a new model for each change. ANSYS FLUENT allows

modeling of the effect of surface condition of the material as well as the effect of phase changes on a body of material. It also allows the optimization of fluid flow, material feed and containing structure. Due to the nature of cement production, ASPEN PLUS is identified as the most suitable since this package has the ability to simulate chemical reactions within solid, liquid and vapour phases [20].

Modeling of the cement manufacturing process can also be done in Microsoft Excel. The Microsoft Excel model is much simpler than the other model; however, this model is not able to consider the chemical processes, the physical layout of the plant or the thermal properties of the materials. In this study, Microsoft Excel is used for modeling as there were some technical difficulties with the Aspen Plus software which we have a license for and due to the unavailability of technical support. The Microsoft Excel simulation is done based on the required input in order to account for the output. The outcomes of this model are sufficient to predict the overall effects of the alternative fuels on the feed requirements of the cement plant, but cannot account for any changes in the chemical composition due to the alternative fuels. Creating the Excel model can be broken into two distinct considerations: energy required by the process and the feed material required by the process. For the purposes of this model, the energy required was simplified to 3.05 mega joules per kilogram. The energy output and composition of each fuel set is shown in Table 1. The fuel required to generate the required energy is calculated using the following equation.

$$FuelReq = \left(\frac{Energy\ required * Clinker\ Produced}{Energy\ per\ kg\ of\ \ fuel * Fuel\%} \right)_{Fuel1} + \left(\frac{Energy\ required * Clinker\ Produced}{Energy\ per\ kg\ of\ \ fuel * Fuel\%} \right)_{Fuel2} + \cdots\cdots \quad (1)$$

The primary purpose of this study was to identify the properties of the fuels being tested in terms of their effect on the cement manufacturing process. Additionally, this study identified the requirements for storing, handling and feeding of these fuels. While calculating the emissions for each fuel, only carbon dioxide has been considered. This was calculated under an ideal case where all carbon atoms are reacted to CO_2. This assumption is suitable for the purposes of this study and, when applied in the same way to all fuel options, provides a suitable comparison between the fuel outputs.

The generalized data from a number of sources and the actual plant data from the regional cement plant are used to run the model. The required information was split into the following categories:

Fuel Properties: The properties of the alternative fuel in terms of energy content and chemical composition were needed in order to calculate the amount of fuel needed and the various emissions.

Table 1: Fuel Composition

		Coal	**SCL**	**Tyres**	**Used Oil**
	Energy Content (MJ/kg)	**27.43**	**8**	**31**	**33.54**
Components (% of fuel)	Water	8.1	—	—	1.0
	Carbon	69.9	36.59	72.0	74.2
	Hydrogen	0.379	—	6.07	15.0
	Nitrogen	0.15	—	0.2	1.8
	Sulphur	0.37	—	1.06	1.34
	Oxygen	6.32	—	1.12	—
	SiO_2	8.2957	10.2	2.292	0.31
	Al_2O_3	4.07	18.4	3.056	1.4
	Fe_2O_3	1.193	3.0	12.5247	4.95
	CaO	0.3	1.9	0.4011	—
	MgO	0.168	0.81	0.6112	—
	K_2O	0.267	0.7	—	—
	Na_2O	0.0487	14.0	0.665	—
	SO_3	0.4386	—	—	—
	F	—	14.4	—	—

Material Feed: To calculate the contribution of the fuel to the raw material required by the process, the material content of the fuel had to be known.

The proposed Microsoft Excel model could not simulate chemical reactions but could predict the suitability of fuels based on the required material input. The feed material content required and the content of the alternative fuels are taken from the available cement manufacturing plant data. The resulting feed material was calculated using the following equation.

$$FeedReq_{Material} = (Mass\ Fraction * Output) + (Mass\ Fraction * Output * Loss\ on\ Ignition) \quad (2)$$

Due to the simple nature of the model, the following assumptions were made:

- There were no chemical reactions accounted for.
- The feed required only related to the total input required and did not account for feeding fuel into the preheater or kiln.
- The emissions were calculated as an ideal conversion of carbon to carbon dioxide; this was necessary to allow excel to calculate emissions.
- Energy requirement was assumed to be 3.05 mega joules per kilogram of clinker production.
- Assuming that 100kg of clinker was to be produced, the required feed material is shown in Table 2. According to the previous assumption, the total energy required is 305MJ.
- To meet the energy requirement, the required amount of coal was 11.12 kg which was calculated on the basis of the assumptions stated earlier.

Table 2: Feed Material Required

Component	Mass %	Required (kg)	Loss on Ignition (kg)	Final Requirement (kg)
SiO_2	21.84%	21.84	7.788	29.628
Al_2O_3	5.72%	5.72	2.040	7.760
Fe_2O_3	3.89%	3.89	1.387	5.277
CaO	66.55%	66.55	23.732	90.282
MgO	1.10%	1.10	0.392	1.492
K_2O	0.37%	0.37	0.132	0.502
Na_2O	0.31%	0.31	0.111	0.421
SO_3	0.22%	0.22	0.078	0.298
Total	100	100.000	35.660	135.660

With a working simulation model, the next step was to run the required simulations in order to produce a set of results suitable for analysis. Using the Excel spreadsheet, production of the results was a simple process of changing the percentage inputs for each fuel. The testing took place in two phases, the first to test each fuel against coal and the second using a combination of the alternatives in order to select the most beneficial mixture. For each fuel composition test, the following procedure was used:

- Set the fuel percentage for the composition to be tested.
- Make up to 100% using coal.
- Check the results to ensure no component is oversupplied.
- If material is over supplied, reduce the step size to best pinpoint the limiting point.
- Repeat the process of checking the amount of the components until either a limit point is found or 100% of alternative fuel is used in the mixture.

4. Results and Discussion

Three different alternative fuels for the cement industry have been studied through use of a Microsoft Excel model. The input data consisted of an energy requirement, amount of feed material required and the chemical composition of the feed material and fuels. The model provided the percentage changes in different components of the required feed material as well as changes in CO_2 emission. Figure 2 shows the resultant component breakdown for the 100% exchange of coal with different alternative fuels. This result gives an idea of the possible maximum exchange rate of coal to the alternative fuels.

The changes in feed material requirements have been plotted in Figure 3 for the usage of the maximum limit of each alternative fuel. Figure 3 indicates that SCL reduces the feed material requirements more than the other alternative fuel options.

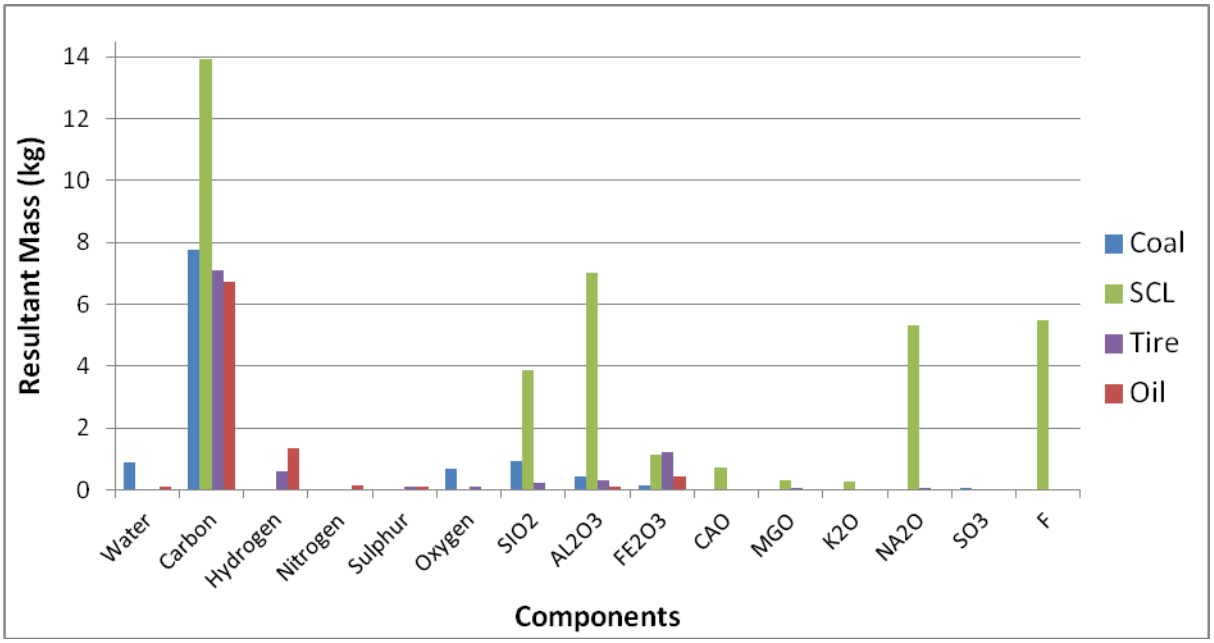

Fig. 2: Comparative component breakdown for 100% exchange of coal to alternative fuels

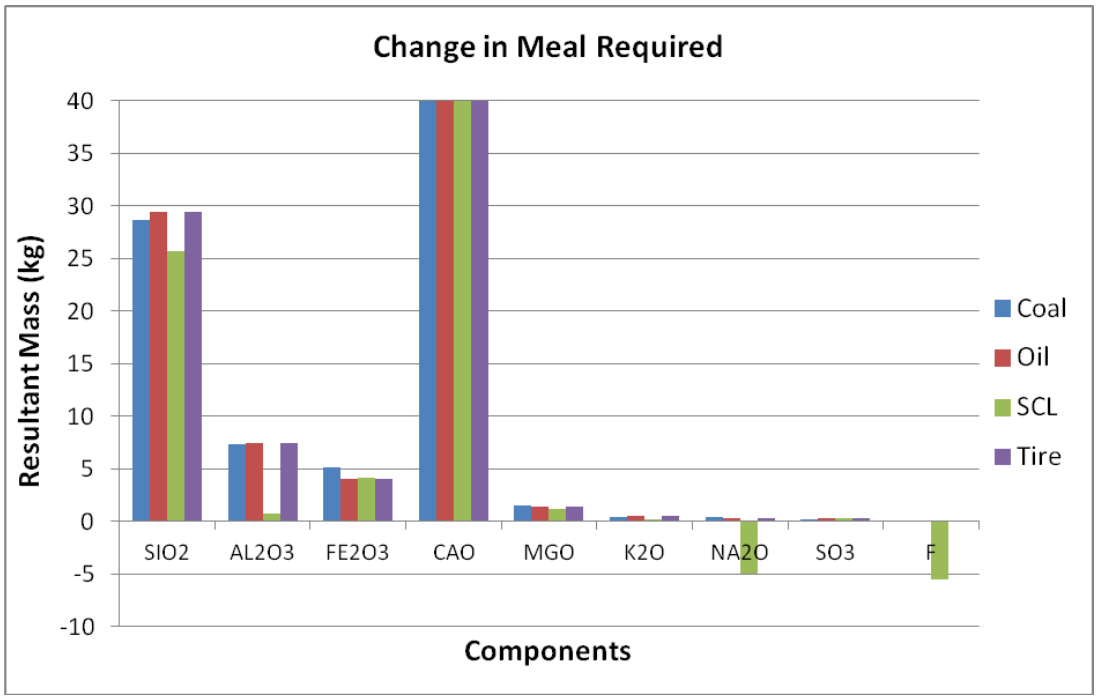

Fig. 3: Change in feed material required for different alternative fuels

4.1. Spent carbon lining

Upon examination of the results of replacing the coal with SCL it was found that SCL is a viable substitute. The use of SCL does not provide significant thermal energy; rather it reduces the feed material requirements and is a source of fluorine. The disadvantage of using SCL is an increase in carbon dioxide emissions. The limiting factor for the use of SCL is the sodium oxide or alkali content which in this case limits the feed rate to 7.8% of the total fuel feed.

In terms of energy content and emissions savings, SCL is the worst performing of the tested alternative fuels. Due to the low energy content of SCL, it required 2.42 times of the amount of coal and produced 79% more carbon dioxide. At the limiting point, SCL increased the CO_2 emissions by 6.18% resulting in an additional 1.76kg of CO_2 when assuming that all carbon is converted to CO_2. SCL is a very good source of the feed materials required for the process, amounting to 14.83% of the total requirements at the limiting point.

4.2. Used industrial lubricant

It was found that the use of used industrial lubricants was beneficial to the process. This fuel was able to produce the required energy with two kilograms less fuel compared to coal. CO_2 emissions increased 13% while coal is completely substituted by used industrial lubricants. The largest concern is that many used lubricants can be treated for reuse which is a more sustainable option. As such, burning in cement kilns should be a last resort and undertaken only for material which is too contaminated for recycling

This study was able to show that, for the specific used lubricant considered, the energy and emissions make it a suitable replacement for coal. However, before implementation, the specific material to be used should be analysed to ensure that it will reduce the required feed material and CO_2 emissions. Used industrial lubricants were found to be the simplest alternative to implement. Due the liquid nature of the material, the storage and handling equipment requires little space and can be easily incorporated into an existing plant.

4.3. Used tires

Used tires were shown to require 1.2 kg less material than coal in order to generate the required energy. Used tires produced 9% less carbon dioxide than pure coal. In addition, tires are a good source of iron due to the steel strapping within the rubber. The incineration of used tires is a sustainable practice as the recycling applications currently cannot consume the amount of material generated. Combustion of tires in the kiln was found to be a clean process due to the very high temperature and long residence times. In this study the tires were assumed to combust instantaneously. If the whole tire is not combusted entirely, that can result in less efficient firing and additional fuel requirement. Further study should be undertaken on specific firing situations to quantify the effect of this.

Storage handling and feeding of tires can be problematic, particularly if the tires are being fed in whole. The feeding involves a high level of manual handling. This can be overcome through the use of shredded tires, but the shredding equipment involves a higher capital cost and energy for preparation.

5. Conclusions

This study investigated three alternative fuels which were selected and analyzed for their suitability for use in a cement kiln. This analysis identified the benefits or detriments to the process using a computer simulation of the required process inputs. With suitable data being available for each of the fuels, a Microsoft Excel model was used to create a simplified solution. While this model was not able to calculate the chemical output, it was able to find the changes to the material input caused by each fuel which, for this study, was enough to make a preliminary judgment on the fuel's suitability.

In the case of the spent carbon lining, it was found to be a suitable alternative fuel. Uniquely, this alternative is recommended for use not because of its value as an energy source, but for its ability of offset a portion of the feed material required. SCL was limited though by its sodium content which could not exceed the maximum overall input for the feed requirements. This fuel was found to be the easiest to implement as the storage, handling and feed requirements are very similar to that for coal and would require minimal alterations.

Used industrial lubricants were found to be the fuel most suited to replacing coal. The energy content for the used lubricants analyzed was the highest of all the fuels examined and produced the lowest overall carbon dioxide emissions. In terms of the change in feed material, this fuel provided little to no material and therefore the cost of the additional feed would need to be weighed against the savings in coal. The logistics of using waste lubricants is fairly simple and would require minimal changes to the current plant. The largest modification would be the area needed for the storage, pumping and blending.

As an alternative fuel, used tires were found to be a suitable replacement for coal. The tires had a high energy content allowing them to provide a better emissions profile than coal. The largest weakness with using this option is that tires require a complicated handling setup which often includes a large amount of manual handling.

Overall this study has successfully identified the strengths and weaknesses of each of the fuels considered. This study has proven that this process could be used to model an alternative fuel without the need for expensive testing, allowing many

more fuels to be considered, and having substantial benefit to both plant operators and the sustainability of the cement industry.

References

[1] WHD Microanalysis Consultants, 2011. Cement History. http://www.understanding-cement.com/history.html [Accessed 10 October 2011]

[2] Hendriks, C.A., Worrell, E., de Jager, D., Blok, K., Riemer, P., 2004, Emission Reduction of Greenhouse Gases from the Cement Industry. IEA Greenhouse Gas R&D Progeamme. Breakeley, 2004. Lawrence Berkeley National Laboratory, http://www.wbcsdcement.org/pdf/tf1/prghgt42.pdf, ed. [Accessed 10 October 2011]

[3] Hewlett, P.C., 2003, Lea's Chemistry of Cement and Concrete. 4th ed. United Kingdom: Butterworth-Heinemann ltd.

[4] European Commission, Reference Document on the Best Available Techniques in the Cement and Lime Manufacturing Industries. BAT Reference Document (BREF), European IPPC Bureau, Seville, Spain, 2011.

[5] Vdz Media release, 2009, Environmental Data of the German Cement Industry, www.vdz-online.de/uploads/media/Environmental_data_2009.pdf [Accessed 19 June 2012]

[6] Kaantee, U., Zevenhoven, R., Backman, R., Hupa, M., 2004, Cement Manufacturing Using Alternative Fuels and the Advantages of Process Modelling, Fuel Processing Technology, 85 (4), p. 293– 301.

[7] Lechtenberg, D., 2009, Spent Cell Linings from The Aluminium Smelting Process as an Alternative Fuel and Raw Material for Cement Production, Global Cement Magazine, January, p. 36-37.

[8] Ranade, V.V., Mujumdar, K.S., 2003, CFD Simulations of Solid Motion in the Transverse Plane of Rotating Kilns, Third International Conference on CFD in the Minerals and Process Industries, CSIRO, Melbourne, Australia, 2003.

[9] Ranade, V.V., 2003, Modeling of Rotary Cement Kiln, Third International Conference on CFD in the Minerals and Process Industries, CSIRO, Melbourne, Australia, 2003.

[10] Mastorakos, E., Massias, A., Tsakiroglou, C.D., Goussis, D.A., Burganos, V.N., 1999, CFD Predictions for Cement Kiln Including Flame Modeling, Heat Transfer And Clinker Chemistry, Applied Mathematical Modelling 23, p. 55–76

[11] Mujumdar, K.S., Ranade, V.V., 2006, Simulation of Rotary Cement Kilns Using a One-Dimensional Model, Trans IChemE, Part A, Chemical Engineering Research and Design, 84(A3), p. 165–177

[12] Mujumdar, K.S., Ganesh, K.V., Kulkarni, S.B., Ranade, V.V., 2007, Rotary Cement Kiln Simulator (RoCKS): Integrated Modelling Of Pre-Heater, Calciner, Kiln And Clinker Cooler, Chemical Engineering Science. 62, p. 2590 – 2607

[13] Marin, O., Charon, O., Dugue, J., Dukhan, S., Zhou, W., 2001, Simulating the Impact of Oxygen Enrichment in a Cement Rotary Kiln Using Advanced Computational Methods, Combust. Sci. and Tech. 164, p. 193-207

[14] Zhang, Y., Cao, S., Shao, S., Chen, Y., Liu, S., Zhang, S., 2011, Aspen Plus-Based Simulation of a Cement Calciner and Optimization Analysis of Air Pollutants Emission, Clean Techn. Environ Policy, 13(3), p. 459–468

[15] Mokrzycki, E., Uliasz-Bochenczyk, A., 2003, Alternative Fuels For The Cement Industry, Applied Energy, 74, p. 95–100.

[16] Kaantee, U., Zevonhoven, R., Backman, R., Hupa, M., 2002, Cement Manufacturing Using Alternative Fuels and the Advantages of Process Modelling. in Proc. of R'2002 Recovery Recycling Re-Integration, Geneva, February 12-15.

[17] Alcoa Worldwide Sustainability: Sustainability of Operations: Environmental: Emissions & Waste, 2012, http://www.alcoa.com/sustainability/en/info_page/operations_env_emissions.asp. [Accessed 1st March 2012]

[18] Alcoa in Australia: Environmental Management: Waste, 2012, http://www.alcoa.com/australia/en/info_page/environ_waste.asp. [Accessed 1st March 2012]

[19] de Vos, S., Gortzen Mulder, J.E., Ligthart, T., Hesseling, W., 2007, LCA of Thermal Treatment of Waste Streams in Cement Kilns in Belgium, TNO report I&T-A R 2007/036, Netherland Org. for Applied Sci. Res.

[20] Aspen One, 2011. Aspen Plus. Product Disclosure Statement. Houston, TX USA: AspenTech AspenTech.

[21] Ansys, 2011. Ansys Fluent Features. Product Disclosure Statement. Ansys.